



D2.6 USE CASE DEFINITIONS AND INITIAL SAFETY-CRITICAL SCENARIOS

Primary Author(s) András Bálint | Chalmers University of Technology
Volker Labenski, Markus Köbe, Carina Vogl, Johan Stoll | Audi AG
Lars Schories, Lena Amann, Ganesh Baroda Sudhakaran | ZF Friedrichshafen AG
Pedro Huertas Leyva, Thomas Pallacci | University of Florence
Martin Östling | Autoliv
Daniel Schmidt | Robert Bosch GmbH
Ron Schindler | Chalmers University of Technology

Related Work Package WP2

Version/Status 1.0 | Submitted to the EC

Issue date 30/Sep/2021

Deliverable type R

Dissemination Level PU

Project Acronym SAFE-UP

Project Title proactive SAFETy systems and tools for a constantly UPgrading road environment

Project Website www.safeup.eu

Project Coordinator Núria Parera | Applus IDIADA

Grant Agreement No. 861570



This project has received funding from the European Union's Horizon 2020 research and innovation programme under Grant Agreement 861570.

Document Distribution

Version	Date	Distributed to
0.7	28/Sep/2021	Coordination Team
1.0	30/Sep/2021	Submission in the EC System
1.0	17/03/2022	Approved by the EC

Acknowledgment

We thank all SAFE-UP project partners, especially the T2.1 team, for supporting the work that led to this document and for their active participation in project meetings! Special thanks go to Marilee Nugent (UniFi) for suggestions regarding the terminology used in this report, and to the reviewers of the document for their valuable insights and suggestions.



Copyright statement

The work described in this document has been conducted within the SAFE-UP project. This document reflects only the views of the SAFE-UP Consortium. The European Union is not responsible for any use that may be made of the information it contains.

This document and its content are the property of the SAFE-UP Consortium. All rights relevant to this document are determined by the applicable laws. Access to this document does not grant any right or license on the document or its contents. This document or its contents are not to be used or treated in any manner inconsistent with the rights or interests of the SAFE-UP Consortium or the Partners detriment and are not to be disclosed externally without prior written consent from the SAFE-UP Partners.

Each SAFE-UP Partner may use this document in conformity with the SAFE-UP Consortium Grant Agreement provisions.



Executive summary

The aim of the SAFE-UP project is to improve traffic safety by developing tools and innovative methods that proactively address the safety challenges of future mobility systems. This deliverable, which is reporting the work performed in SAFE-UP task T2.1, specifies scenarios that will be considered in later stages of the project. Relevant data sets and results are identified by a literature review. The specific goal of the task is to identify initial safety-critical scenarios that work packages investigating active and passive safety systems as part of different demonstrators, can consider for their application. Results described in this deliverable will be further investigated in traffic simulation (in SAFE-UP tasks T2.2 - T2.5) to characterize scenarios that are expected to be safety-critical in future traffic.

In line with the SAFE-UP project focus and the requirements of the various work packages that need input, this report describes existing crash scenarios from the viewpoint of a passenger car (ego vehicle) and taking all traffic participants into account. In particular, the scope of analysis ranges from situations with high risk for ego occupants, e.g., in car-to-car and car-to-heavy goods vehicle (HGV, with gross weight $\geq 3.5\text{t}$) crashes, to scenarios with limited injury risk for occupants of the ego vehicle but high injury risk for the opponent, e.g., car-to-vulnerable road user (VRU, including pedestrian, bicyclist and powered two-wheeler) conflicts.

To prevent serious injuries and fatalities of car occupants, the SAFE-UP project evaluates potential occupant restraint systems for in-crash protection in WP4. For the protection of VRUs, primarily pedestrians and bicyclists, active safety systems and infrastructure-based or on-user warning systems are considered in WP3 with the aim of avoiding the crashes or mitigating crash consequences. These considerations guide the analysis so that the analysis of car-to-vehicle crashes is focused on the crash configuration at the moment of collision while the analysis of car-to-VRU crashes is focused on the last seconds before the collision. Additionally, aspects related to adverse weather conditions (i.e., conditions like rain, snow or fog that could adversely affect sensor performance) are relevant for the work on improved sensing algorithms. Crash causation, especially the role of infrastructure, is relevant input to infrastructure-based and on-user warning systems that will be referred to as Cooperative Intelligent Transport Systems (CITS).

In SAFE-UP T2.1, an extensive analysis of road crash data in the EU community database on road accidents (CARE) database was conducted to obtain a general overview of car occupant injuries and fatalities. This analysis has identified the relevance of occupant restraint systems in both car-to-car and car-to-HGV crashes and analyzed the most frequently occurring general crash types for each case. Various assumptions have been investigated to identify the scenarios in which occupants of cars with automated driving functions are expected to need protection. These aspects have contributed to the definition of occupant use cases described in deliverable D4.1, which includes a description of these analysis steps. The corresponding analysis is briefly summarized and extended in this deliverable.



A similar analysis of CARE data has provided general statistics on car-to-VRU crashes in the EU, mainly in urban environment. As CARE provides police-reported information on all road crashes in the EU with personal injury, the corresponding analysis results give a good representation of the crash situation in Europe. As a first step, the relationship of the location of crashes to junctions was investigated, to facilitate appropriate placement of infrastructure-based systems for VRU protection. It was found that **for car-to-bicycle crashes in urban areas, crashes at junctions are most relevant, especially in bad weather**. However, it was found that **crashes at junctions have smaller prevalence in car-to-pedestrian crashes**.

Additionally, various in-depth analyses have been performed to enable a deeper understanding of the main scenarios and trends on EU level identified in CARE. This step is essential for a more detailed understanding because the level of detail in CARE does not allow a sufficiently detailed characterization of critical situations such that it can be used for the assessment of safety systems. An analysis of data from the German In-Depth Accident Study (GIDAS) supported this work. For the vehicle-based active safety systems for VRU protection, the GIDAS analysis included the extraction of main parameters contributing to system specification as well as a study of factors influencing different sensor principles. Additionally, crash configuration parameters such as vehicle speeds, angles, etc. were analyzed using the GIDAS database for improved car occupant restraint systems. A final group of in-depth analyses was focused on pedestrian crashes in the German in-depth crash database GIDAS complemented by an analysis of near-crashes in naturalistic driving data sets (AMP, JAAD), analyzing specifically the role of infrastructure and traffic rules in car-to-VRU scenarios.

Analyses of GIDAS are performed to identify injured road users considering all injury levels as well as killed or seriously injured (KSI) road users. Fatalities as a separate category are only used in the CARE-based analyses, because of the limited number of fatalities in GIDAS. As a result of the analyses described above, the following initial safety-critical scenarios have been defined in this report:

1. **For the avoidance of AV occupant fatalities in mixed traffic**, it was identified that future work in SAFE-UP (related to SAFE-UP Demonstrator 1) should focus on **car-to-car (C2C) and car-to-heavy goods vehicle (C2HGV) crash scenarios**. Due to project timing, much of the analysis of C2C and C2HGV crashes was reported in SAFE-UP deliverables D4.1 and further developed in D4.2. In SAFE-UP D4.1, **a target population of fatalities in modern cars (with registration year 2000 or later) in C2C and C2HGV crashes, excluding crashes with parking vehicles**, was defined. According to CARE analysis, the target population included 2 085 such fatalities in 2018 in the EU. The scenarios that were selected for further analysis were the crash types identified as the most frequent ones in specific traffic environments. Due to a large number of unknown values in the crash type classification in CARE, the relative frequency of different crash types is expressed as intervals rather than single values. The lower ends of the intervals indicate the share of the given crash type as a percentage of the total sample while the



upper ends indicate their share among cases with known crash types. The scenarios selected for further analysis are as follows:

- a) **C2C head-on and C2HGV head-on crashes** (covering 11.1-25.0% and 5.2%-11.9% of the target population; such crashes are common among fatal crashes away from junctions in rural areas);
- b) **C2C crossing or turning and C2HGV crossing or turning crashes** (covering 0.2-4.4% and 0.1%-1.8% of the target population; such crashes are common among fatal crashes at a junction in rural areas);
- c) **C2C rear-end and C2HGV rear-end crashes** (covering 1.1-2.2% and 1.2%-2.2% of the target population; such crashes are common among fatal crashes on motorways away from junctions).

Further work with occupant protection (OP) requires the specification of crash configurations (e.g., kinematic parameters, angles, and other relevant parameters describing the moment of impact) within the above crash scenarios. **Publications in the field of traffic safety as well as previous project results will be used in WP4 to specify relevant crash configurations for C2C crashes.** As such results are not available for C2HGV crashes, C2HGV head-on and C2HGV rear-end crashes were analyzed further in GIDAS data, and the following crash configurations were identified as starting points for further analysis:

- a) **OP-C2HGV-HO1: head-on collision in which the front of a passenger car of weight 1.5-2.5 t at a speed 39 km/h collides with the front of a heavy goods vehicle of weight 10-18 t having collision velocity 36 km/h, at an angle of 10°, with 50% overlap.**
- b) **OP-C2HGV-RE1: rear-end collision in which the front of a heavy goods vehicle of weight 10-18 t having collision velocity 29 km/h, at an angle close to 0°, with 100% overlap, strikes the rear-end of a passenger car of weight 1.5-2.5 t that is standing at the moment of collision.**

These crash configurations are very specific and, depending on the outcome of finite element simulations, may need to be modified to get relevant results. To facilitate this process, the **distributions of relevant kinematic parameters (collision speeds of car and HGV, relative speed, impact angle, hit point, weight)** are described in this report (Section 4.2.2) so that appropriate parameter ranges can be considered.

2. **Car-to-VRU crashes in adverse weather conditions (AWC): precipitation like rain, snow, hail, or sleet was found to be the most common conditions that could adversely affect sensor performance while fog was found to be less relevant as it is present in 0-1% of crashes.** Therefore, the use cases that are recommended to be addressed by safety systems with improved performance in AWC (addressed in SAFE-UP Demonstrators 2 and 3) are **scenarios with a larger-than-average prevalence of precipitation.** The precipitation amounts observed in crashes are quantified in the paragraph under points a)-d) below. The car-to-pedestrian (C2P, further abbreviated by



the letter P in the name of use cases) and car-to-bicycle (C2B, further abbreviated by the letter B in the name of use cases) AWC use cases are defined as follows:

- a) **AWC-P1** (identical to CITS-P2 below): **Pedestrian crossing from left, without sight obstruction** (P-CLwoSO, 19.5% of KSI, 15.3% of all injured within C2P), **with common initial speeds of 30-50 km/h for the passenger car. 23.1% of KSI and 21.5% of all injuries** within this scenario occur in weather conditions **with precipitation**. The intensity of precipitation in the corresponding crashes is 63% “light”, 31% “moderate”, 3% “heavy” and 3% “not identifiable”.
- b) **AWC-P2: Pedestrian in conflict with passenger car turning left** (P-PCTurnL, 9.2% of KSI, 11.1% of all injured within C2P), **with common initial speeds of 10-28 km/h for the passenger car. 23.2% of KSI and 25.3% of all injuries** within this scenario occur in weather conditions **with precipitation**. The intensity of precipitation in the corresponding crashes is 60% “light”, 31% “moderate”, 6% “heavy” and 3% “not identifiable”.
- c) **AWC-B1** (identical to CITS-B1 below): **Bicyclist crossing from right while passenger car moves forward** (B-CR, 37.8% of KSI, 35.2% of all injured within C2B), **with common initial speeds of 5-30 km/h for the passenger car and 10-18 km/h for the cyclist. 7.7% of KSI and 7.2% of all injuries** within this scenario occur in weather conditions **with precipitation**. The intensity of precipitation in the corresponding crashes is 59% “light”, 30% “moderate”, 6% “heavy” and 5% “not identifiable”.
- d) **AWC-B2, identical to CITS-B3: Bicyclist in conflict with passenger car turning left** (B-PCTurnL, 10.0% of KSI, 17.1% of all injured within C2B), **with common initial speeds of 11-29 km/h for the passenger car and 12-21 km/h for the cyclist. 11.8% of KSI and 12.8% of all injuries** within this scenario occur in weather conditions **with precipitation**. The intensity of precipitation in the corresponding crashes is 71% “light”, 27% “moderate”, and 2% “heavy”.

To allow the simulation and testing of scenarios with realistic precipitation amounts that can be observed in real-world crashes, GIDAS data was linked to rainfall amounts around the crash site as measured in weather stations of the German Meteorological Service (Deutscher Wetterdienst, DWD). This study (see Section 4.3.4) shows that the **subjective intensity label “light” in GIDAS can be mapped to the median value of 0.42 mm/h, “moderate” to the median value of 0.84 mm/h, and “heavy” to the median value of 1.2 mm/h, while the 90th percentiles** (indicating the precipitation amount that includes 90% of GIDAS crashes with the given intensity label) **are 1.5 mm/h for “light,” 3.6 mm/h for “moderate” and 5.8 mm/h for “heavy”.**

3. **Car-to-pedestrian (C2P) crashes**, including the following scenarios suggested for consideration for work related to advanced intervention functions and CITS (addressed in SAFE-UP Demonstrators 3 and 4):



- a) **C2P-1: Pedestrian crossing from right, without sight obstruction (P-CRwoSO, 23.2% of KSI, 22.8% of all injured within C2P), with common initial speeds of 26-48 km/h for the passenger car.**
- b) **C2P-2 (identical to AWC-P1 above): Pedestrian crossing from left, without sight obstruction (P-CLwoSO, 19.5% of KSI, 15.3% of all injured within C2P), with common initial speeds of 30-50 km/h for the passenger car.**
- c) **C2P-3: Pedestrian crossing from right, with sight obstruction (P-CRwSO, 18.7% of KSI, 17.1% of all injured within C2P), with common initial speeds of 26-45 km/h for the passenger car.**
- d) **C2P-4: Pedestrian crossing from left, with sight obstruction (P-CLwSO, 14.0% of KSI, 12.4% of all injured within C2P), with common initial speeds of 28-45 km/h for the passenger car.**

The speed of pedestrians is not quantified in the GIDAS and is therefore not specified above.

Most crashes in the above scenarios happen in urban areas away from junctions at non-designated crossing locations, where the infrastructure is not meant to support the pedestrians in crossing the road. The corresponding analysis (presented in Section 4.3.1.3) focused on non-designated crossing revealed that **crashes at non-designated crossings often are characterized by missing or failing interaction of both participants.** These crashes tend to happen more frequently than crashes at designated crossings and seem to lead more often to severely or fatally injured pedestrians. In crossing scenarios of pedestrians, where interaction is needed there is the opportunity for CITS to provide a safety benefit.

4. **Car-to-bicyclist (C2B) crashes**, for which the most common scenarios, suggested for the consideration of advanced intervention functions and CITS (Demonstrators 3 and 4), are as follows:
 - a) **C2B-1: Bicyclist crossing from right while passenger car moves forward (B-CR, 37.8% of KSI, 35.2% of all injured within C2B), with typical initial speeds of 5-30 km/h for the passenger car and 10-18 km/h for the cyclist.**
 - b) **C2B-2: Bicyclist crossing from left while passenger car moves forward (B-CL, 25.5% of KSI, 22.4% of all injured within C2B), with typical initial speeds of 7-32 km/h for the passenger car and 12-20 km/h for the cyclist.**
 - c) **C2B-3 (identical to AWC-P2 above): Bicyclist in conflict with passenger car turning left (B-PCTurnL, 10.0% of KSI, 17.1% of all injured within C2B), with typical initial speeds of 11-29 km/h for the passenger car and 12-21 km/h for the cyclist.**
 - d) **C2B-4: Bicyclist in conflict with passenger car turning right (B-PCTurnR, 7.5% of KSI, 12.3% of all injured within C2B), with typical initial speeds of 10-30 km/h for the passenger car and 14-20 km/h for the cyclist.**

These scenarios almost exclusively happen at junctions.



This report also includes a characterization of precipitation and daylight conditions, as well as the specification of trajectories for both participants in each of the above scenarios (as well as for other, less frequent C2P and C2B scenarios, for completeness). Furthermore, while the SAFE-UP systems for VRU protection are primarily targeting pedestrians and cyclists, the most frequent crash scenarios between cars and powered two-wheelers (PTWs) are also identified. Crash data and naturalistic riding data are analyzed for a better understanding of the behavior of PTW riders and their interaction with other traffic participants (Section 4.3.3).

The analyses described so far address the question of which existing issues in current traffic should be tackled by future safety systems. Additionally, SAFE-UP is also considering new safety-critical situations that could be relevant for the protection of vehicle occupants as well as VRUs after an assumed introduction of automated vehicles in traffic, and traffic simulations in WP2 are an essential tool for identifying such situations. **The results in this report (Section 4.1) show that crashes in the EU are distributed over all periods of the day, including night-time that is especially relevant for car-to-pedestrian crashes of all injury levels. Furthermore, in each group of car-involved crashes, the night-time period makes up a larger share among crashes with a fatal outcome compared to all injury crashes.**

Further work will be performed to support the definition of metrics and calibration of model parameters that would allow WP2 to analyze future safety-critical interactions by micro-simulation. This requires an investigation of relevant parameter ranges in naturalistic driving data, and continuous discussion between WP2 partners needs to be performed to ensure that the relevant parameters are selected in the best way for the simulation needs. The corresponding work will be performed in task T2.2, with the findings reported in deliverable D2.14.



Table of contents

1. Introduction	24
1.1 <i>Future view of current safety-critical scenarios</i>	25
1.2 <i>New safety-critical scenarios in mixed traffic</i>	27
2. Literature review	28
2.1 <i>VRU fatalities worldwide</i>	28
2.2 <i>VRU fatalities in the USA</i>	29
2.3 <i>VRU fatalities in the EU.....</i>	30
2.4 <i>VRU crashes in Germany</i>	32
2.5 <i>Influence of precipitation on road crashes</i>	34
3. Method and data.....	35
3.1 <i>Method</i>	35
3.1.1 <i>Vulnerable road users.....</i>	35
3.1.2 <i>Car occupants.....</i>	35
3.2 <i>Crash databases.....</i>	36
3.2.1 <i>Community Accident Database (CARE).....</i>	36
3.2.2 <i>German In-Depth Accident Study (GIDAS).....</i>	37
3.2.3 <i>Initiative for the Global harmonization of Accident Data (IGLAD).....</i>	38
3.3 <i>Naturalistic driving data.....</i>	38
3.3.1 <i>Joint Attention in Autonomous Driving (JAAD)</i>	39
3.3.2 <i>Automated Mobility Partnership (AMP).....</i>	40
4. Results	41
4.1 <i>General crash statistics in the EU.....</i>	41
4.2 <i>Car occupants.....</i>	47
4.2.1 <i>Selecting occupant use cases by CARE analysis</i>	47
4.2.2 <i>In-depth analysis of occupant use cases based on GIDAS.....</i>	49
4.2.2.1 <i>Head-on collisions</i>	51
4.2.2.2 <i>Rear-end collisions</i>	52
4.3 <i>In-depth analysis of car-to-VRU crashes</i>	53



4.3.1	Car-to-pedestrian crashes	54
4.3.1.1	Filter criteria for the analysis of car-to-pedestrian crashes in GIDAS	54
4.3.1.2	Clustering of car-to-pedestrian crashes	55
4.3.1.2.1	Conflict scenario P-CLwoSO	57
4.3.1.2.2	Conflict scenario P-CLwSO	59
4.3.1.2.3	Conflict scenario P-CRwoSO	61
4.3.1.2.4	Conflict scenario P-CRwSO	63
4.3.1.2.5	Conflict scenario P-Long	65
4.3.1.2.6	Conflict scenario P-PCRev	67
4.3.1.2.7	Conflict scenario P-PCTurnL	69
4.3.1.2.8	Conflict scenario P-PCTurnR	71
4.3.1.3	Designated vs non-designated crossings of pedestrians	73
4.3.1.4	Implications of the infrastructure-based analysis on safety measures	78
4.3.2	Car-to-bicyclist crashes.....	78
4.3.2.1	Filter criteria for the analysis of car-to-bicycle crashes in GIDAS.....	78
4.3.2.2	Clustering of car-to-bicycle crashes.....	80
4.3.2.2.1	Conflict scenario B-CR	82
4.3.2.2.2	Conflict scenario B-CL.....	84
4.3.2.2.3	Conflict scenario B-LongSD	86
4.3.2.2.4	Conflict scenario B-LongOD	88
4.3.2.2.5	Conflict scenario B-PCRev	90
4.3.2.2.6	Conflict scenario B-PCStat	92
4.3.2.2.7	Conflict scenario B-PCTurnL	94
4.3.2.2.8	Conflict scenario B-PCTurnR	96
4.3.3	Powered two-wheelers.....	98
4.3.3.1	Car-to-PTW crashes	98
4.3.3.2	Clustering of Car-to-PTW crashes	100
4.3.3.3	Small PTW vs. PC crashes.....	101
4.3.3.4	Large PTW vs. PC crashes	101
4.3.3.5	PTW crash contributing factors from MAIDS data and naturalistic riding data	102



4.3.3.5.1	In-depth crash data involving PTWs.....	102
4.3.3.5.2	Analysis of Naturalistic Riding Data.....	104
4.3.4	VRU crashes in adverse weather conditions	107
4.3.4.1	Databases and variables for the analysis of weather conditions	107
4.3.4.1.1	Variables in GIDAS.....	107
4.3.4.1.2	Variables in the DWD database	107
4.3.4.2	Linkage of DWD and GIDAS data	108
4.3.4.2.1	Precipitation baseline	109
4.3.4.2.2	Objective rainfall amounts	111
4.3.4.3	Use cases for car-to-VRU-crashes with precipitation	116
4.4	<i>Future crash scenario outlook in IGLAD</i>	119
4.5	<i>Summary</i>	123
4.5.1	Use cases for car occupant protection	123
4.5.2	Use cases for advanced intervention functions and CITS	125
4.5.2.1	Most common car-to-pedestrian crashes	125
4.5.2.2	Most common car-to-bicycle crashes	127
4.5.3	Use cases for car-to-VRU crashes in adverse weather conditions.....	128
4.5.4	Most common crash scenarios for powered two-wheelers.....	130
5.	Discussion and outlook	132
5.1	<i>Discussion of the method, results, and limitations</i>	132
5.2	<i>Suggested future directions and open points</i>	133
6.	Conclusions	134
7.	References	135
	Appendix	139



List of figures

Figure 1 The role of T2.1 in supporting other SAFE-UP tasks.....	25
Figure 2 Distribution of fatalities by type of mobility mode, by WHO region (WHO, 2018)	28
Figure 3 Pedestrian fatalities as a percentage of total traffic fatalities, 2007-2016 - Source: SAFE-UP T2.1 analysis in FARS.....	30
Figure 4 Cyclist fatalities in EU countries, 2000-2019. Source: Eurostat.....	31
Figure 5 Cyclist fatalities in Germany 2008-2019 (Eurostat, 2021)	32
Figure 6 Data in JAAD (Rasouli, Kotseruba, & Tsotsos, 2017)	39
Figure 7 Time-of-the-day distribution of car-involved crashes of any injury level in urban areas in the EU in 2018	43
Figure 8 Time-of-the-day distribution of fatal car-involved crashes in urban areas in the EU in 2018	43
Figure 9 Relation to infrastructure in car-to-pedestrian crashes in urban areas in the EU in 2018	45
Figure 10 Relation to infrastructure in car-to-bicycle crashes in urban areas in the EU in 2018	45
Figure 11 Relation to infrastructure in car-to-pedestrian crashes in urban areas in the EU in 2018 in adverse weather conditions	46
Figure 12 Relation to infrastructure in car-to-bicycle crashes in urban areas in the EU in 2018 in adverse weather conditions	46
Figure 13 Defining the target population for protecting future car occupants	47
Figure 14 Crash scenarios for car occupant protection in SAFE-UP	48
Figure 15 Share of HGV>3.5t weight groups in head-on collisions by crash site	51
Figure 16 Illustration of Q50 passenger car-to-HGV>3.5t head-on crash configuration	52
Figure 17 Share of HGV>3.5t weight groups in rear-end collisions by crash site.....	52
Figure 18 Illustration of Q50 passenger car vs. HGV3.5 rear-end crash configuration	53
Figure 19 Overview of conflict scenarios for C2P crashes – schematic representation	56



Figure 20 Results summary for C2P conflict scenario 1: P-CLwoSO 57

Figure 21 P-CLwoSO trajectories showing the relative motion of pedestrians w.r.t. the passenger car 58

Figure 22 Trajectories of pedestrians and passenger cars relative to the collision point in P-CLwoSO scenarios - passenger car heading east (to the right) at collision point..... 58

Figure 23 Results summary for C2P conflict scenario 2: P-CLwSO 59

Figure 24 P-CLwSO trajectories showing the relative motion of pedestrians w.r.t. the passenger car 60

Figure 25 Trajectories of pedestrians and passenger cars relative to the collision point - in P-CLwSO scenarios - passenger car heading east (to the right) at collision point..... 60

Figure 26 Results summary for C2P conflict scenario 3: P-CRwoSO 61

Figure 27 P-CRwoSO trajectories showing the relative motion of pedestrians w.r.t. the passenger car 62

Figure 28 Trajectories of pedestrians - and passenger cars relative to the collision point in P-CRwoSO scenarios - passenger car heading east (to the right) at collision point. 62

Figure 29 Results summary for C2P conflict scenario 4: P-CRwSO 63

Figure 30 P-CRwSO trajectories showing the relative motion of pedestrians w.r.t. the passenger car 64

Figure 31 Trajectories of pedestrians - and passenger cars relative to the collision point in P-CRwSO scenarios - passenger car heading east (to the right) at collision point. 64

Figure 32 Results summary for C2P conflict scenario 5: P-Long 65

Figure 33 P-Long trajectories showing the relative motion of pedestrians w.r.t. the passenger car 66

Figure 34 Trajectories of pedestrians - and passenger cars relative to the collision point in P-Long scenarios - passenger car heading east (to the right) at collision point. 66

Figure 35 Results summary for C2P conflict scenario 6: P-PCRev 67

Figure 36 P-PCRev trajectories showing the relative motion of pedestrians w.r.t. the passenger car 68



Figure 37 Trajectories of pedestrians - and passenger cars relative to the collision point in P-PCRev scenarios -passenger car heading east (to the right) at collision point. 68

Figure 38 Results summary for C2P conflict scenario 7: P-PCTurnL 69

Figure 39 P-PCTurnL trajectories showing the relative motion of pedestrians w.r.t. the passenger car 70

Figure 40 Trajectories of pedestrians - and passenger cars relative to the collision point in P-PCTurnL scenarios -passenger car heading east (to the right) at collision point. 70

Figure 41 Results summary for C2P conflict scenario 8: P-PCTurnR 71

Figure 42 P-PCTurnR trajectories showing the relative motion of pedestrians w.r.t. the passenger car 72

Figure 43 Trajectories of pedestrians - and passenger cars relative to the collision point in P-PCTurnR scenarios - passenger car heading east (to the right) at collision point. 72

Figure 44 Illustration of "designated" (source: JAAD) and "non-designated" (source: AMP) crossings 73

Figure 45 Description of the GIDAS analysis filters and sample sizes for designated and non-designated crossing 75

Figure 46 Overview of GIDAS Parameter "HURSU" and "HURSAU", stating the main crash cause in non-designated crossings; green pedestrian means the pedestrian behaved correct; red pedestrian means improper behavior by the pedestrian..... 76

Figure 47 Overview of GIDAS Parameter "HURSU" and "HURSAU", stating the main crash cause in designated crossings; green pedestrian means the pedestrian behaved correct; red pedestrian means improper behavior by the pedestrian..... 77

Figure 48 Overview of conflict scenarios for C2B crashes – schematic representation 81

Figure 49 Results summary for C2B conflict scenario 1: B-CR 82

Figure 50 B-CR trajectories showing the relative motion of bicyclists w.r.t. the passenger car 83

Figure 51 Trajectories of bicyclists - and passenger cars relative to the collision point in B-CR scenarios -passenger car heading east (to the right) at collision point..... 83

Figure 52 Results summary for C2B conflict scenario 2: B-CL..... 84



Figure 53 B-CL trajectories showing the relative motion of bicyclists w.r.t. the passenger car 85

Figure 54 Trajectories of bicyclists - and passenger cars relative to the collision point in B-CL scenarios -passenger car heading east (to the right) at collision point. 85

Figure 55 Results summary for C2B conflict scenario 3: B-LongSD 86

Figure 56 B-LongSD trajectories showing the relative motion of bicyclists w.r.t. the passenger car 87

Figure 57 Trajectories of bicyclists - and passenger cars relative to the collision point in B-LongSD scenarios -passenger car heading east (to the right) at collision point. 87

Figure 58 Results summary for C2B conflict scenario 4: B-LongOD 88

Figure 59 B-LongOD trajectories showing the relative motion of bicyclists w.r.t. the passenger car 89

Figure 60 Trajectories of bicyclists - and passenger cars relative to the collision point in B-LongOD scenarios -passenger car heading east (to the right) at collision point..... 89

Figure 61 Results summary for C2B conflict scenario 5: B-PCRev 90

Figure 62 B-PCRev trajectories showing the relative motion of bicyclists w.r.t. the passenger car 91

Figure 63 T Trajectories of bicyclists - and passenger cars relative to the collision point in B-PCRev scenarios -passenger car heading east (to the right) at collision point..... 91

Figure 64 Results summary for C2B conflict scenario 6: B-PCStat 92

Figure 65 B-PCStat trajectories showing the relative motion of bicyclists w.r.t. the passenger car 93

Figure 66 Trajectories of bicyclists - and passenger cars relative to the collision point in B-PCStat scenarios -passenger car heading east (to the right) at collision point..... 93

Figure 67 Results summary for C2B conflict scenario 7: B-PCTurnL 94

Figure 68 B-PCTurnL trajectories showing the relative motion of bicyclists w.r.t. the passenger car 95

Figure 69 Trajectories of bicyclists - and passenger cars relative to the collision point in B-PCTurnL scenarios -passenger car heading east (to the right) at collision point..... 95



Figure 70 Results summary for C2B conflict scenario 8: B-PCTurnR 96

Figure 71 B-PCTurnR trajectories showing the relative motion of bicyclists w.r.t. the passenger car 97

Figure 72 Trajectories of bicyclists - and passenger cars relative to the collision point in B-PCTurnR scenarios -passenger car heading east (to the right) at collision point. 97

Figure 73 Distribution of crash site and injury severity for small and large PTW in GIDAS99

Figure 74 Overview of conflict scenarios for car-to-small PTW crashes – schematic representation 101

Figure 75 Overview of conflict scenarios for car-to-large PTW crashes – schematic representation 101

Figure 76 Maximum longitudinal deceleration in braking maneuvers of the PTW 105

Figure 77 Road infrastructure, interaction type, and lead vehicle in braking maneuvers from naturalistic PTW riding (data from a single volunteer) 105

Figure 78 Infrastructure context and type of lead vehicle in braking events from naturalistic riding after excluding braking events without interaction 106

Figure 79 Infrastructure, interaction type, and type of lead vehicle for the 100 sharpest braking maneuvers 106

Figure 80 Heat Map of GIDAS crashes with rain (Hanover, 2010-2017) (blue-green-red) and considered DWD weather stations (black dots). Data from GIDAS and DWD Climate Data Center (DWD, 2020)..... 108

Figure 81 GIDAS crashes with rain (Dresden, 2010-2017) and considered DWD weather stations. Data from GIDAS and DWD Climate Data Center (DWD, 2020) 108

Figure 82 Precipitation baselines for Dresden and Hanover (2010-2019). Data from the DWD Climate Data Center 109

Figure 83 Rain and snow intensity shares in Dresden and Hanover based on the intensity ranges defined by the DWD (2010-2019). Data from the DWD Climate Data Center (DWD, 2020)..... 110

Figure 84 Methodology for extracting objective rainfall amounts of the DWD data for the intensity labels in GIDAS 111



Figure 85 Box plot for the distance between GIDAS crashes with rain (2010-2017) to the nearest considered weather station. Data from GIDAS and DWD Climate Data Center (DWD, 2020) 112

Figure 86 Projection of the minutes of the crash time in GIDAS to the 10-minute interval of the DWD according to the description in (DWD, 2020)..... 112

Figure 87 Cumulative distribution functions for rain amount recorded by the DWD at different rain intensity labels in GIDAS (2010-2017, max. 15 km distance to weather station). Data from GIDAS and DWD Climate Data Center (DWD, 2020), x-axis is limited to the interval [0,5] mm per 10 min. 113

Figure 88 Box plots for the amount of rain recorded by the DWD at different rain intensity labels in GIDAS (2010-2017, max. 15km distance to weather station). Data from GIDAS and DWD Climate Data Center (DWD, 2020), y-axis is limited to the interval [0,2] mm per 10 min. 113

Figure 89 Cumulative distribution functions for the amount of rain recorded by the DWD at different rain intensity labels in GIDAS (2010-2017, up to three stations with max. 15 km distance to weather station). Data from GIDAS and DWD Climate Data Center (DWD, 2020), x-axis is limited to the interval [0,5] mm per 10 min 115

Figure 90 Box plots for the amount of rain recorded by the DWD at different rain intensity labels in GIDAS (2010-2017, up to three stations with max. 15km distance to weather station). Data from GIDAS and DWD Climate Data Center (DWD, 2020), y-axis is limited to the interval [0,2] mm per 10 min 115

Figure 91 Precipitation intensity shares for SAFE UP use cases in adverse weather conditions 118

Figure 92. Crash distributions for the main crash type categories 121

Figure 93 Time-of-the-day distribution of car-involved crashes of any injury level in rural areas in the EU in 2018 139

Figure 94 Time-of-the-day distribution of car-involved crashes of any injury level on motorways in the EU in 2018 139

Figure 95 Time-of-the-day distribution of fatal car-involved crashes in rural areas in the EU in 2018 140

Figure 96 Time-of-the-day distribution of fatal car-involved crashes on motorways in the EU in 2018 140



List of tables

Table 1 Injured and killed VRUs in crashes with passenger cars by location and injury severity in Germany in 2019 (DESTATIS, 2020a)	33
Table 2 Survey criteria for GIDAS.....	38
Table 3 Number of non-fatally injured road users in car-involved crashes in the EU in 2018 by road user type and area type	42
Table 4 Fatalities in car-involved crashes in the EU in 2018 by road user type and area type	43
Table 5 Weather conditions in car-to-pedestrian crashes in urban areas in the EU in 2018	44
Table 6 Weather conditions in car-to-bicycle crashes in urban areas in the EU in 2018...	44
Table 7 Passenger car front row occupants in crashes with HGV>3.5t by area type	49
Table 8 Applied filter criteria for vehicles in GIDAS dataset to identify front-to-rear collisions	50
Table 9 Front row passenger car occupants (MBAIS1+) by crash types (PC and HGV>3.5t)	50
Table 10 Distributions of crash configuration parameters for passenger car-to-HGV>3.5t head-on collisions in GIDAS	51
Table 11 Distributions of crash configuration parameters for passenger car vs. HGV3.5 rear-end collisions in GIDAS	53
Table 12 Criteria for the selection of car-to-pedestrian crashes in the GIDAS dataset	54
Table 13 Scenario clustering in passenger car-to-pedestrian crashes	55
Table 14 Classification of different crash types within the P-CLwoSO conflict scenario ...	57
Table 15 Classification by crash type within P-CLwSO	59
Table 16 Classification by crash type within P-CRwoSO.....	61
Table 17 Classification by crash type within P-CRwSO.....	63



Table 18 Classification by crash type within P-Long.....	65
Table 19 Classification by crash type within P-PCRev	67
Table 20 Classification by crash type within P-PCTurnL	69
Table 21 Classification by crash type within P-PCTurnR.....	71
Table 22 Result summary of key findings from NDD analysis (JAAD and AMP) of pedestrians crossing at designated and non-designated locations	74
Table 23 Criteria for the selection of car-to-bicycle crashes from the GIDAS database....	79
Table 24 Scenario clustering in passenger car-to-bicycle crashes.....	80
Table 25 Classification by crash type within B-CR	82
Table 26 Classification by crash type within B-CL	84
Table 27 Classification by crash type within B-LongSD.....	86
Table 28 Classification by crash type within B-LongOD	88
Table 29 Classification by crash type within B-PCRev	90
Table 30 Classification by crash type within B-PCStat	92
Table 31 Classification by crash type within B-PCTurnL	94
Table 32 Classification by crash type within B-PCTurnR.....	96
Table 33 Criteria for the selection of car-to-PTW crashes from the GIDAS database.....	99
Table 34 Scenario clustering in passenger car-to-PTW crashes.....	100
Table 35 Definition of the seven merged crash configurations selected and frequency distribution (Huertas-Leyva, Baldanzini, Savino, & Pierini, 2021).....	103
Table 36 Relation between primary crash contributing factor and configuration. PTW: PTW rider; OV: Other Vehicle driver. Adapted from Huertas-Leyva, et al. (2021).....	104
Table 37 Intensity ranges defined by the DWD for rain and snow (DWD, 2020b).....	110
Table 38 Comparison of the extracted values to the ranges defined by the DWD for the intensity labels. Data from GIDAS, DWD Climate Data Center (DWD, 2020), and (DWD, 2020b).....	114



Table 39 Comparison of the extracted weighted values to the ranges defined by the DWD for the intensity labels. Data from GIDAS, DWD Climate Data Center (DWD, 2020), and (DWD, 2020b).	116
Table 40 Precipitation shares within the C2P conflict scenarios (with values above the precipitation baseline of 11.95% written in bold) and the total precipitation shares within car-to-pedestrian cases.	117
Table 41 Precipitation shares within the C2B conflict scenarios (with values above the precipitation baseline of 11.95% written in bold) and the total precipitation shares within car-to-bicycle cases.	117
Table 42. Systems implemented in IGLAD for car-involved crashes.	120
Table 43. Overview of different crash types and the expected changes in the crash type distribution based on an analysis of IGLAD data	122
Table 44 Car-to-HGV crash configurations recommended for further consideration for car occupant protection.	124
Table 45 Most common car-to-pedestrian crashes and corresponding use cases.	125
Table 46 Overview of the most frequent car-to-pedestrian scenarios, recommended for consideration for CITS	126
Table 47 Most common car-to-bicycle crashes and corresponding use cases	127
Table 48 Overview of the most frequent car-to-bicyclist scenarios, recommended for consideration for advanced intervention systems and CITS.	128
Table 49 Car-to-VRU scenarios recommended for consideration for safety systems with improved sensor performance	129
Table 50 Schematic illustrations of car-to-PTW crashes by size of the PTW	131
Table 51 Summary statistics of environmental and kinematic parameters in car-to-pedestrian conflict scenarios.	141
Table 52 Summary statistics of crash causation in car-to-pedestrian conflict scenarios.	142
Table 53 Summary statistics of environmental and kinematic parameters in car-to-bicycle conflict scenarios	143
Table 54 Summary statistics of crash causation in car-to-bicycle conflict scenarios.	144



List of abbreviations

Abbreviation	Meaning
AV	Automated Vehicle
AIS	Abbreviated Injury Scale, indicates injury severity
AWC	Adverse Weather Conditions – applied to weather conditions like rain, snow or fog that can adversely affect sensor performance
CARE	EU Community database on road crashes, including data from police-reported crashes in EU and EFTA member states and the United Kingdom
CITS	Cooperative Intelligent Transport Systems
C2C	Car-to-car, a crash involving exactly two passenger cars
C2HGV	Car-to-heavy goods vehicle, a crash involving exactly one passenger car and exactly one goods vehicle with total weight $\geq 3.5t$
C2B	Car-to-bicycle, a crash involving exactly one passenger car and a bicycle
C2P	Car-to-pedestrian, a crash involving exactly one passenger car and a pedestrian
C2PTW	Car-to-PTW, a crash involving exactly one passenger car and a powered two-wheeler
D	Deliverable within SAFE-UP (e.g., D2.6 denotes SAFE-UP deliverable 2.6)
DWD	German Meteorological Service (Deutscher Wetterdienst)
EU	European Union, including the member states in 2021
EFTA	European Free Trade Association, including Iceland, Liechtenstein, Norway, and Switzerland
GIDAS	German In-Depth Accident Study
HGV	A goods vehicle with total weight $\geq 3.5t$
IQR	Interquartile range, specified by the 25 th and 75 th percentiles of a distribution
KSI	Killed or Seriously Injured
MBAIS	Maximum known AIS value, indicates the severity of the most serious injury in the crash disregarding injuries with unknown severity
NDD	Naturalistic Driving Data
NRD	Naturalistic Riding Data
OP	Occupant Protection
PC	Passenger Car
PTW	Powered Two-Wheeler



T	Task within SAFE-UP (e.g., T2.1 denotes SAFE-UP task 2.1)
VRU	Vulnerable Road User – applied to pedestrians, cyclists and PTW riders
WP	Work Package within SAFE-UP (e.g., WP2 denotes SAFE-UP work package 2)



1. Introduction

The SAFE-UP project aims to improve traffic safety by proactively addressing the safety challenges of future mobility systems. Therefore, one of the main goals of the SAFE-UP project is to identify future safety-critical scenarios and develop new safety technologies and assessment methods accordingly. An essential element in the description of the expected future road traffic is an increasingly widespread introduction of Automated Vehicles (AVs) on the roads. These vehicles are expected to co-exist with traditional vehicles for an extended period and, over the time, comprise an increasing percentage of all vehicles on the roads. The appearance of AVs is likely to change the traffic in various ways.

For example, if AVs are designed to conform to traffic rules, they will not initiate a road crash by a violation of these rules. Additionally, AVs may help avoiding crashes related to human errors that have been identified to contribute to a large portion of crashes. On the other hand, the introduction of AVs in the current traffic landscape could potentially generate safety-critical situations that are AV-specific and may not be present in today's traffic. Overall, it is reasonable to expect that a widespread fleet penetration of AVs will change both the absolute number of road crashes and the distribution of various crash types and will potentially introduce new safety-critical situations.

Forecasting future traffic safety is a very challenging task. The results of the analysis will always depend on the assumptions made and their accuracy depends on different factors. Recent research projects (e.g., the EU project OSCCAR, see Dobberstein, Lich, & Schmidt (2019)) found that an analysis of current crash data has limitations that cannot be overcome by purely relying on the analysis of crash data sources. Therefore, the approach taken by the SAFE-UP project includes traffic simulation which will indicate our best estimate regarding future safety-critical traffic scenarios. The development and adaptation of the traffic simulation tools, and the analysis of results will be performed in tasks T2.2 – T2.5, while the work on the development of safety systems and their evaluation will be dealt with in WP3-WP5.

The aim of this deliverable, reporting the work performed in SAFE-UP task T2.1, is to specify scenarios to be considered for simulation studies and physical testing, based on crash data, naturalistic driving data and other available information. Relevant approaches, data sets and results are identified by a literature review. In particular, the literature review concerning crashes with the involvement of Vulnerable Road Users (VRUs) quantifies the amount of traffic fatalities of different VRU groups (e.g., pedestrians and cyclists) worldwide, as well as more detailed characteristics of fatal VRU-related crashes in the USA, in the EU, and in Germany. As the SAFE-UP project aims to develop safety systems that work in all weather conditions including rain and snow, further results from the research literature are reviewed for an understanding of the influence of precipitation on road crashes. Additional literature review regarding safety measures for both safety-critical and non-critical situations was performed in T2.1. The corresponding results were perfectly aligned with the topic of SAFE-



UP deliverable D2.5 (Adjenughwure, Huertas-Leyva, Prinz, Tejada, & Wang, 2021), hence they were reported in that document.

As the main result in this deliverable, initial safety-critical scenarios are identified, so that other work packages investigating active and passive safety systems can start working with them. The initial safety-critical scenarios reflect the most relevant safety-critical scenarios (e.g., most frequent crash scenarios overall and with serious or fatal consequences) for the protection of VRUs as well as for occupants of modern passenger cars (registration year 2000 or later); see section 1.1 for further details. These scenarios reflect current traffic safety issues. Results described in this deliverable will be further investigated in traffic simulation (in SAFE-UP tasks 2.2 - 2.5).

1.1 Future view of current safety-critical scenarios

In line with the SAFE-UP project focus and the requirements of the various work packages that need input, this report describes existing crash scenarios from the viewpoint of a passenger car (ego vehicle) and taking all traffic participants into account as possible opponents to the passenger car. In particular, the scope of analysis ranges from situations with high risk for ego occupants (e.g., in car-to-car and car-to-HGV crashes) to scenarios with limited injury risk for occupants of the ego vehicle but high injury risk for the opponent (e.g., car-to-VRU conflicts); see Figure 1. A more detailed graphical representation of the role of task 2.1 is available in Nugent & Bálint (2021).

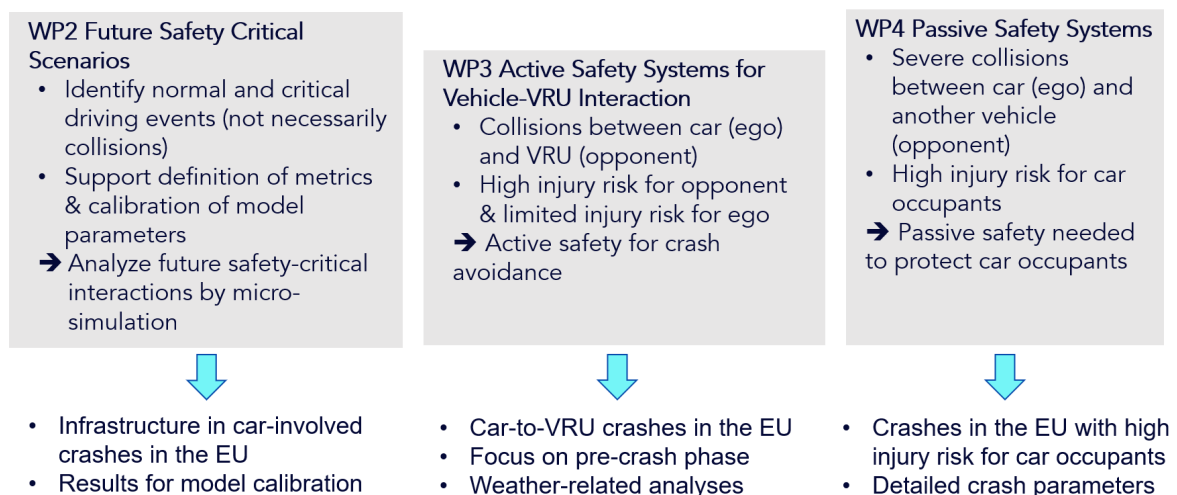


Figure 1 The role of T2.1 in supporting other SAFE-UP tasks

In SAFE-UP, in order to prevent serious injuries and fatalities, different safety systems are going to be evaluated. Regarding injuries and fatalities related to car occupants, the project evaluates potential occupant restraint systems for in-crash protection, while for injuries and fatalities related to VRUs, active safety systems and infrastructure-based or on-user warning systems are considered. These considerations guide the analysis so that the analysis of car-

to-vehicle crashes is focused on the crash configuration at the moment of collision while the analysis of car-to-VRU crashes is focused on the last seconds before the collision. In the latter case, aspects related to adverse weather conditions are relevant for the work on improved sensing algorithms, while crash causation and the role of infrastructure are relevant input to infrastructure-based and on-user warning systems.

In T2.1, an extensive analysis of road crash data from all EU countries in the EU community database on road accidents (CARE) database was conducted to obtain a general overview of car occupant injuries and fatalities. This analysis has identified the relevance of occupant restraint systems in both car-to-car and car-to-HGV crashes and analyzed the most frequently occurring crash types for each case. Various assumptions have been investigated to identify those scenarios in which occupants of cars with automated driving functions are expected to need protection. These aspects have contributed to the definition of occupant use cases described in deliverable D4.1, which includes a description of these analysis steps. The corresponding analysis is briefly summarized and extended in this deliverable.

A similar analysis of CARE data has provided general statistics on car-to-VRU crashes in the EU. As CARE provides police-reported information on all road crashes in the EU with personal injury, the corresponding analysis results give a good representation of the crash situation in Europe. As a first step, the relationship of the location of crashes to junctions was investigated, to facilitate appropriate placement of infrastructure-based systems for VRU protection.

Additionally, various in-depth analyses have been performed to enable a deeper understanding of the main scenarios and trends on EU level identified in CARE. This step is essential for a more detailed understanding because the level of detail in CARE does not allow a sufficiently detailed characterization of the critical situations that is required for the assessment of safety systems. Specifically, crash configuration parameters such as vehicle speeds, angles, etc. were analyzed using data from the German In-Depth Accident Study (GIDAS) for an improved evaluation of possible car occupant restraint systems. The corresponding results have provided valuable insights for the project work on on-user warning systems.

Further analysis of GIDAS with more focus on vehicle-based active safety systems was performed to ensure that WP3 receives all relevant input, including the extraction of main parameters contributing to system specification and analyzing factors influencing different sensor principles. In a detailed analysis using this database, also the influence of adverse weather conditions to crash risk was investigated. Finally, one group of in-depth analyses was focused on pedestrian crashes in the German in-depth crash database GIDAS complemented by an analysis of near-crashes in naturalistic driving data sets (from the Automated Mobility Partnership (AMP) and the Joint Attention in Autonomous Driving (JAAD) projects), analyzing specifically the role of infrastructure and traffic rules in car-to-VRU scenarios.



1.2 New safety-critical scenarios in mixed traffic

The analyses described so far address the question of which existing issues in current traffic are expected to be relevant in the future. Additionally, SAFE-UP is also considering new safety-critical situations that could be relevant after an assumed introduction of AVs in traffic, and traffic simulations in WP2 are an essential tool for identifying such situations. Therefore, further T2.1 work will support the definition of metrics and calibration of model parameters that would allow WP2 to analyze future safety-critical interactions by micro-simulation. This requires an investigation of relevant parameter ranges in naturalistic driving data, and continuous discussion between WP2 partners to ensure that the relevant parameters are selected in the best way for the simulation needs. It was identified in T2.1 that two databases that could support the corresponding analysis are the naturalistic driving data based on the Scenario-Based Platform for the Inspection of Automated Driving Functions (SePIA, 2021) and the Traffic Accident Scenario Community (TASC) database (including pre-crash data reconstructed from police reports (Urban, Erbsmehl, Mallada, Puente Guillen, & Tanigushi, 2020; Urban, et al., 2020)). However, due to delays in gaining data access, this analysis is planned to be performed in T2.2, with the findings reported in deliverable D2.14



2. Literature review

This section reviews results about VRUs, starting with a worldwide perspective based on publications by the World Health Organization (WHO). Afterwards, the USA, Europe, and Germany are considered separately, to be able to identify the similarities and particularities of the respective areas. The literature-based results are extended with a few relevant results from SAFE-UP T2.1 analysis to give a more complete picture; the source of information is clearly indicated for each result.

Note that a literature review regarding car occupant protection was included in the SAFE-UP deliverable D4.1 (Odriozola, et al., 2021) and the research literature about surrogate measures of safety by TNO, IKA and other partners, was reviewed in deliverable D2.5 (Adjenughwure, Huertas-Leyva, Prinz, Tejada, & Wang, 2021).

2.1 VRU fatalities worldwide

According to the World Health Organization (WHO), the European percentage of cyclists and pedestrians killed in traffic crashes is above the global average (WHO, 2018). The high percentage of pedestrians killed in Africa (40%) and in the Eastern Mediterranean region with 34%, shown in Figure 2, are particularly noticeable. More than half of all people killed in traffic crashes are part of the group of vulnerable road users.

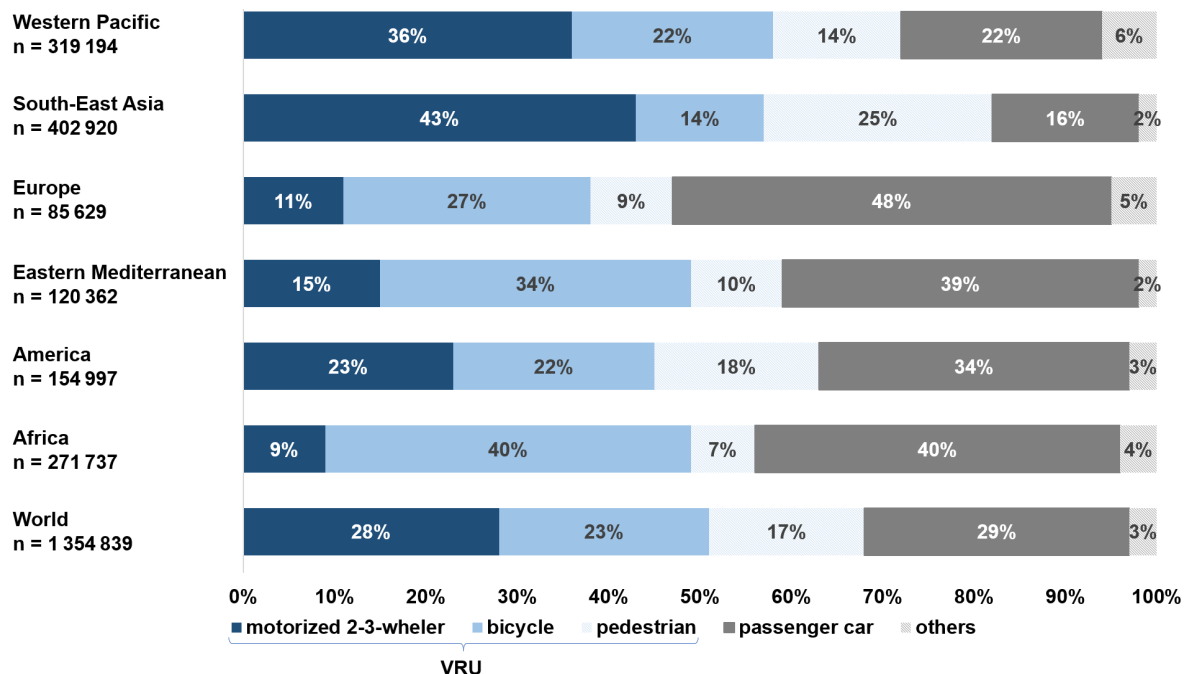


Figure 2 Distribution of fatalities by type of mobility mode, by WHO region (WHO, 2018)



More than half of the estimated 1.27 million road deaths in 2018 can be attributed to the group of VRUs. While improvements are emerging among vehicle occupants, no sufficient improvement has been achieved for VRUs yet. The lowest death rates are found in high-income countries such as the Netherlands, Sweden and the United Kingdom, while the highest fatality rates are found in Africa and the Eastern Mediterranean. Regarding the group of motorized two-wheelers, one of the main reasons for the high proportion of fatalities among this group can be traced back to the legal situation regarding helmet requirements. While helmets are compulsory in 90% of the countries, only 40% of the countries have laws related to the use of helmets for riders as well as passengers and standards for helmets (Sminkey, 2021).

More than 270 000 of the road users killed worldwide are pedestrians. Thus, they represent 22% of the total traffic fatalities. In terms of gender, men are overrepresented in this group. While senior citizens are at higher risk of having a fatal accident in high-income countries, younger people are more likely to die in a crash in low-income countries. About the location of the crash, differences between high- and low-income countries can also be identified. Pedestrian crashes in high-income countries predominantly take place in urban areas, while in medium- and low-income countries, those happen in rural areas, out of town. Most pedestrian crashes happen while pedestrians are crossing the street. Regarding the time of the day, there is worldwide tendency for pedestrian crashes to occur to a high percentage at night or at poor lighting conditions.

The first separate region considered is USA, which can be seen as a representative of a high-income country.

2.2 VRU fatalities in the USA

Data from the Fatality Analysis Reporting System (FARS) crash database (FARS, 2021) shows that while the number of road fatalities in the United States decreased by 14% in the period 2007-2016, the percentage of pedestrian deaths relative to the total of road fatalities is steadily increasing (+27%). The proportion of pedestrian deaths rose from 11% in 2007 to 16% in 2016 (as shown in Figure 3). According to Retting (2018), the number of states with a death rate of ≥ 2.0 per 100 000 inhabitants rose from 7 in 2014 to 15 in 2016 (based on data from the FARS database). The risk for pedestrians is particularly high at night. 75% of fatal pedestrian crashes nationwide occur in the dark (as of 2016). In 33% of the fatal pedestrian collisions there was a blood alcohol content $BAC \geq 0.08g/dL$ recorded for the pedestrian as well as 13% of the drivers. The top five cities with most pedestrian fatalities include New York, Los Angeles, Chicago, Houston, and Philadelphia. Four of the five cities mentioned show an increase in pedestrian deaths between 2015 and 2016.

In addition to pedestrian fatalities, data from the National Safety Council (NSC, 2021) shows that the number of fatalities of bicyclists increased by 6% in 2019 and 37% in the last 10



years, from 793 in 2010 to 1089 in 2019. However, the number of bicyclist injuries decreased by 40% from 515 861 in 2010 to 308 864 in 2019, with a rise of 7% from 2018 to 2019.

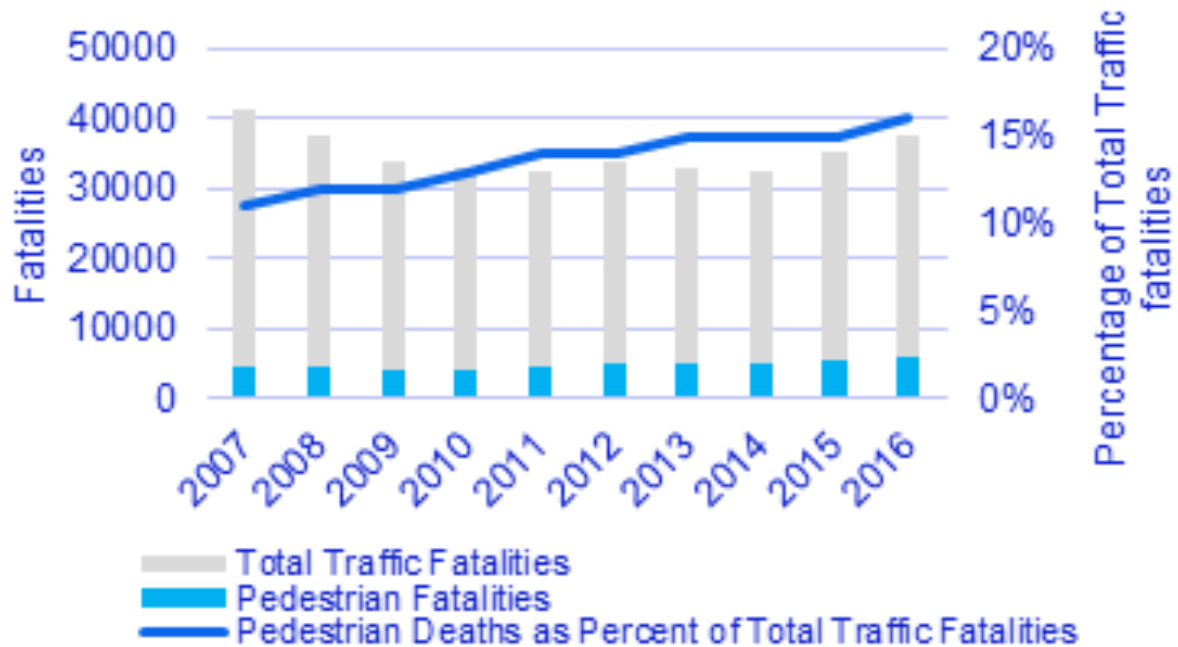


Figure 3 Pedestrian fatalities as a percentage of total traffic fatalities, 2007-2016 - Source: SAFE-UP T2.1 analysis in FARS

2.3 VRU fatalities in the EU

An analysis from Evgenikos et al. (2016) shows that in the European Union, 55% of fatal cycling crashes take place in urban areas, with large differences between the member states. While 80% of fatal cyclist crashes in Romania occur in urban areas, the percentage in Belgium is only about 40%. Germany represents the EU average share with 60% fatal cyclist crashes in urban areas. The same applies for the cyclist fatality rates per million population in Germany. In the USA, on the other hand, the proportion of 68% (NSC, 2021) is higher than the EU average (58%). Compared to other road users, cyclists have the largest proportion of fatal crashes in junctions, followed by motorized two-wheelers. The Netherlands with 63% and Denmark (58%) lead the statistics on the proportion of cyclists fatally injured in junction areas (as of 2013).

Data from a Eurostat article, based on data from the CARE database (Eurostat, 2021) shows that while the total number of fatally injured cyclists in the EU is decreasing, this value is stagnating in Germany; see Figure 4. Consequently, the percentage share of Germany has increased from 22.5% in 2000 to 27.2% in 2019.



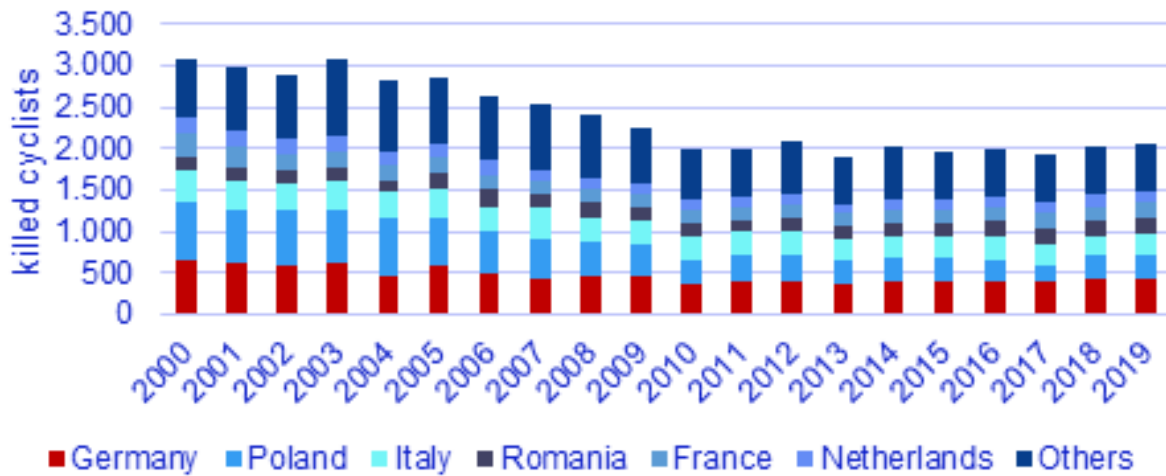


Figure 4 Cyclist fatalities in EU countries, 2000-2019. Source: Eurostat

According to the Eurostat data browser (Eurostat, 2021), around 4 800 pedestrians were killed in road crashes in the EU in 2018. These represent 20.7% of all traffic fatalities. However, these proportions vary greatly in the different member states from 8.4% in the Netherlands to 37% in Romania. The European average (EU-27 as of 2018) is 10.9 pedestrian fatalities and 4.3 cyclist fatalities per million inhabitants. Romania is particularly striking with 9.3 cyclists and 35.3 pedestrians. Latvia and Lithuania are also particularly noticeable with 25.8 and 28.8 killed pedestrians per one million inhabitants. In the Netherlands the number of killed cyclists is above average with 7.1 but the pedestrian fatality rate of 2.9 is below the EU average. Similarly, Germany has a slightly higher-than-average fatality rate for cyclists at 5.4 but a below-average rate of 5.6 for pedestrians. With 2.6 cyclist fatalities and 7.0 pedestrians per million inhabitants, France is below the European average for both VRU groups.

The Eurostat statistics by type of vehicle (Eurostat, 2021) show that in absolute terms, Germany has the highest annual number of cyclist fatalities (445), followed by Romania (220) and Italy (219). The number of fatal crashes including a bicycle in Estonia, Cyprus, Latvia, Luxembourg, Malta, Slovenia, Iceland, and Norway is below 10. For pedestrian fatalities, Poland has the highest number with 873, followed by Romania with 690 and Italy with 612. Germany ranks 6th with 464.

Further statistics from the Eurostat data browser (Eurostat, 2021) indicate that in the time interval from 2008-2018, a decrease of 30% road fatalities overall was achieved in the EU-27 countries, whereas only 15% was achieved within cyclists. At the same time, the number of passenger car occupants killed has decreased by 40%. Among the cyclists there are particularly strong decreases in Switzerland, Finland, and Latvia with reductions over 49%. In Germany only a change of -12% could be achieved, comparable with Italy (-14%), Romania (-16%) and Bulgaria (-11%).



Of the European countries, data from Germany is especially relevant, partly as the EU country with the largest population and, as pointed out above, because of its high absolute number of VRU fatalities. Additionally, in-depth data from Germany (from the GIDAS database) will be used as an essential part of the analysis in this report. Therefore, VRU fatalities in Germany will be described in the next section.

2.4 VRU crashes in Germany

In Germany, the overall number of road fatalities is decreasing, while the number of cyclist fatalities remains at a relatively constant level. This increases the percentage of this group in relation to the total number of road fatalities as shown in Figure 5.

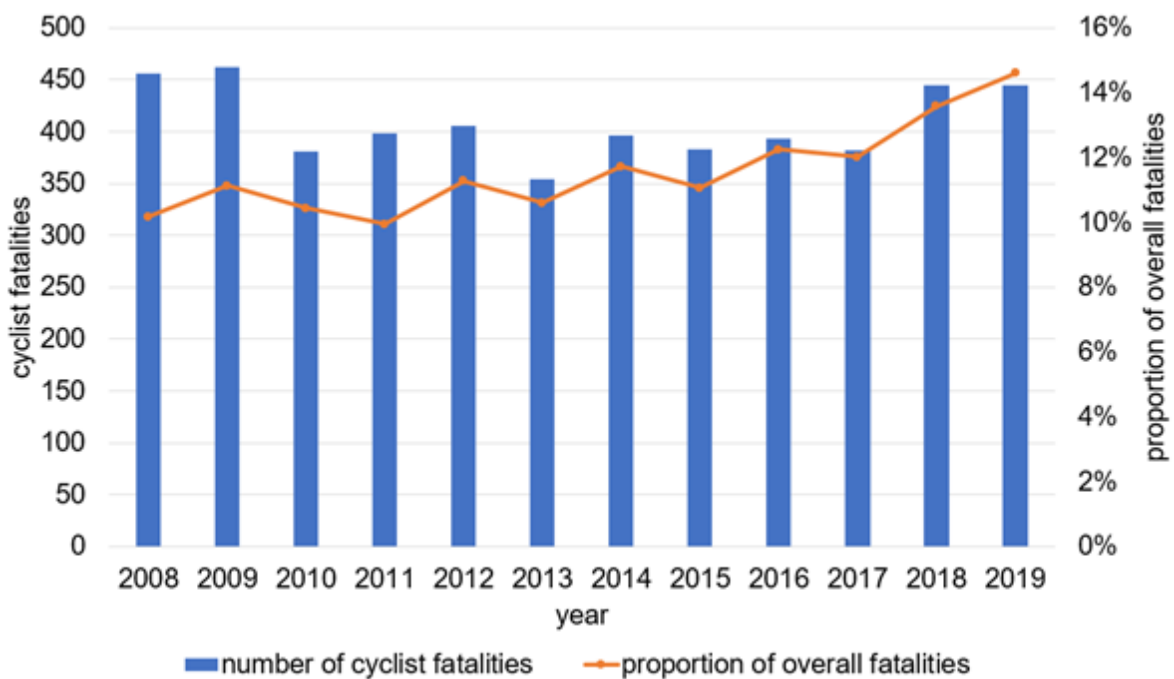


Figure 5 Cyclist fatalities in Germany 2008-2019 (Eurostat, 2021)

Among crashes with personal injury, the share of cyclist crashes is 17% and the share of pedestrian crashes is 6%. In crashes with fatalities, cyclists represent 19% whereas pedestrians represent 9%. A total of 87 253 bicycle crashes with injury were recorded in 2019. It is noticeable that 45.4% of the cyclists involved were classified as main causers of the crash. Passenger cars are the most frequent opponent of crashes for cyclists with a share of 75.3%. Table 1 shows the assessment of the main causer classification for injured and killed VRUs in crashes with cars, classified by injury severity and the location.



Table 1 Injured and killed VRUs in crashes with passenger cars by location and injury severity in Germany in 2019 (DESTATIS, 2020a)

Crash causation classification	Injury severity	Area type	Cyclists	Pedestrians
VRU as the main causer	Injured	Urban	11 033	4 680
		Rural	899	250
	Killed	Urban	45	55
		Rural	52	30
VRU as opponent of passenger car (Passenger car is main causer)	Injured	Urban	33 996	15 327
		Rural	2 304	595
	Killed	Urban	40	125
		Rural	35	35

Further statistics from the German Federal Statistical Office (DESTATIS, 2020a) indicate that 33.4% of all injured road users and 34.5% of all road fatalities in 2019 were users of motorcycles or bicycles (129 207 in total) of which 68% consist of bicyclists including riders of pedelecs (i.e., electric cycles). The proportion of people in the oldest age group (65+ years) among the killed cyclists (including pedelec riders) is particularly high. According to a report by the German Federal Ministry of Transport and Digital Infrastructure (Infas, 2019), during the period from 2002 to 2017, the share of trips by bicycle per day remained fairly constant (25% in 2002 and 28% in 2017) while the number of kilometers traveled rose sharply from 82 to 112 million per day. This increase in exposure was coupled with an increase in the number of cyclists involved in crashes: according to DESTATIS, a doubling from 1999 (7 902) to 2019 (15 560) can be observed here (DESTATIS, 2020a). However, the number of bicycles has decreased during this period – 74.1 million in 1999 compared to 68.3 million in 2019.

Further statistics from the German Federal Statistical Office (DESTATIS, 2021a; DESTATIS, 2021b; DESTATIS, 2021c; DESTATIS, 2020a) show that the number of injured cyclists increased by 15.7% between 2017 and 2020 and an increase of 11.5% was recorded in the number of cyclists killed over the same period. Fatal crashes involving cyclists occur predominantly in the summer months from May to September and primarily during the week.

On the other hand, fatal pedestrian crashes occur primarily in the winter months from November to January. Over 50% of fatal pedestrian crashes occur in the dark.

It is noticeable that 2.5% of all participants of crashes with injury were under the influence of alcohol. More than 80% among these people were passenger car drivers (51.3%) and cyclists (31.2%) (DESTATIS, 2020b).



2.5 Influence of precipitation on road crashes

As the focus of the analysis in section 4.3.4 is to analyze car-to-VRU crashes in adverse weather conditions, a literature review on the influence of precipitation on the occurrence of crashes was conducted.

For identifying the influence of variables on the crash frequency, the relative risk is often considered. This value shows to which extent the risk of a crash changes under a certain condition. A value less than one implies that the risk of a crash is lower under the given condition, and a value greater than one that the risk of a crash is higher. If the value is equal to one, the crash risk remains unchanged despite the condition.

In Stevens, Schreck, Saha, & Bell (2019), they analyze 125 012 fatal crash data from the US were analyzed and it was found that the relative risk of a fatal crash during precipitation is on average 1.34, which means that the probability of a fatal crash increases by 34% due to precipitation. While the relative risk of a fatal crash during night hours is around 1.0 despite precipitation and therefore no increased risk is assumed, it reaches the highest value of 1.6 in morning rush hour traffic. In addition, it was concluded that the precipitation amount has a significant influence on the relative risk of a fatal crash. For example, a value of 1.29 on average for light rain and a value of 2.46 for heavy rain was reported. In the analysis by Andrey, Mills, Leathy, & Suggett (2003) where crashes in six Canadian cities over a four-year period were investigated, it is stated that the relative risk of a road crash under precipitation is 1.75 and the relative risk of an injury within a crash under precipitation is 1.45.

The results of the EU-project DENSE, in which the French crash database BAAC and the European crash database CARE were analyzed, show that the crash frequency increases under rain in comparison to dry weather and that snow, hail, and freezing rain are more often connected with more severe crashes (DENSE, 2017b). Additionally, the project also found that rain in combination with darkness leads to more frequent and more severe crashes.

Overall, it can be concluded that precipitation has an influence on the occurrence of crashes and leads to an increased risk of crashes.



3. Method and data

The analysis methods for the relevant studies and the corresponding data sources are described in this section.

3.1 Method

The method for selecting the most relevant use cases is based on an analysis of real-world data, to ensure the relevance of results for EU traffic. In line with the project objectives, results relevant for active safety systems for the protection of vulnerable road users in car-to-VRU crashes and those for car occupant protection by passive safety systems are required, see below. The analysis is based on data from several sources, including police-reported crash data on EU-level and in-depth crash data, as well as naturalistic driving data; see the description of the corresponding databases in sections 3.2-3.3.

3.1.1 Vulnerable road users

Car-to-VRU crashes are considered to identify and characterize the most common scenarios including vulnerable road users. Active safety systems aimed at preventing or mitigating car-to-pedestrian and car-to-bicycle crashes will be developed in the project. The analysis described here also includes car-to-PTW crashes, for completeness. To assess whether an active safety system can possibly support crash avoidance, a description of the position and kinematic parameters of the participants a few seconds before the crash (pre-crash data analysis) will be provided for car-to-VRU crashes.

Special attention is paid to crashes occurring in weather conditions that can adversely affect sensor performance (i.e., rain, snow, and fog). Therefore, besides the most common scenarios, the ones with the largest prevalence of adverse weather conditions are also identified.

3.1.2 Car occupants

Car occupant injuries and fatalities are analyzed to identify the scenarios in which occupants of AVs in the near future will require additional protection.

Different occupant restraint systems will be evaluated in such scenarios in the project, to understand the best ways to protect occupants of future vehicles. Such safety systems are meant to provide protection in the case that a crash occurs, and relevant parameters for the analysis include kinematic parameters and the crash configuration (described in terms of angles) at the moment of crash.

The use cases for the protection of car occupants have been extensively described in SAFE-UP deliverable D4.1 (Odriozola, et al., 2021). Therefore, a summary of the corresponding



results is provided in this report, together with the description of further details that were not included in D4.1 but are relevant for a general understanding of crashes including car occupants. The use cases in D4.1 include the crash type based on police-reported data, and further details were not available at the time of writing that report. Such details, including vehicle speeds and angles, are provided in the current report.

3.2 Crash databases

The main data source used for the analysis described in this report are crash databases, containing information about real-world crashes. In the EU, all crashes of sufficient severity (i.e., those with personal injury or, in some countries, with property damage) occurring on public roads are investigated by the police. Consequently, analyzing police-reported crash data provides a good characterization of road crashes in the EU. However, police-reported data has a limited level of detail that does not suffice to analyze all requirements of safety system development and evaluation. Therefore, various crash databases have been included in the analysis, including both police-reported data and in-depth crash data; see below.

3.2.1 Community Accident Database (CARE)

CARE is a database that contains information about every road crash with a personal injury reported by the police from all EU and European Free Trade Association (EFTA) countries, as well as the United Kingdom (CARE, 2021). Data collected by the police in the different countries, using different data collection methods, are re-coded to the data format used in CARE, called the Common Accident Data Set (CADaS). The corresponding variables are described in a publicly available document, called the CADaS glossary (CADaS, 2021). In this document, each variable in CARE is defined and classified to have high reliability (H) or low reliability (L).

The aim with the CARE analysis was the identification of current and future traffic safety issues, and for this purpose, it is relevant to analyze the most recent data year reported to CARE. However, the latest reported data year differs by country, and it was deemed important to choose a year for which almost all countries have data available to ensure the representativeness of results on EU level. At the time of performing most CARE-related analyses (late 2020), the data year for which data from all EU countries except Ireland were available was crash year 2018, which was therefore used in all CARE-related analysis described in this report. For Ireland, data from 2016, which is the latest available crash year at the time of analysis, was used. Note that although the United Kingdom (UK) was an EU country in 2018, data from the UK are excluded from EU-level results, to ensure that the results are most relevant for the current EU countries. Consequently, in this report, EU will be used to denote the EU countries in 2021, even when presenting EU level results from 2018.



3.2.2 German In-Depth Accident Study (GIDAS)

The recording of the road crashes by the police and preparation of the crash report aims to identify the main perpetrator and clarify the question of guiltiness. A sound foundation research in vehicle safety requires detailed, so-called in-depth crash investigations. Crash research teams collect a large amount of data and information about the crash itself, the people and vehicles involved as well as the environment. This is done directly at the scene of the crash or immediately after the crash. The data collection for German In-Depth Accident Study (GIDAS) is carried out by the Hannover Medical School and Technische Universität Dresden in the regions of Hannover and Dresden which are meant to have a good representation of Germany as the selected areas cover urban, rural and highway environment. The survey criteria are given in Table 2 below.

At both locations, survey teams consisting of technicians and physicians are alerted together with rescue forces and police. The scope of the survey includes information about persons, vehicles and the environment around the crash scene, as follows.

- Person-related information in the GIDAS survey:
 - Survey of the persons involved about person-specific information and possible courses of the crash;
 - Collision points of occupants or other road users;
 - Injuries, cause and severity of the injury;
 - Preclinical and clinical care.
- Vehicle-related information:
 - Technical data of the vehicle as well as equipment;
 - Deformations and damage to the vehicle;
 - Collision opponents and collision objects.
- Environment-related information:
 - Environmental conditions such as weather and lighting conditions;
 - Road design and traffic control;
 - Structural features;
 - Road conditions;
 - Crash sequence with sketch.

With the existing consent of the parties involved, epi-crises, rescue protocols, road crash reports by the police as well as through discussions with police, rescue workers, doctors and nursing staff additional information is obtained. Subsequently, during the reconstruction of traffic crashes, the entire course of the crash is analyzed, from the initiation of the crash to the reaction of the participants up to the final position of the vehicles. In this case,



characteristic variables such as brake decelerations, initial or collision speeds as well as angular changes are reconstructed using the computer software PC-Crash. A subset of this database contains the kinematic information of the pre-crash phase, including trajectories and speed information from the initiation of the conflict situation, through the actual collision and up to the final position of the participants involved, in the so called GIDAS-PCM database. Based on information from the crash reconstruction, the pre-crash phase is described up to TTC=5 seconds before the collision and stored as a pre-crash matrix format (PCM). It contains information on static objects, visual obstacles, the infrastructure, and the movements of participants involved in the crash.

Table 2 Survey criteria for GIDAS

Sampling description	Team Dresden	Team Hanover
Radius of sampling	35 km – 40 km	30 km – 35 km
Inhabitants in sampling area	~1.0 million	~1.2 million
Size of sampling area	~3 000 km ²	~2 289 km ²
Geographical features	Lowlands and mountain ranges up to 700 m	Flat terrain
Duration of sampling, week 1	0-6 am and 12-6 pm	0-6 am and 12-6 pm
Duration of sampling, week 2	6 am-12 pm and 6 pm-0 am	6 am-12 pm and 6 pm-0 am

3.2.3 Initiative for the Global harmonization of Accident Data (IGLAD)

The database compiled in the Initiative for Global Harmonization of In-depth Data project, called the IGLAD database, contains in-depth crash data from more than 10 countries worldwide, including several EU countries. IGLAD does not have an own data collection process but rather crash data collected by established data collection projects are re-coded to the IGLAD scheme to obtain a harmonized database with comparable data from different countries. The IGLAD codebook, available online from the IGLAD webpage (IGLAD, 2021), includes the description of all variables (123 variables describing information on crash level, participant level, vehicle occupants and safety systems). The data used in the analysis described in section 4.4 is the IGLAD data release from 2021, contains more than 7 000 crashes in total of which more than 3 000 are from EU countries.

3.3 Naturalistic driving data

Naturalistic driving data (NDD) includes time series data (typically also video recordings) of road users participating in real-world traffic. The corresponding cameras and sensors may



be placed in vehicles and/or the environment, and data recording is performed continuously during a trip or during a given time period. The recorded traffic may thereby include all possible levels of criticality, from normal everyday traffic to safety-critical events, potentially including crashes. NDD may thereby be an essential data source for understanding road user behavior in safety-critical and non-critical situations.

3.3.1 Joint Attention in Autonomous Driving (JAAD)

The naturalistic driving database JAAD – Joint Attention in Autonomous Driving, (JAAD, 2021) – was established for the study of pedestrian and driver behaviors in the context of automated driving. JAAD consists of 346 annotated video clips, 5 - 10 s long, derived from 240 hours of driving; see Figure 6 below. The videos have been recorded in locations of North America and Eastern Europe. The data shall offer insights into everyday driving in urban environment which includes also different weather conditions. The purpose of the database was to study the interactions between pedestrians and the vehicle/driver and involves normal driving conditions. The database does not include conflict or collision situations.

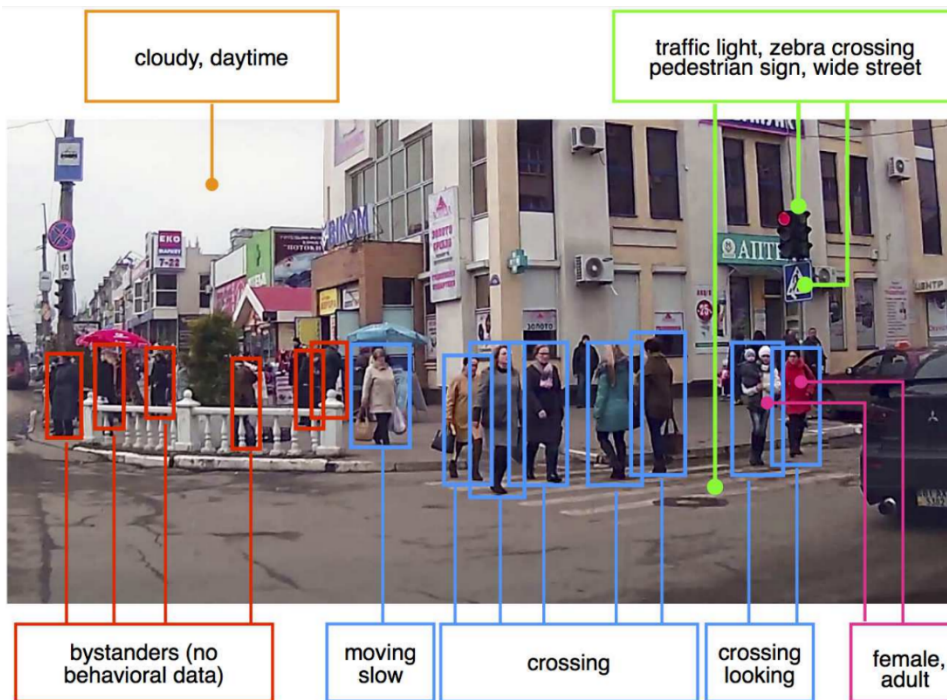


Figure 6 Data in JAAD (Rasouli, Kotseruba, & Tsotsos, 2017)

The database provides a wide variety of traffic scenarios involving VRUs, but it is limited in terms of representativeness due to its small sample size.



3.3.2 Automated Mobility Partnership (AMP)

The Automated Mobility Partnership (AMP) lead by Virginia Tech Transportation Institute (VTTI) provides members with access to variety of real-world driving data from the US and a suite of supporting tools for the development and evaluation of automated driving technologies. The data and tools are provided through a web portal. The AMP Portal is based on 36.7 million miles of extensive naturalistic driving data, including vehicles equipped with advanced driver-assistance systems, which provides true driving behavior and performance. This is characterised by a rich amount of datapoints including information about the driver, vehicle status and dynamics in all relevant driving scenarios. It results in a rich database for subsequent analysis of scenarios for development of automated driving and safety functions. The database currently contains about 60 000 cases which includes approximately 7 000 near crash and approximately 1 000 crash scenarios.

Based on the specific research question, the portal database can be used to filter the scenarios with different filter parameters such as infrastructure, daytime / night, involved traffic, presence of VRUs etc. The different AMP scenarios can be replayed for visualization or provided in different simulation formats for function development.



4. Results

The results from T2.1 are described here, starting with general crash statistics on EU level indicating the number of crash participants in crashes in Europe as well as the most common times-of-the-day when crashes happen. This provides input to traffic simulations; in particular, the time of the day can then be linked to traffic flow-related data to conclude the relevant extent of traffic flow to be simulated in the Aimsun Next traffic simulation in WP2. Afterwards, fatalities and injuries of car occupants are analyzed, in a future-oriented study aimed at identifying the most relevant crash scenarios in which occupants of AD vehicles are expected to need protection by occupant restraint systems (WP4). Finally, car-to-VRU crashes are analyzed – the purpose with this analysis is to study the crash avoidance potential of active safety systems as well as systems based on Cooperative Intelligent Transport Systems (e.g., systems utilizing potential connection of vehicles and/or VRUs).

Analyses of GIDAS are performed to identify injured road users considering all injury levels as well as killed or seriously injured (KSI) road users. Fatalities as a separate category are only used in the CARE-based analyses, because of the limited number of fatalities in GIDAS.

4.1 General crash statistics in the EU

This section provides general statistics about casualties in road crashes in the EU. As indicated in section 3.2.1, the results refer to crash year 2018 (with data from 2016 used for Ireland) and EU means the current EU countries in 2021, hence results from the United Kingdom are excluded from the EU statistics.

The next tables provide an overview of the number of road users injured or killed in car-involved crashes in 2018 in the EU in different areas, as classified by the variable R-X in the CADaS glossary (CADaS, 2021).

Table 3 below shows that there were about 1 million road users in the EU who were non-fatally injured in car-involved crashes, with the largest groups being car occupants in urban areas (33%), car occupants in rural areas (23%), cyclists and pedestrians in urban areas (9% each), car occupants on motorways (8%) and motorcycle riders in urban areas (7%).

Table 4 indicates that of the 17 119 fatalities in car-involved crashes in the EU in 2018, the three largest groups are car occupants in rural areas (41%), pedestrians in urban areas (13%), car occupants in urban areas (13%), followed by car occupants on motorways (6%), motorcyclists in rural areas (5%), pedestrians in rural areas (5%) motorcyclists in urban areas (4%), cyclists in urban areas (3%) and cyclists in rural areas (3%).



Table 3 Number of non-fatally injured road users in car-involved crashes in the EU in 2018 by road user type and area type

Type of road user	All	Urban	Rural	Motorway
Car occupants	649 016	336 139	234 617	77 854
HGV occupants	3 188	880	1 355	953
LGV occupants	17 566	8 049	6 412	3 099
Cyclists	98 247	88 345	9 663	109
Pedestrians	94 633	89 848	4 434	285
Motorcycle riders	91 453	71 976	15 788	3 681
Moped riders	34 746	30 446	4 185	80
Bus occupants	8 404	6 921	1 210	272
Other	4 778	3 410	1 247	121
Unknown	5 667	2 775	1 887	974
Total	1 007 698	638 789	280 798	87 428

For creating simulations within SAFE-UP, it is important to know the time period when the corresponding crashes occur to cover the times of the day in the simulation when safety-critical situations may be expected. Figure 7 provides this information for all injury crashes in urban areas with the involvement of exactly two traffic participants of which at least one is a passenger car, while Figure 8 addresses fatal crashes. The names of the columns indicate the traffic participants in the crash: C2P refers to car-to-pedestrian crashes, C2B refers to car-to-bicycle crashes, etc. The analyzed sample size, i.e., the number of corresponding crashes in the EU in 2018, is specified between parentheses. Corresponding figures for car-involved crashes in rural areas and car-involved crashes on motorways are provided in the Appendix.

It is visible from the figures that all time periods considered have non-negligible shares of crashes. In particular, while night-time crashes have lower shares in general, they are relevant for car-to-pedestrian crashes of all levels and have higher proportions for each group among fatal crashes (compared to their share among crashes of all injury severity levels).



Table 4 Fatalities in car-involved crashes in the EU in 2018 by road user type and area type

Type of road user	All	Urban	Rural	Motorway
Car occupants	10 349	2 225	7 066	1 056
HGV occupants	83	7	27	49
LGV occupants	166	31	98	37
Cyclists	1 006	527	474	4
Pedestrians	3 283	2 303	833	147
Motorcycle riders	1 651	647	926	77
Moped riders	319	146	169	4
Bus occupants	31	13	11	7
Other	126	47	74	5
Unknown	105	23	32	50
Total	17 119	5 969	9 710	1 436

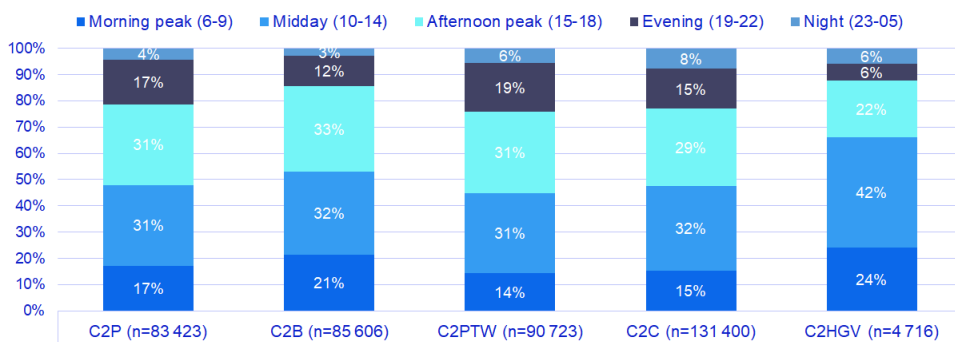


Figure 7 Time-of-the-day distribution of car-involved crashes of any injury level in urban areas in the EU in 2018

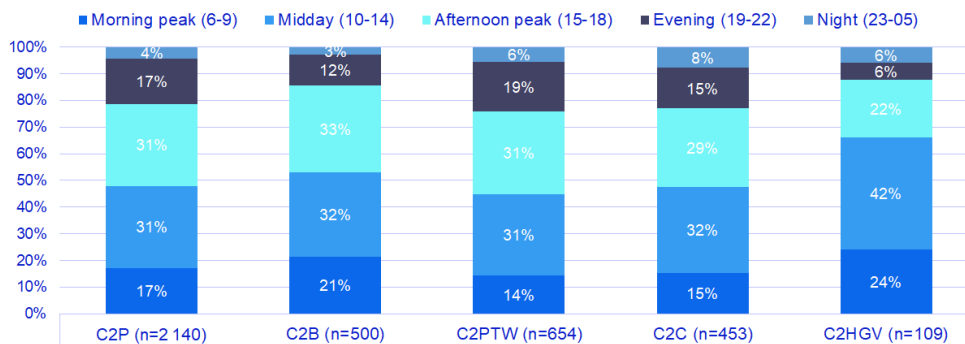


Figure 8 Time-of-the-day distribution of fatal car-involved crashes in urban areas in the EU in 2018



One focus area of the SAFE-UP project is to improve safety in adverse weather conditions. Table 5 indicates the prevalence of different weather conditions in car-to-pedestrian crashes of various severities.

Table 5 Weather conditions in car-to-pedestrian crashes in urban areas in the EU in 2018

Weather condition	All injury crashes (n= 60 454)	KSI crashes (n = 12 556)	Fatal crashes (n=1 925)
Dry / Clear	80%	78%	79%
Fog, Mist, Smoke	1%	1%	1%
Other	4%	6%	6%
Rain	13%	13%	13%
Severe winds	0%	0%	0%
Sleet, Hail	0%	0%	0%
Snow	1%	2%	1%
Snow or Sleet, Hail	0%	0%	0%
Sample size	60 454	12 556	1 925

Similar statistics for car-to-bicycle crashes are provided in Table 6 below.

Table 6 Weather conditions in car-to-bicycle crashes in urban areas in the EU in 2018

Weather condition	All injury crashes (n= 60 454)	KSI crashes (n = 12 556)	Fatal crashes (n=1 925)
Dry / Clear	80%	78%	79%
Fog, Mist, Smoke	1%	1%	1%
Other	4%	6%	6%
Rain	13%	13%	13%
Severe winds	0%	0%	0%
Sleet, Hail	0%	0%	0%
Snow	1%	2%	1%
Snow or Sleet, Hail	0%	0%	0%
Sample size	60 454	12 556	1 925



For infrastructure-based systems, e.g., those relevant to Demonstrator 4, it is also important to know the relation to junction in car-to-VRU crashes. Figure 9 indicates this for urban car-to-pedestrian crashes. In particular, the results show that car-to-pedestrian crashes in urban areas, especially those leading to higher injury severity or fatality, occur primarily away from junctions.

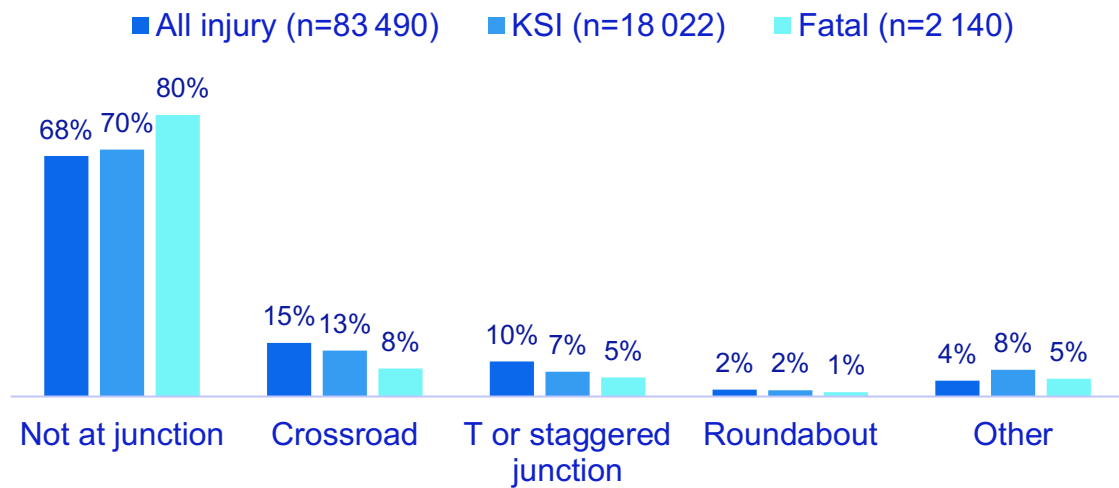


Figure 9 Relation to infrastructure in car-to-pedestrian crashes in urban areas in the EU in 2018

Similar statistics for cyclists, see Figure 10 below, lead to a different conclusion. Most urban car-to-bicycle crashes happen at a junction which can be a crossroad, T or staggered junction, or roundabout (i.e., circular junction). Note, however, that slightly more than half of fatal car-to-bicycle crashes in urban areas happen away from junctions.

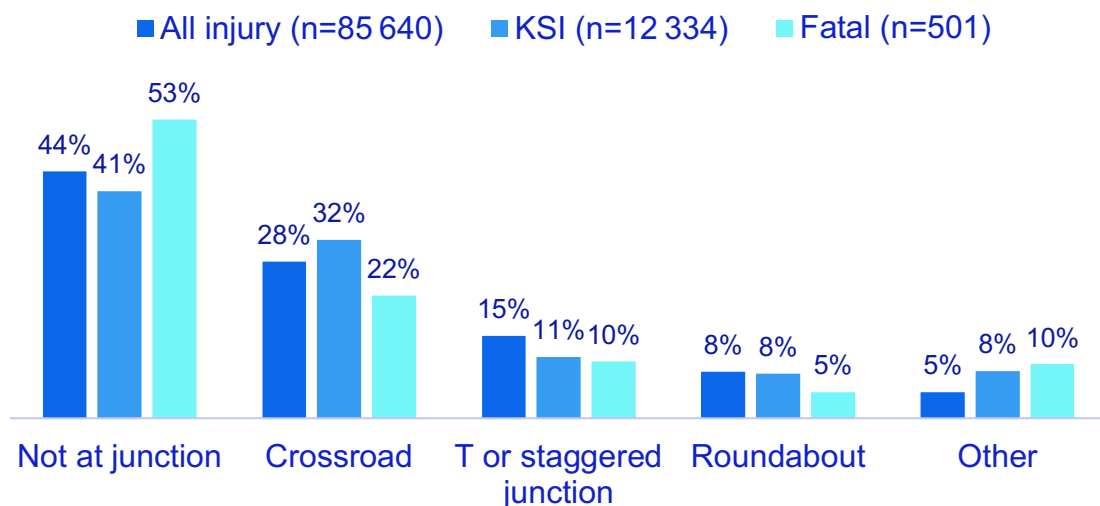


Figure 10 Relation to infrastructure in car-to-bicycle crashes in urban areas in the EU in 2018



An analysis of relation to junctions can also be affected by the weather conditions. In particular, analysis of CARE indicates that the percentage of crashes in junctions increases when bad weather conditions are considered, both for pedestrians (Figure 11) and for cyclists (Figure 12).

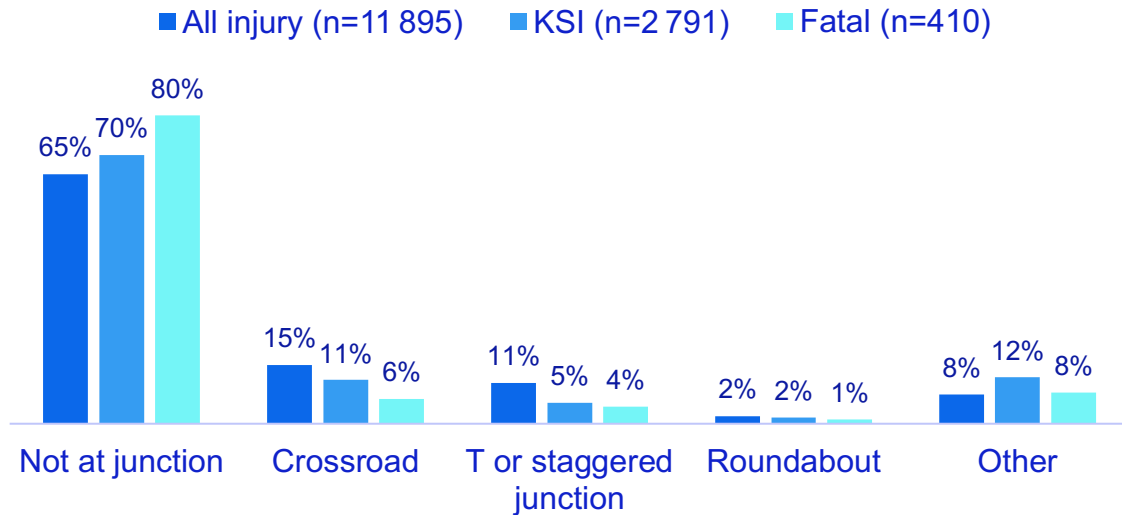


Figure 11 Relation to infrastructure in car-to-pedestrian crashes in urban areas in the EU in 2018 in adverse weather conditions

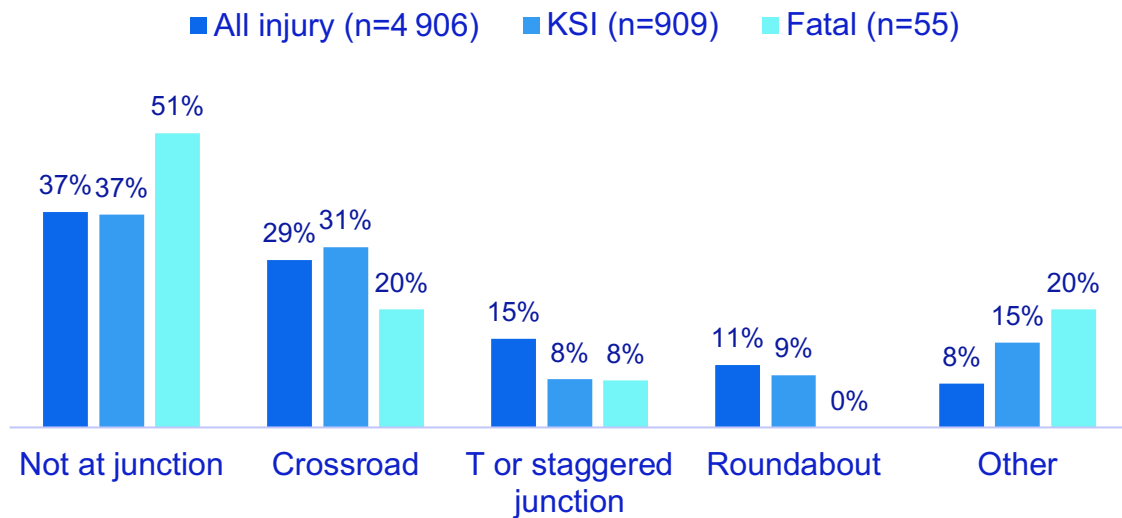


Figure 12 Relation to infrastructure in car-to-bicycle crashes in urban areas in the EU in 2018 in adverse weather conditions

These EU-level statistics guide the scope for further in-depth analysis of crashes. The relation to infrastructure is used in Section 4.3.1. Additionally, for car occupants, Section 4.2.1 describes how CARE-based statistics helped to derive the use cases to be addressed in WP4.



4.2 Car occupants

This section briefly summarizes how occupant use cases in SAFE-UP D4.1 (Odriozola, et al., 2021) were derived from crash data analysis in CARE and describes further details of the selected use cases based on GIDAS analysis.

4.2.1 Selecting occupant use cases by CARE analysis

The main research question stated in SAFE-UP D4.1 (Odriozola, et al., 2021) related to the work in this report is as follows: “Which crash configurations would L3 (in both manual and automated driving modes) and L4 cars be exposed to in mixed traffic?” The complete answer to this question will require the traffic simulation work conducted in tasks T2.2-T2.5. However, an initial answer can be given based on analysis of crash data and expert assessment, aided by an extensive literature review.

Due to the timing of the project tasks, the first part of the crash data analysis based on CARE data was already reported in SAFE-UP D4.1, hence this part will only be summarized here. For an initial answer regarding the crash population of future vehicles, crashes in the EU leading to fatalities in modern cars (with registration year 2000 or later) were analyzed in CARE. This analysis revealed that there were 6 431 fatalities in modern cars in the EU in 2018 (Table 1 in SAFE-UP D4.1).

The first step in the analysis, illustrated in Figure 13 below, was the specification of a target population that could be relevant for future vehicles and potentially feasible to address. Future-oriented considerations excluded single-vehicle crashes from the analysis because future cars are expected to avoid essentially all single vehicle crashes (Dobberstein, Lich, & Schmidt, 2019; Fahrenkrog, et al., 2019). Addressing crashes with the involvement of at least 3 vehicles was judged too complex. Therefore, further analysis addressed those crashes with exactly two vehicles, and Table 2 in SAFE-UP D4.1 revealed that the most common crash opponents in such crashes are passenger cars, heavy goods vehicles (HGVs) with a gross weight $\geq 3.5t$ and light goods vehicles (LGVs) with a gross weight $< 3.5t$. Besides car-to-car crashes (C2C), crashes between a car and an HGV or road tractor (C2HGV crashes) were analyzed further. Finally, crashes with parking vehicles were excluded, based on the same future-oriented considerations that were used to exclude single vehicle crashes. This process led to the identification of a target population for the analysis, including 2 085 fatalities in modern cars.

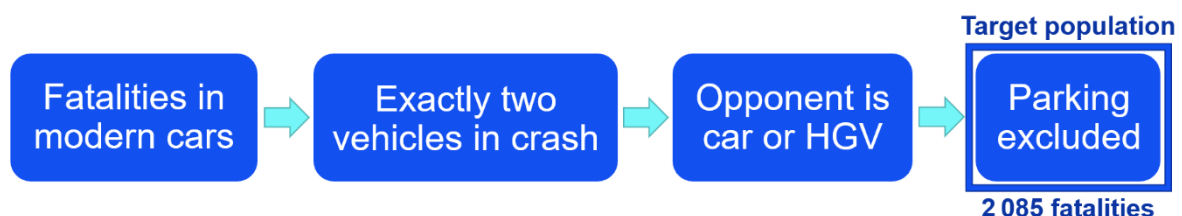


Figure 13 Defining the target population for protecting future car occupants



The crashes in the target population were further analyzed based on the general focus for the SAFE-UP project proposal which indicated that car occupant protection would be mainly considered in peri-urban conditions and on motorways. The area classification used in CARE data (CADaS variable R-X (CADaS, 2021)) defines urban areas, rural areas, and motorways. It was decided that crashes in rural areas and on motorways are considered in the analysis. Crashes in rural areas may have similar characteristics as crashes in peri-urban areas; additionally, as shown in Table 4, the large majority of car occupant fatalities occur in rural areas. As crashes close to junctions are generally different from those away from junctions, crashes were further split into those at a junction (more precisely, within 20m of a junction) and those not at a junction (using the classification in CADaS variable R-13). As crashes at junctions are not relevant for motorways, the next step was an analysis of the most common crash types in C2C and C2HGV crashes in rural areas at or away from a junction as well as those on motorways away from a junction; see Figure 14 below.

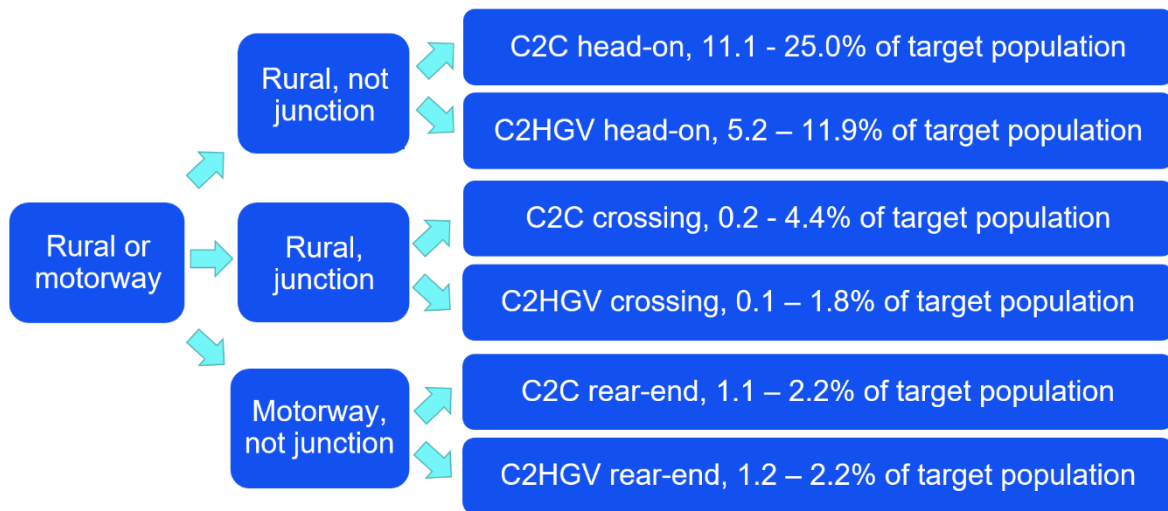


Figure 14 Crash scenarios for car occupant protection in SAFE-UP

The percentage intervals in Figure 14 indicate the shares of fatalities in the target population that occur in the given crash type. The reason why intervals are specified rather than a single value is the large number of unknown values in the crash type classification in CARE (which is the reason why the crash type-related variables are indicated to have low reliability in the CADaS glossary, see variables A8-A12 (CADaS, 2021)). The lower bounds indicate the share of the given crash type as a percentage of the total sample while the higher bounds indicate their share among cases with known crash types.

As indicated in SAFE-UP D4.1, there are various results in the literature regarding and experience from previous projects like OSCCAR about the C2C crashes, which allows the corresponding evaluation of occupant protection concepts. However, such results are not available for C2HGV crashes which were therefore further analyzed in the in-depth crash data from GIDAS (see section 3.2.2 for the description of the database). In particular, C2HGV head-on and C2HGV rear-end crashes were analyzed further in section 4.2.2 to define the most relevant crash configurations within these crash types.



4.2.2 In-depth analysis of occupant use cases based on GIDAS

Based on the CARE analysis regarding fatally injured passenger car occupants in modern vehicles, respected through the year of first registration of 2000 and later two main use cases for passenger car occupants in crashes with two participants had been derived. As opponent for passenger cars heavy goods vehicle above 3.5t (HGV>3.5t) had been identified in rural head-on collisions and in rear-end collisions on motorways (see 3.3.1). To parametrize simulations of passenger car occupant models input on a higher level of detail is necessary. Therefore, the In-Depth database GIDAS (German-In-Depth Accident Study) has been analyzed to identify necessary input for simulations in WP4.

The GIDAS dataset from June 2020 had been used. The following basic assumptions have led to the relevant dataset.

- Belted front row occupants with the age of 15 or older
 - In passenger cars (KLASSECE=1),
 - year of first registration 2000 and later,
 - with its most severe collision regarding injury against an N2/N3 vehicle (KLASSECE=5,6), and
 - the exclusion of crashes with rollover events.
 - Based on the injury severity classes: MBAIS1+, MBAIS2+, and MBAIS3+.

MBAIS means that the maximum (known) single injury based on AIS according to the AIS 2015 is given. Injuries with an unknown severity of injury (AIS9) are not considered in the calculation of this value.

Table 7 shows the number of occupants matching the criteria above distributed by site.

Table 7 Passenger car front row occupants in crashes with HGV>3.5t by area type

Injury severity level	Urban	Rural	Motorway	Total
MBAIS1+	205	89	130	424
MBAIS2+	41	28	34	103
MBAIS3+	10	11	10	31

In total, 424 belted front row passenger car occupants in collisions against HGV>3.5t with the injury severity of MBAIS1+ matched the criteria, most of them in urban environments. Applying the filter criteria to the GIDAS dataset in Table 8 the collision between passenger cars and HGV>3.5t can be described. With that for example, the share of passenger cars got hit at the rear by the front of an HGV>3.5t can be identified.



Table 8 Applied filter criteria for vehicles in GIDAS dataset to identify front-to-rear collisions

Collision type	Applied GIDAS coding
Front	(VDI1=10,11,12,1,2 AND VDI2=1) OR (VDI1=12 AND VDI2=2,4 AND VDI3=50,81)
Rear	(VDI1=4,5,6,7,8 AND VDI2=3) OR (VDI1=6 AND VDI2=2,4 AND VDI3=70,91)

An overview of all 424 MBAIS1+ injured front row occupants, categorized by collision configuration, is given in Table 9. The collision type of passenger cars (PC) is noted in rows. The collision type of HGV>3.5t is given in columns.

Table 9 Front row passenger car occupants (MBAIS1+) by crash types (PC and HGV>3.5t)

Collision type PC	Collision type HGV>3.5t	Front	Side, left	Side, right	Rear	Other	Total
Front		50	27	10	95	1	183
Side, left		44	1	21	2	1	69
Side, right		17	13	0	2	1	33
Rear		129	0	0	0	0	129
Other		3	0	0	2	5	10
Total		243	41	31	101	8	424

According to Table 9, there are 183 front row occupants of passenger cars having a frontal collision with an HGV>3.5t. For 50 of them the HGV3.5t also has a frontal collision. For 129 front row occupants in rear collision the HGV3.5t vehicle collides with the front.

To parametrize simulations for WP4 the following aspects are analyzed for head-on and rear-end collisions:

- Collision velocities, relative velocities (based on collision speeds);
- Impact angles (angles between longitudinal axes);
- Overlap of passenger car;
- Contact/ Hit point;
- Dimensions /weight of all participants.



4.2.2.1 Head-on collisions

Head-on collisions in general are described often with a collision of two participants with their vehicle fronts. Table 9 shows that in the GIDAS dataset there are 50 MBAIS1+ injured front row occupants matching those criteria. As only 24 of them were involved in crashes on rural roads, it was decided to use the data of all 50 passenger car occupants for further analysis. Some further information in the head-on dataset is aggregated in categorical format like the weight of HGV3.5t, given in Figure 15.

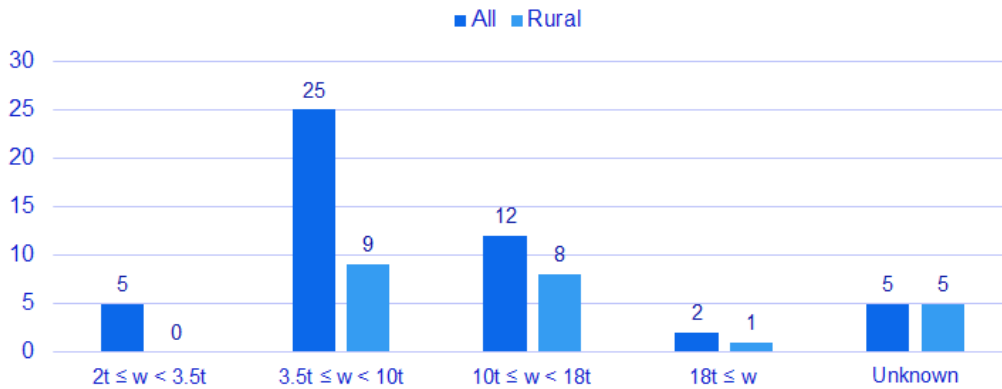


Figure 15 Share of HGV > 3.5t weight groups in head-on collisions by crash site

The overall result for head-on situations is summarized in Table 10 to generate input for further simulations based on in-depth data.

Table 10 Distributions of crash configuration parameters for passenger car-to-HGV > 3.5t head-on collisions in GIDAS

Variable	Q25	Q50	Q75
Overlap [%]	Up to 25%	50%	80%
Vc-PC [km/h]	24	39	56
Vc-HGV3.5 [km/h]	27	36	53
Vrel [km/h]	57	72	92
Impact Angle [°]	Up to ±5°	±10°	>10°
Contact/ Hit point [%]	Up to 20%	Up to 40%	80%
Weight PC [t]		1.5 t	2.5 t
Weight HGV3.5 [t]		Up to 10 t	Up to 18 t
Dimensions PC (W/L/H)	Basic car shape		
Dimensions HGV3.5	Basic HGV shape		



For the overview in Table 10, all results are described based on distribution percentiles for every parameter. Three quartiles of the distributions are given, namely Q25, where 25% of the values are below that value, the Q50, where 50% of the values are below that value and 50% are greater and the Q75, where 75% of the values are below that value. The abbreviations Vc and Vrel stand for collision speed and relative speed, respectively.

Figure 16 below illustrates the collision configuration based on the values given within the Q50 column in Table 10.

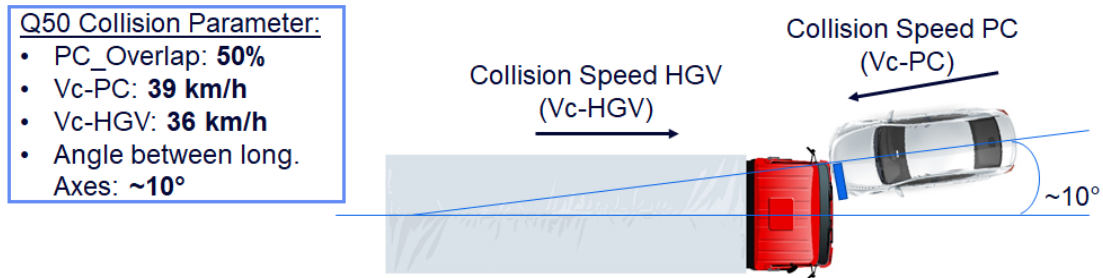


Figure 16 Illustration of Q50 passenger car-to-HGV>3.5t head-on crash configuration

4.2.2.2 Rear-end collisions

Rear-end collisions are described as a collision of two participants where the leading vehicle got hit at the rear by the following HGV with its frontal plane. Table 9 shows that in the GIDAS dataset there are 129 MBAIS1+ injured front row occupants matching those criteria. As only 31 of them have their crashes on motorways, it was decided to use data from all 129 passenger car occupants for further analysis. Some further information in the rear-end dataset is aggregated in categorical format like the weight of HGV3.5t, given in Figure 17.

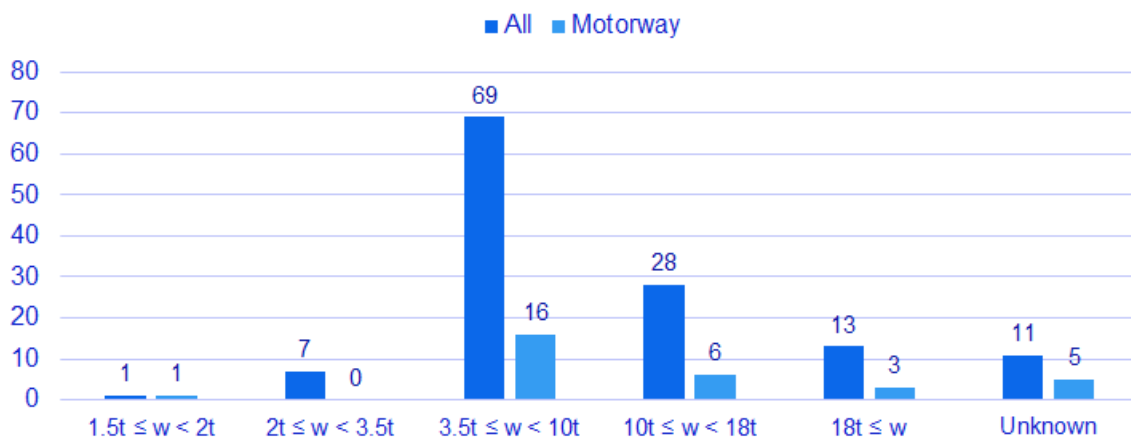


Figure 17 Share of HGV>3.5t weight groups in rear-end collisions by crash site

The overall result for rear-end situations is summarized in Table 11 to generate input for further simulations based on in-depth data, in the same way as the results given for head-on collisions.

Table 11 Distributions of crash configuration parameters for passenger car vs. HGV3.5 rear-end collisions in GIDAS

Variable	Q25	Q50	Q75
Overlap [%]	50%	100%	100%
Vc-PC [km/h]	0	0	7
Vc-HGV3.5 [km/h]	18	29	42
Vrel [km/h]	16	25	35
Impact Angle [°]	Up to ±5°	Up to ±5°	Up to ±5°
Contact/ Hit point [%]	50%	50%	75%
Weight PC [t]	-	1.5 t	2.5 t
Weight HGV3.5 [t]	-	Up to 10 t	Up to 18 t
Dimensions PC (W/L/H)	Basic car shape		
Dimensions HGV3.5	Basic HGV shape		

Figure 18 illustrates the collision configuration based of the values given within the Q50 column Table 11 for rear-end collisions.

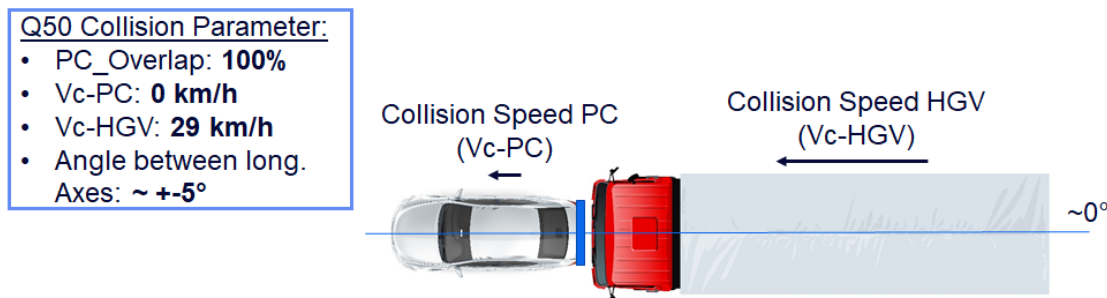


Figure 18 Illustration of Q50 passenger car vs. HGV3.5 rear-end crash configuration

4.3 In-depth analysis of car-to-VRU crashes

The following paragraphs will take a closer look at the car-to-pedestrian (C2P), car-to-bicycle (C2B) and car-to-powered two-wheeler (C2PTW) crashes. Overall, three main road environments are considered for the analysis of in-depth data: urban area, rural area, and motorway. In all cases, the ego vehicle, which is a passenger car, is involved in a conflict with a vulnerable road user (i.e., pedestrian, bicyclist, or PTW rider). The focus of the analysis is on injured VRUs. The crashes are clustered following methodologies applied in EU H2020 PROSPECT, INTERSECTION 2020 and MUSE projects.



4.3.1 Car-to-pedestrian crashes

The results in Section 2 as well as those in Table 3 and Table 4 indicate that pedestrians are the VRU group that is mostly affected by fatal road crashes and underline the importance of car-to-pedestrian crashes. The next sections describe a very detailed study and a clustering of car-to-pedestrian scenarios based on GIDAS data analysis (sections 4.3.1.1 and 4.3.1.2), as well as a study of car-to-pedestrian crashes in relation to traffic infrastructure (section 4.3.1.3).

4.3.1.1 Filter criteria for the analysis of car-to-pedestrian crashes in GIDAS

In the following paragraph the assumptions and the results of the in-depth data analysis of car-to-pedestrian crashes will be described. During the analysis, the conflicts that have led to a crash are described first. In a later step, various aspects including the weather condition as well as sight obstructions are investigated. The data analyzed for the use cases is the GIDAS dataset from June 2020, applying the filter criteria shown in Table 12.

Table 12 Criteria for the selection of car-to-pedestrian crashes in the GIDAS dataset

Filter variable	Value	Explanation
STATUS	4	Cases with completed reconstruction
JAHR	>1999	Data are from the year 2000 or later
FART	3	Identification of passenger cars
FZART	<= 26 OR 56 OR 60-62	
FZGKLASS	< 15	
FGDAT record	Present	FGDAT Record needs to be present
UTYP, UTYP A, UTYP B	All	The crash type variables are considered to describe the conflict before the crash happens. The roles are used to identify the participants in conflict

A set of 3 497 crashes including 3 679 passenger cars and 3 873 pedestrians remained after applying the criteria mentioned in Table 12 to the GIDAS data. Of all identified crashes, 96.7% occurred in urban areas, 2.6% in rural areas and 0.6% on motorways.

The following stepwise approach to identify the final GIDAS dataset was applied:

1. Assign the passenger car a role within the crash, which is causer (A) or non-causer (B) of the conflict.
2. Include the following crashes:
 - a) Pedestrians in collision with passenger cars, which are in role A or B;



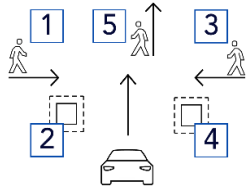

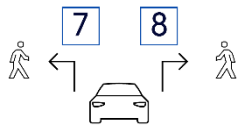
- b) Pedestrians in collision with passenger cars, which are in role A or B and after that in collision with another participant of the crash.
- 3. Assign role A or B to pedestrians within the crash, and include following crashes:
 - a) Pedestrians in collisions with other participants in the crash;
 - b) Pedestrians without contact to passenger cars, which are in role A or B.
- 4. Exclude the following crashes:
 - a) First contact of pedestrians before the conflict with passenger cars in role A or B (to the ground or to another participant);
 - b) All others not matching the criteria above;
 - c) Standing passenger cars in situations defined as “PC moves forward” before its conflict with a pedestrian.

The remaining 3 420 pedestrians in the dataset are the basis for the next steps.

4.3.1.2 Clustering of car-to-pedestrian crashes

Based on the crash type variable the following nine scenarios (shown in Table 13) of conflicts between passenger cars (PC) and pedestrians (P) were defined.

Table 13 Scenario clustering in passenger car-to-pedestrian crashes

Conflict scenario	Abbreviation	Schematic illustration
PC moves forward		
1. P crossing from left without sight obstruction	P-CLwoSO	
2. P crossing from left with sight obstruction	P-CLwSO	
3. P crossing from right without sight obstruction	P-CRwoSO	
4. P crossing from right with sight obstruction	P-CRwSO	
5. P walking in longitudinal direction	P-Long	
PC moves backwards		
6. PC reverse	P-PCRev	
PC turns		
7. PC turning left	P-PCTurnL	
8. PC turning right	P-PCTurnR	
PC in other crashes		
9. Other, excluding all P not in role B, except UTYP=1xx and UTYP=7xx (w./o. 799)	P-Oth	

The data clustering yielded a set of 3 420 pedestrian crash cases of which 1 541 were classified as killed or severely injured (KSI). About 97% of the filtered conflict scenarios were crashes in urban areas; however, 39.5% of all longitudinal cases took place in rural areas.



It is notable that in both conflict scenarios related to pedestrians crossing from the left while PC moves forward, namely, “crossing left without sight obstruction” (15.3% of all cases) and “crossing left with sight obstruction” (12.4%), had a substantially larger share among KSI cases compared to cases of all injury severities (P-CLwoSO: 19.5% of KSI cases, and P-CLwSO: 14.0% of KSI cases). Furthermore, the conflict scenarios with pedestrians crossing from the right, i.e., “crossing right without sight obstruction” (22.8% all / 23.2% KSI) and “crossing right with sight obstruction” (17.2% all / 18.8% KSI) had slightly higher shares in KSI. All the other scenarios had lower shares in KSI cases compared to crash cases overall. Figure 19 shows an overview of results for car-to-pedestrian (C2P) crashes.

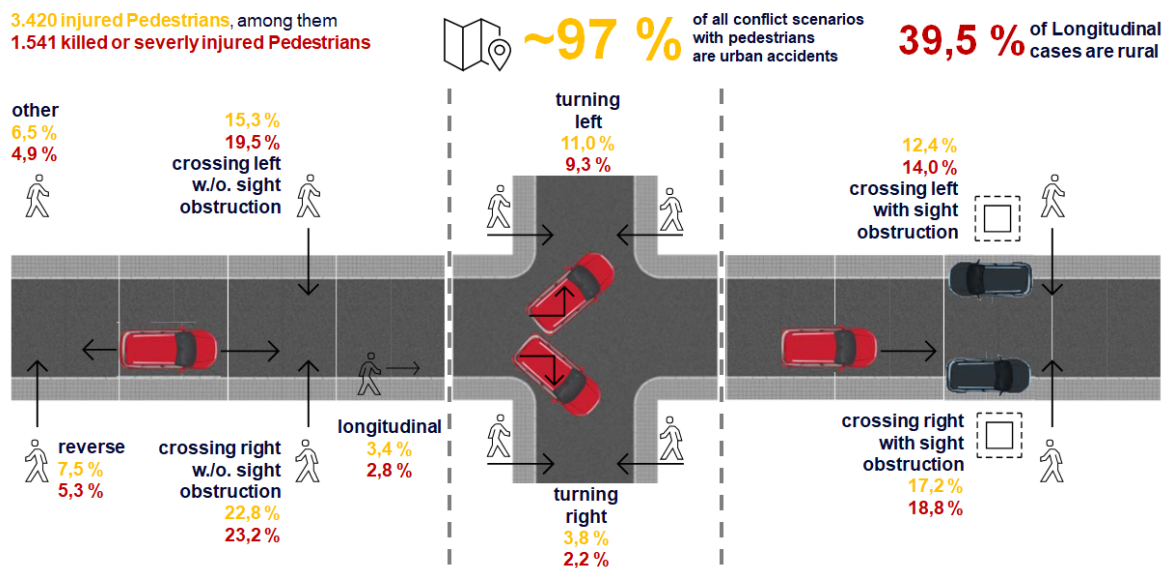


Figure 19 Overview of conflict scenarios for C2P crashes – schematic representation

The final dataset is analyzed for the following aspects:

- Relation to junction;
- Designated / non-designated crossing;
- Passenger car speed distribution (initial / collision);
- Time of day;
- Sight obstruction;
- Weather conditions that adversely affect sensor performance: precipitation (aggregates the following weather conditions: rain, snow, hail and sleet) and fog;
- Conflict-based crash type using the UTYP classification in GIDAS (GDV, 2016);
- Pre-crash trajectories;
- Crash causes.

The walking speeds of pedestrians have not been analyzed as this information is not quantified in the whole GIDAS dataset.



In the following paragraphs, the clusters defined in Table 13 are summarized with the results of all aspects mentioned above. As the cluster “9-Other” does not summarize similar situations, it is not analyzed here. A summary of all presented eight pedestrian clusters with an additional overview of crash causes for participants of C2P crashes is given in Table 51 and Table 52 in the Appendix.

4.3.1.2.1 Conflict scenario P-CLwoSO

An overview of car-to-pedestrian conflict scenario 1: Pedestrian crossing from left without sight obstruction while PC moves forward (P-CLwoSO) is provided in Figure 20 below.

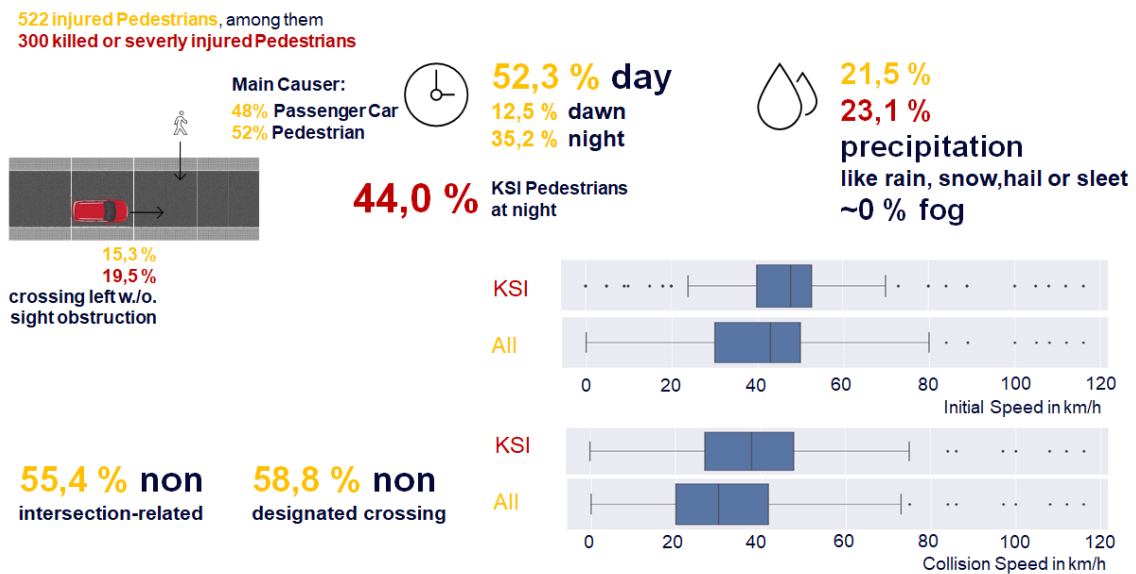


Figure 20 Results summary for C2P conflict scenario 1: P-CLwoSO

In total there are 522 injured pedestrians in the conflict scenario P-CLwoSO, among them 300 were killed or severely injured (KSI). As shown in Table 14 below, most all injury and KSI cases are described by the conflict-based crash type (UTYP) 401: ‘Pedestrian crossing - from left onto roadway without obstacle’.

Table 14 Classification of different crash types within the P-CLwoSO conflict scenario

	UTYP 401	UTYP 431	UTYP 461
Pictogram			
Proportion of injured (all severities)	51.7%	20.5%	17.9%
Proportion of KSI	53.4%	17.7%	19.7%



Figure 21 shows the trajectories of 298 pedestrians including all severities in a relative view, identified based on the GIDAS-PCM 2020-1 dataset. In this view the passenger car is set at the origin of the displayed coordinate system and the dot at the beginning of each trajectory represents the starting point from the pedestrian. The longer the trajectory, the higher the difference in velocity between ego passenger car and pedestrian.

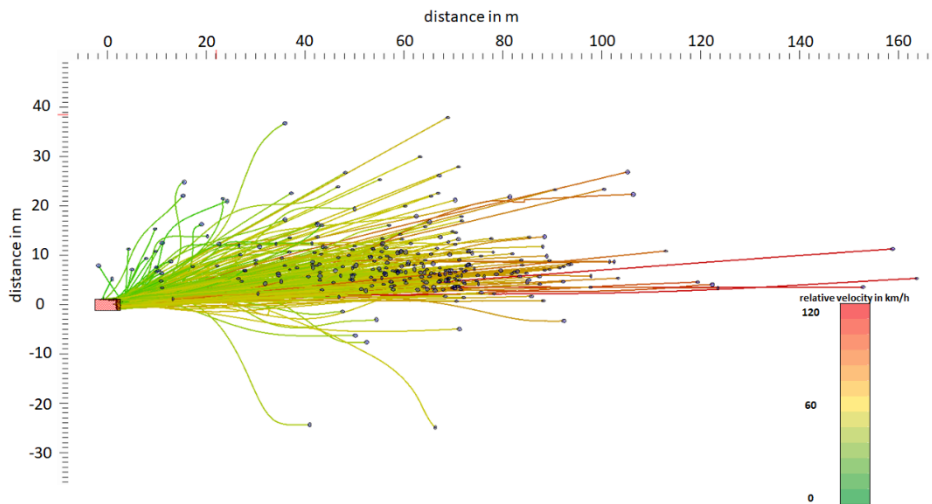


Figure 21 P-CLwoSO trajectories showing the relative motion of pedestrians w.r.t. the passenger car

The same applies for the overview in Figure 22 below which shows absolute trajectories where in each crash the passenger car is facing east at the time of collision. The longer the trajectories of the passenger car, the higher the velocity.

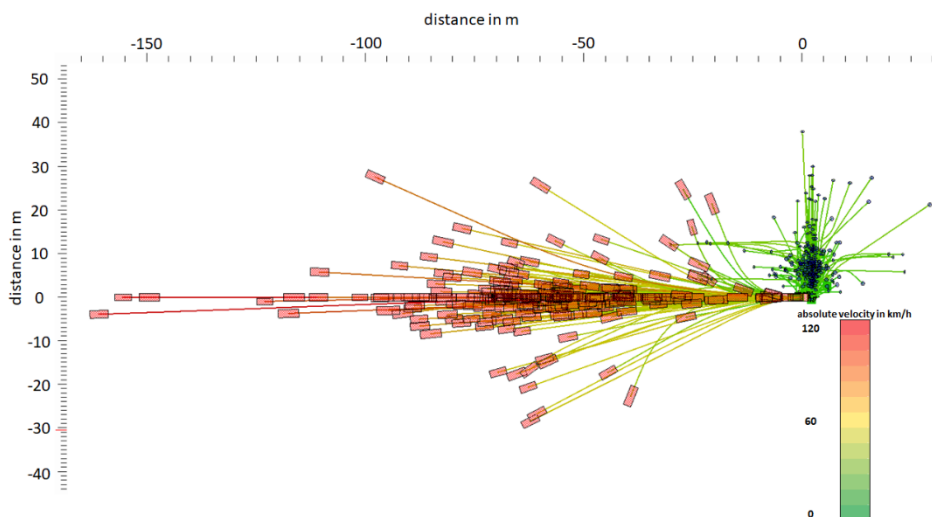


Figure 22 Trajectories of pedestrians and passenger cars relative to the collision point in P-CLwoSO scenarios - passenger car heading east (to the right) at collision point.



4.3.1.2.2 Conflict scenario P-CLwSO

An overview of C2P conflict scenario 2: Pedestrian crossing left with sight obstruction while PC moves forward (P-CLwSO) is provided in Figure 23.

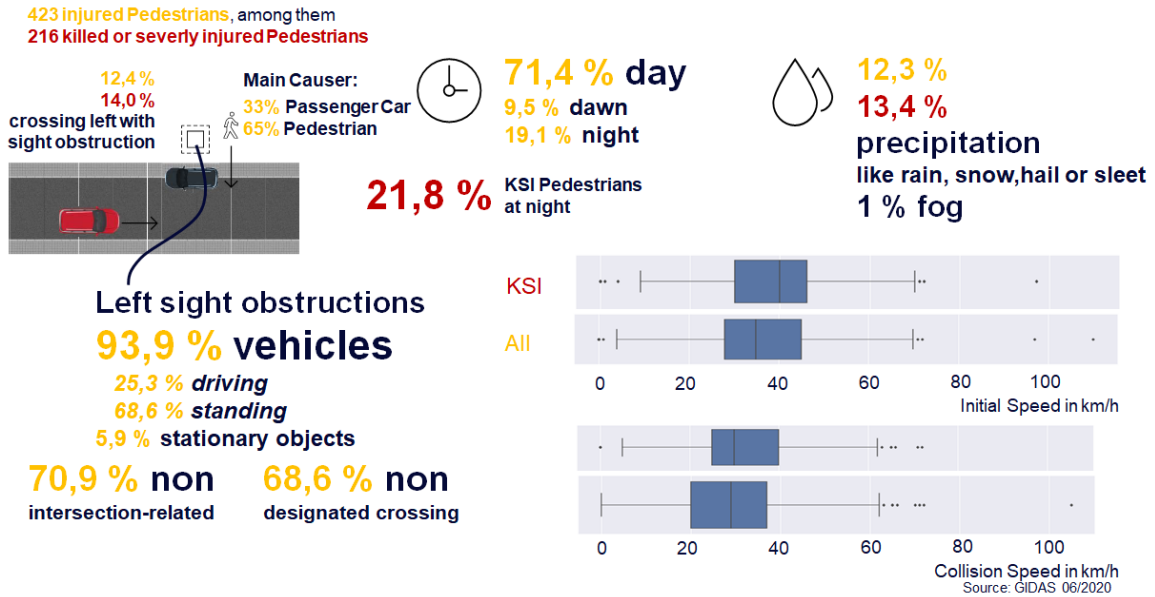


Figure 23 Results summary for C2P conflict scenario 2: P-CLwSO

In total, there are 423 injured pedestrians in P-CLwSO scenarios, among them 216 were killed or severely injured (KSI). As shown in Table 15, most of all injury and KSI cases are described by the conflict accident type with the number 411: 'Pedestrian crossing - from left onto roadway with obstacle'.

Table 15 Classification by crash type within P-CLwSO

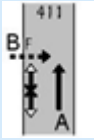
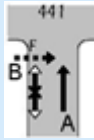
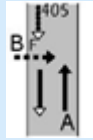
	UTYP 411	UTYP 441	UTYP 405
Pictogram			
Proportion of injured (all severities)	36.3%	11.6%	8.5%
Proportion of KSI	34.1%	10.6%	11.1%

Figure 24 shows the relative trajectories of 263 pedestrians including all severities, identified based on the GIDAS-PCM 2020-1 dataset.



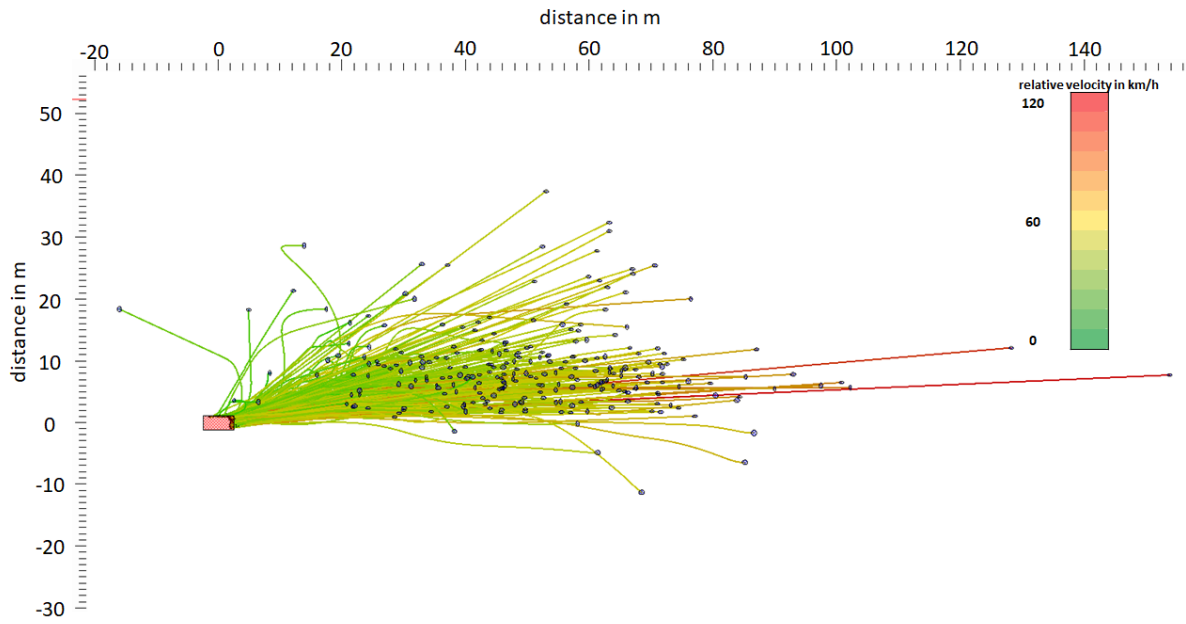


Figure 24 P-CLwSO trajectories showing the relative motion of pedestrians w.r.t. the passenger car

Figure 25 below shows absolute trajectories where in each crash the passenger car is facing east at the time of collision.

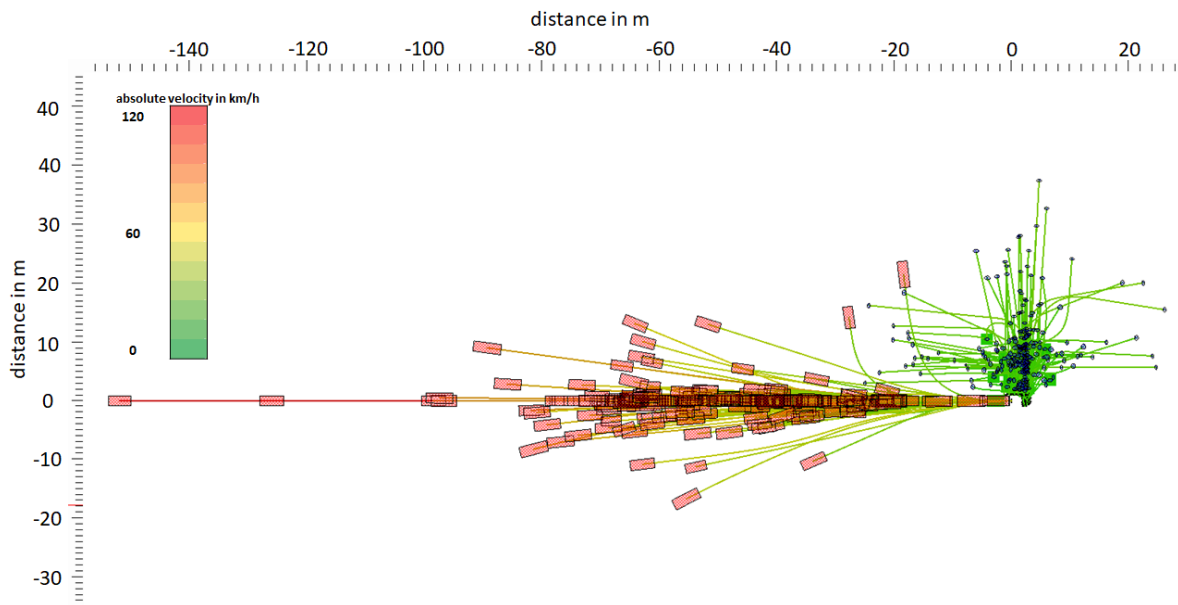


Figure 25 Trajectories of pedestrians and passenger cars relative to the collision point - in P-CLwSO scenarios - passenger car heading east (to the right) at collision point



4.3.1.2.3 Conflict scenario P-CRwoSO

An overview of C2P conflict scenario 3: Pedestrian crossing from right without sight obstruction while PC moves forward (P-CRwoSO) is provided in Figure 26.

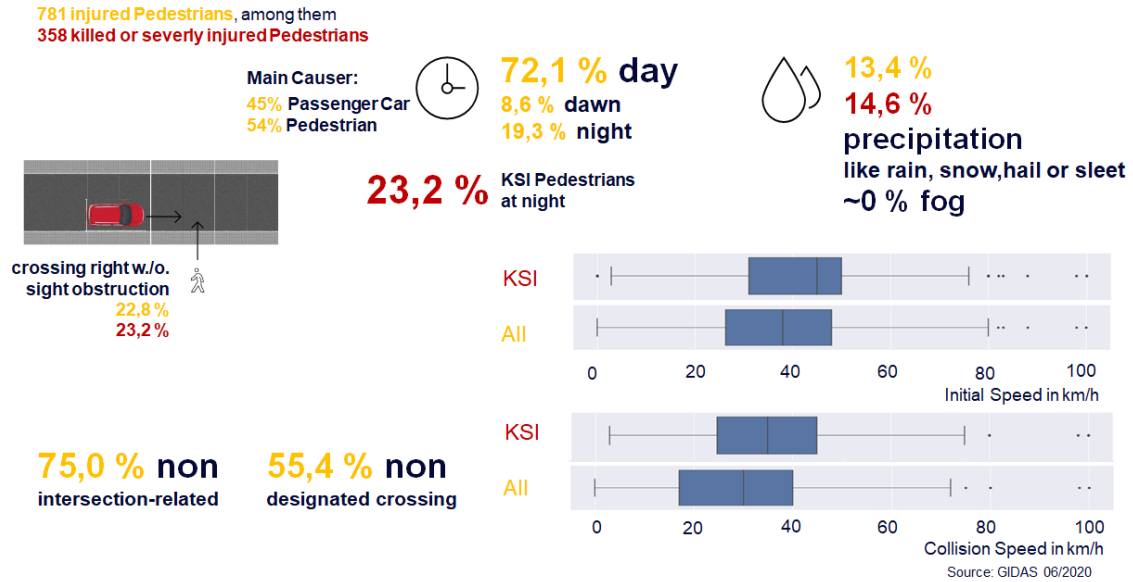


Figure 26 Results summary for C2P conflict scenario 3: P-CRwoSO

In total, there are 781 injured pedestrians in P-CRwoSO scenarios, among them 358 were killed or severely injured (KSI). As shown in Table 16, most of all injury and KSI cases are described by the conflict accident type with the number 421: ‘Pedestrian crossing - from right onto roadway’.

Table 16 Classification by crash type within P-CRwoSO

	UTYP 421	UTYP 451	UTYP 471
Pictogram			
Proportion of injured (all severities)	53.2%	23.3%	19.7%
Proportion of KSI	56.5%	20.3%	20.9%



Figure 27 shows the trajectories of 406 pedestrians including all severities identified based on the GIDAS-PCM 2020-1 dataset.

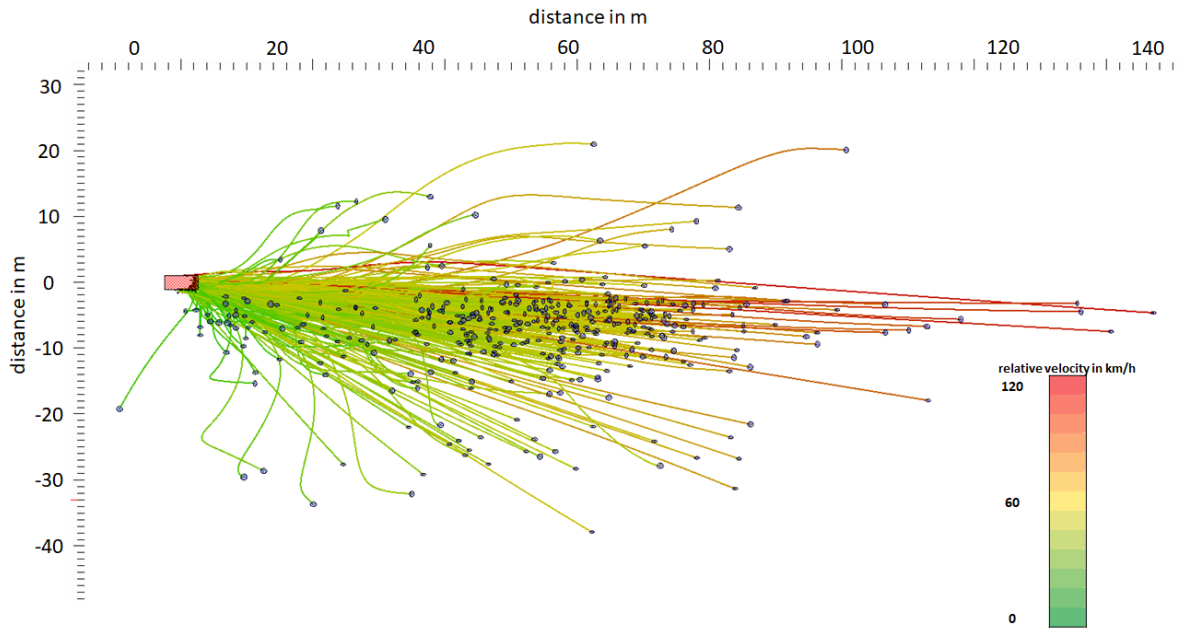


Figure 27 P-CRwoSO trajectories showing the relative motion of pedestrians w.r.t. the passenger car

Figure 28 below shows absolute trajectories where in each crash the passenger car is facing east at the time of collision.

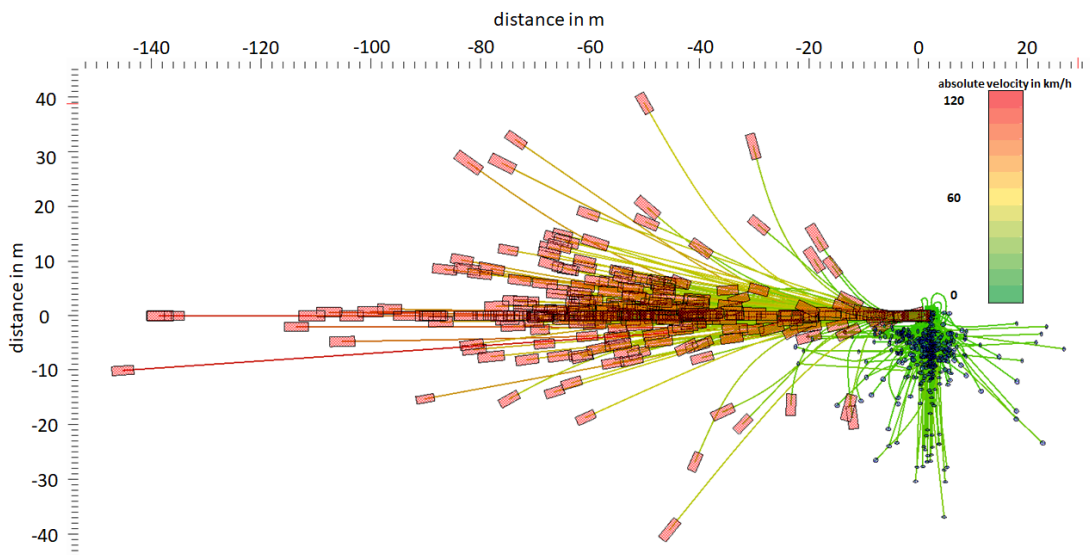


Figure 28 Trajectories of pedestrians - and passenger cars relative to the collision point in P-CRwoSO scenarios - passenger car heading east (to the right) at collision point.



4.3.1.2.4 Conflict scenario P-CRwSO

An overview of C2P conflict scenario 4: Pedestrian crossing from right with sight obstruction while PC moves forward (P-CRwSO) is provided in Figure 29.

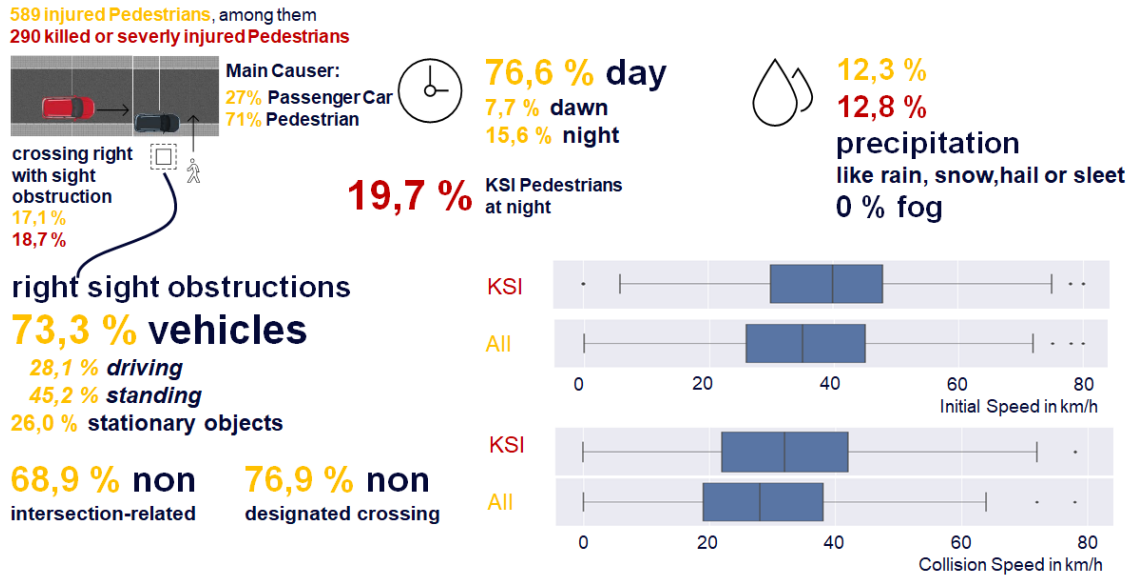


Figure 29 Results summary for C2P conflict scenario 4: P-CRwSO

In total, there are 589 injured pedestrians in P-CRwSO scenarios, among them 290 were killed or severely injured (KSI). As shown in Table 17, most of all injury and KSI cases are described by the conflict accident type with the number 423: ‘Pedestrian crossing - from right onto roadway - while passing’.

Table 17 Classification by crash type within P-CRwSO

	UTYP 423	UTYP 424	UTYP 422
Pictogram			
Proportion of injured (all severities)	38.1%	16.8%	13.4%
Proportion of KSI	39.1%	14.9%	14.5%

Figure 30 shows the trajectories of 379 pedestrians including all severities identified based on the GIDAS-PCM 2020-1 dataset.



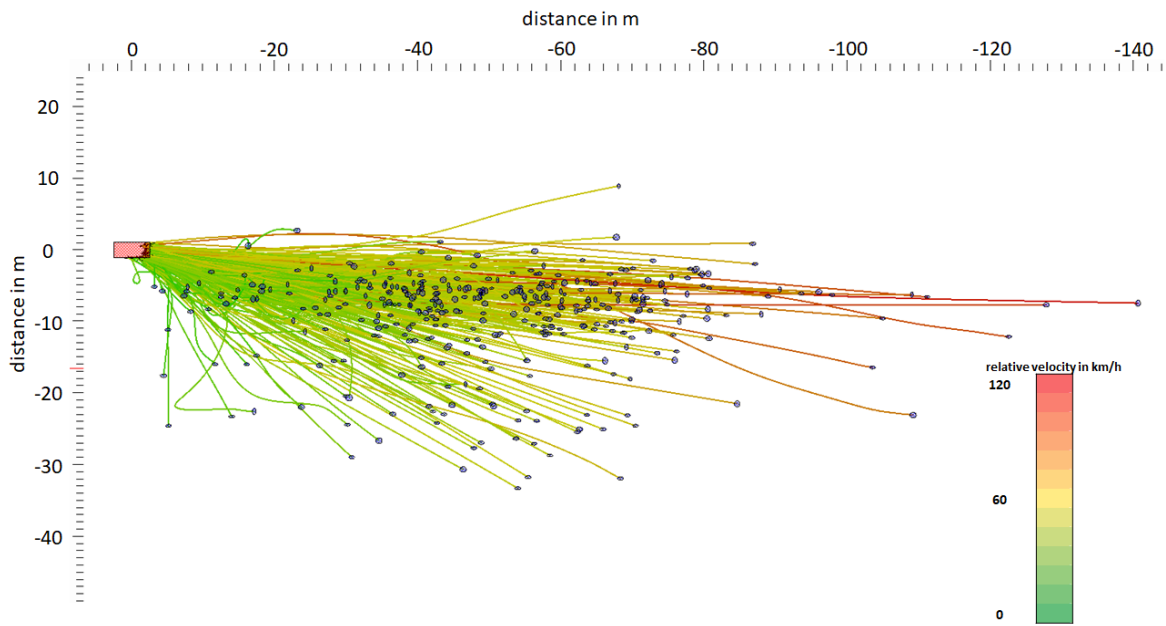


Figure 30 P-CRwSO trajectories showing the relative motion of pedestrians w.r.t. the passenger car

Figure 31 below shows absolute trajectories.

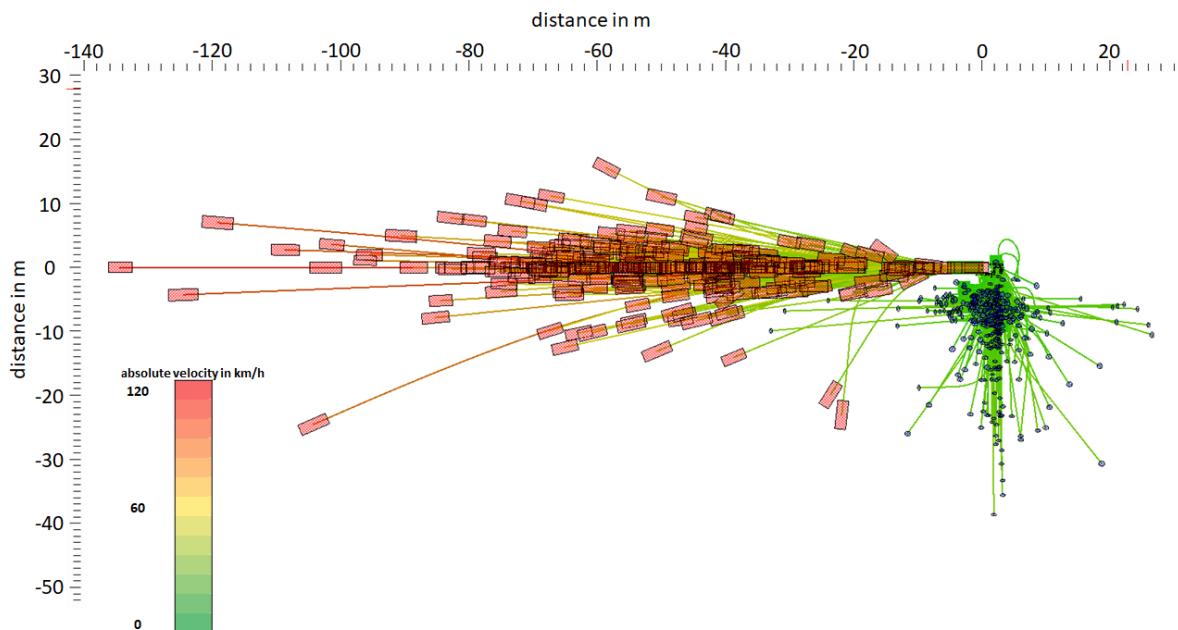


Figure 31 Trajectories of pedestrians - and passenger cars relative to the collision point in P-CRwSO scenarios - passenger car heading east (to the right) at collision point.



4.3.1.2.5 Conflict scenario P-Long

An overview of C2P conflict scenario 5: Pedestrian walking in longitudinal direction (P-Long) is provided in Figure 32.

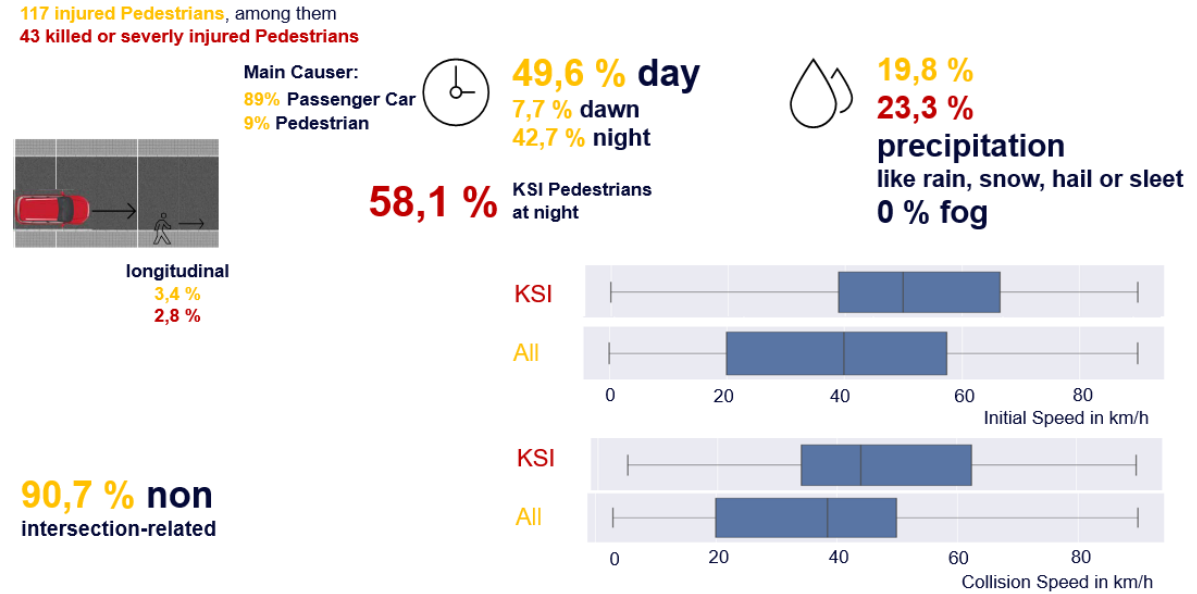


Figure 32 Results summary for C2P conflict scenario 5: P-Long

In total, there are 117 injured pedestrians in P-Long scenarios, among them 43 were killed or severely injured (KSI). As shown in Table 18, most of all injury and KSI cases are described by the conflict accident type with the number 671: ‘Longitudinal Traffic - pedestrian and vehicle. in same direction - right lane’

Table 18 Classification by crash type within P-Long

	UTYP 671	UTYP 672	UTYP 673
Pictogram			
Proportion of injured (all severities)	58.1%	21.4%	10.3%
Proportion of KSI	55.8%	25.6%	7.0%

Figure 33 shows the trajectories of 36 pedestrians including all severities identified based on the GIDAS-PCM 2020-1 dataset.



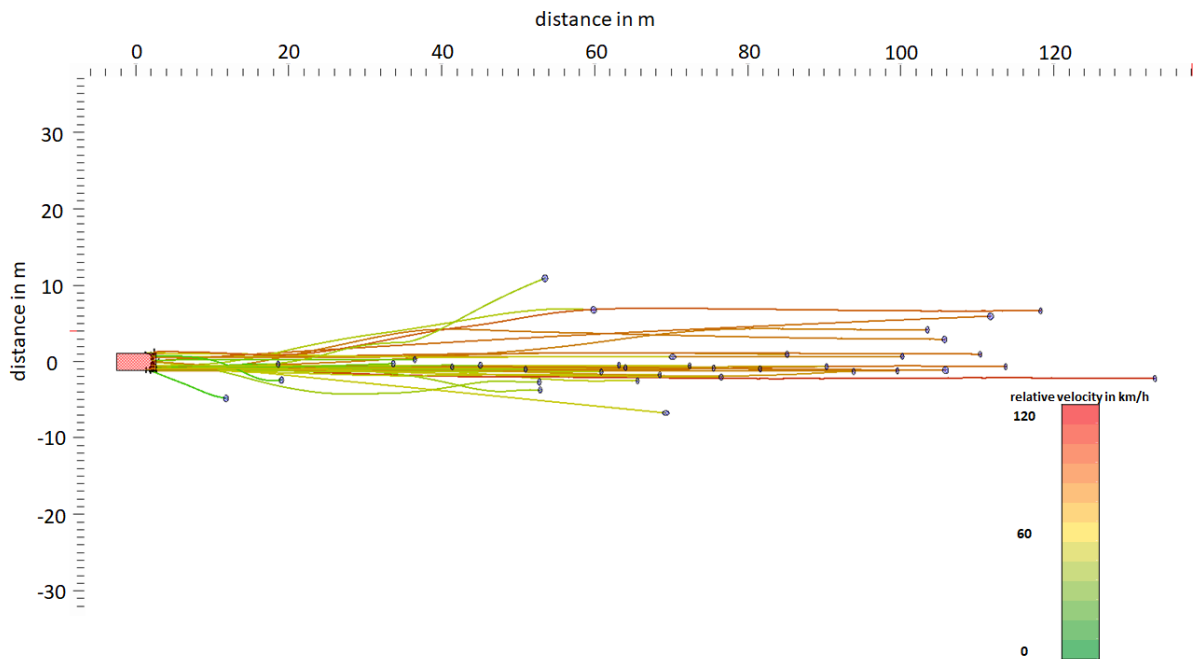


Figure 33 P-Long trajectories showing the relative motion of pedestrians w.r.t. the passenger car

Figure 34 below shows absolute trajectories.

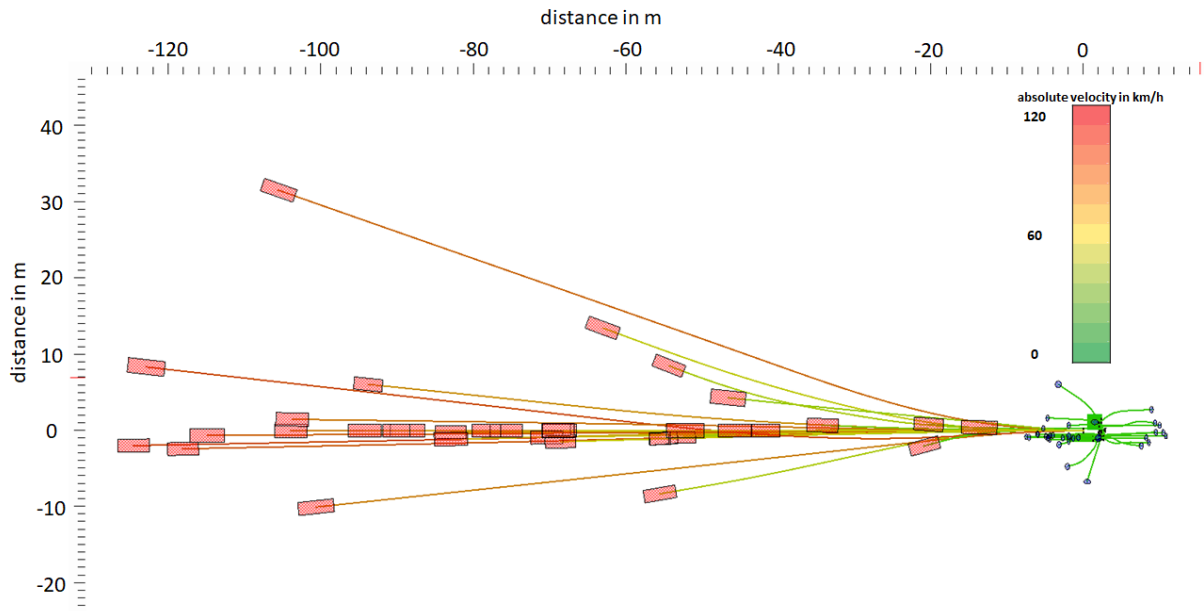


Figure 34 Trajectories of pedestrians - and passenger cars relative to the collision point in P-Long scenarios - passenger car heading east (to the right) at collision point.



4.3.1.2.6 Conflict scenario P-PCRev

An overview of C2P conflict scenario 6: Passenger car reverse (P-PCRev) is provided in Figure 35.

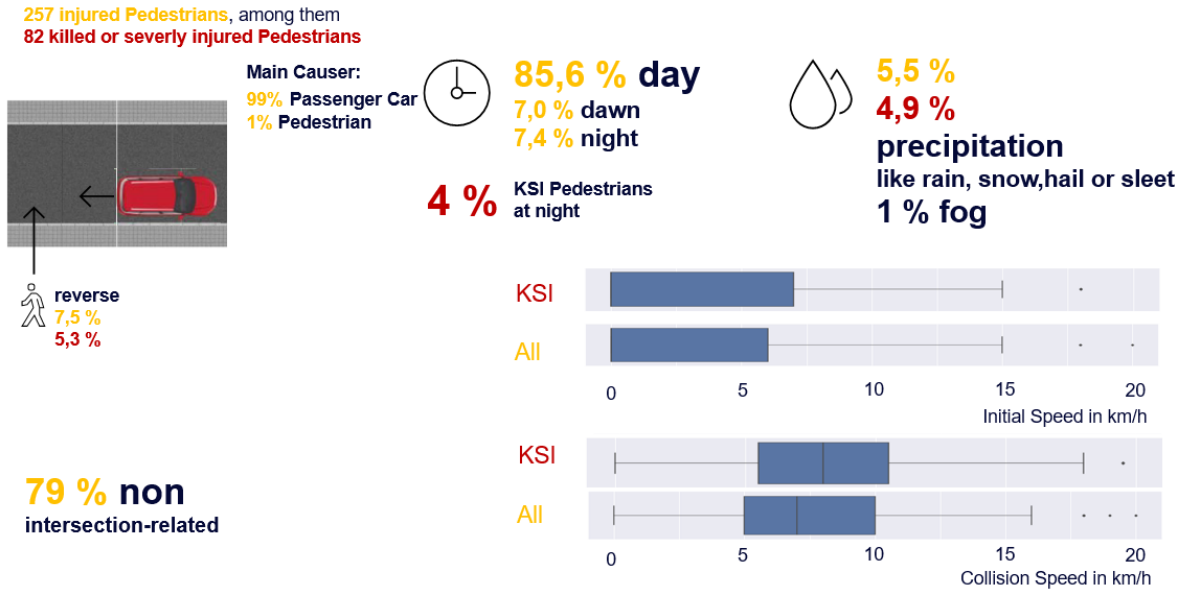


Figure 35 Results summary for C2P conflict scenario 6: P-PCRev

In total, there are 257 injured pedestrians in P-PCRev scenarios, among them 82 were killed or severely injured (KSI). As shown in Table 19, most of all injury and KSI cases are described by the conflict accident type with the number 713: ‘Other Accident - Backing up and collision with ped. Crossing behind the vehicle’

Table 19 Classification by crash type within P-PCRev

	UTYP 713	UTYP 571	UTYP 719
Pictogram			711-715
Proportion of injured (all severities)	87.2%	4.3%	3.1%
Proportion of KSI	86.6%	4.9%	8.5%

Figure 36 shows the trajectories of 47 pedestrians including all severities identified based on the GIDAS-PCM 2020-1 dataset.



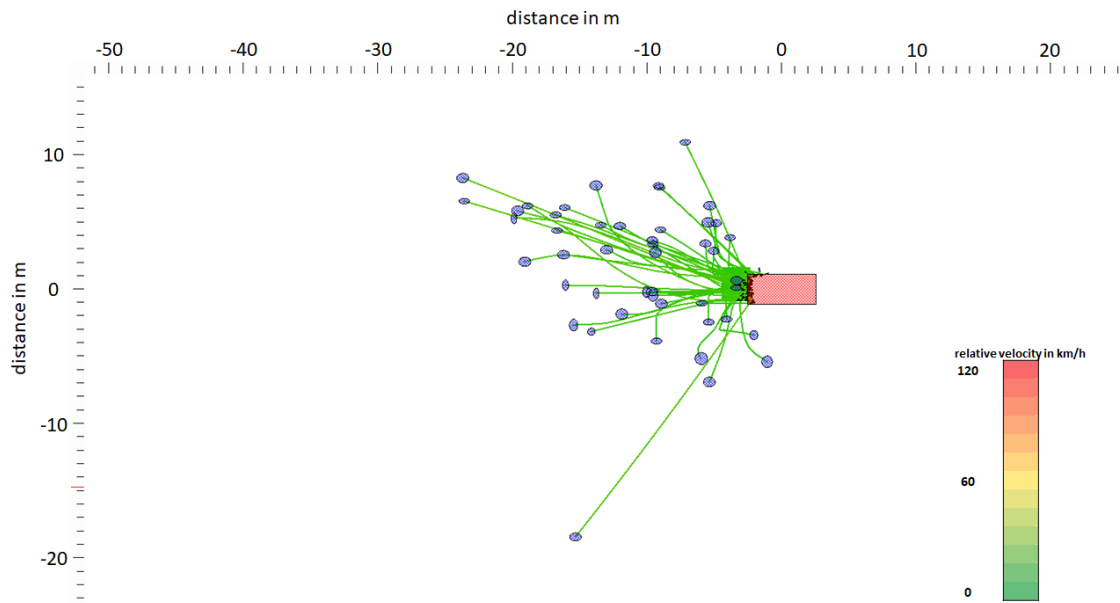


Figure 36 P-PCRev trajectories showing the relative motion of pedestrians w.r.t. the passenger car

Figure 37 below shows absolute trajectories.

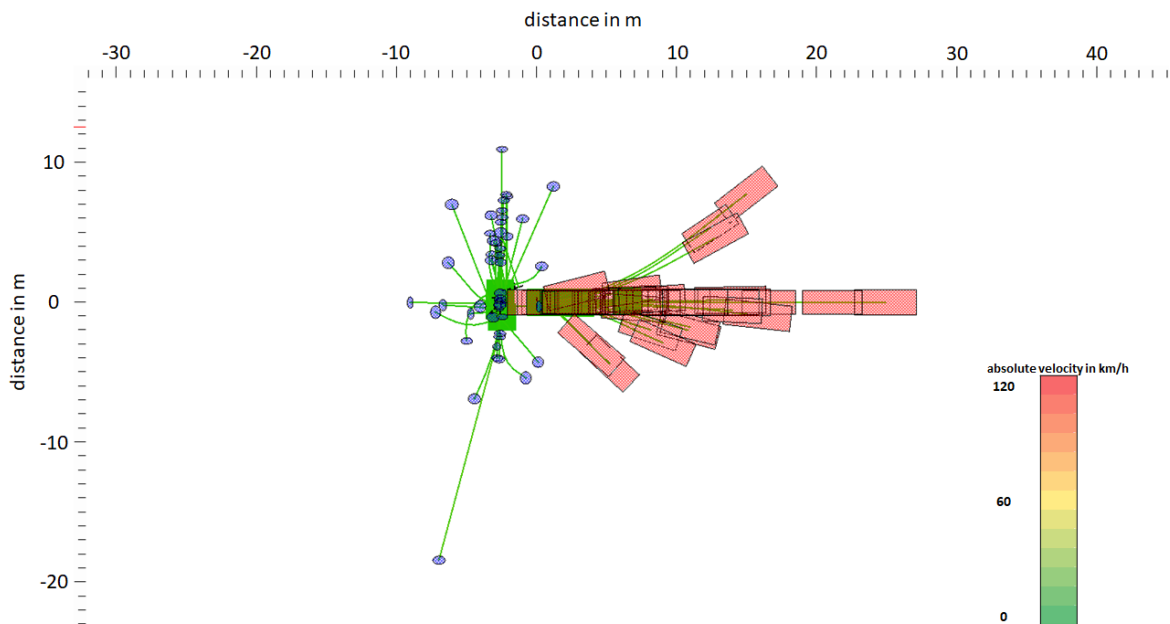


Figure 37 Trajectories of pedestrians - and passenger cars relative to the collision point in P-PCRev scenarios -passenger car heading east (to the right) at collision point.



4.3.1.2.7 Conflict scenario P-PCTurnL

An overview of the C2P conflict scenario 7: Passenger car turning left (P-PCTurnL) is provided in Figure 38.

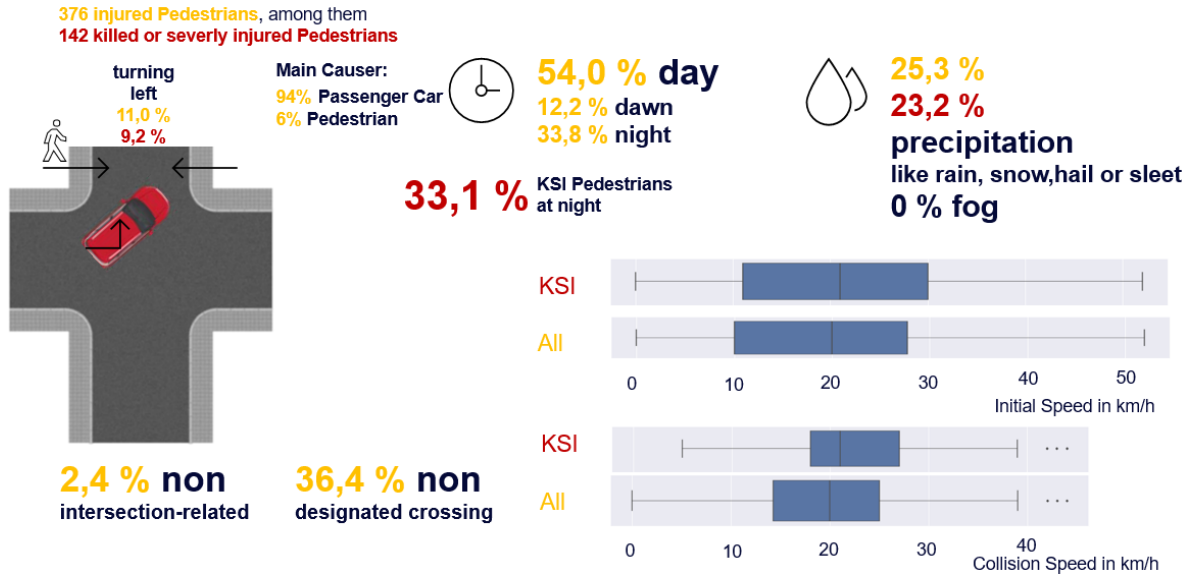


Figure 38 Results summary for C2P conflict scenario 7: P-PCTurnL

In total, there are 376 injured pedestrians in P-PCTurnL scenarios, among them 142 were killed or severely injured (KSI). As shown in Table 10, most of all injury and KSI cases are described by the conflict-based crash type with the number 222: ‘Turning - left turning veh. and pedestrian in opposite direction’.

Table 20 Classification by crash type within P-PCTurnL

	UTYP 222	UTYP 221	UTYP 282
Pictogram			
Proportion of injured (all severities)	53.7%	43.6%	1.1%
Proportion of KSI	50.0%	45.1%	2.8%

Figure 39 shows the trajectories of 151 pedestrians including all severities identified based on the GIDAS-PCM 2020-1 dataset.



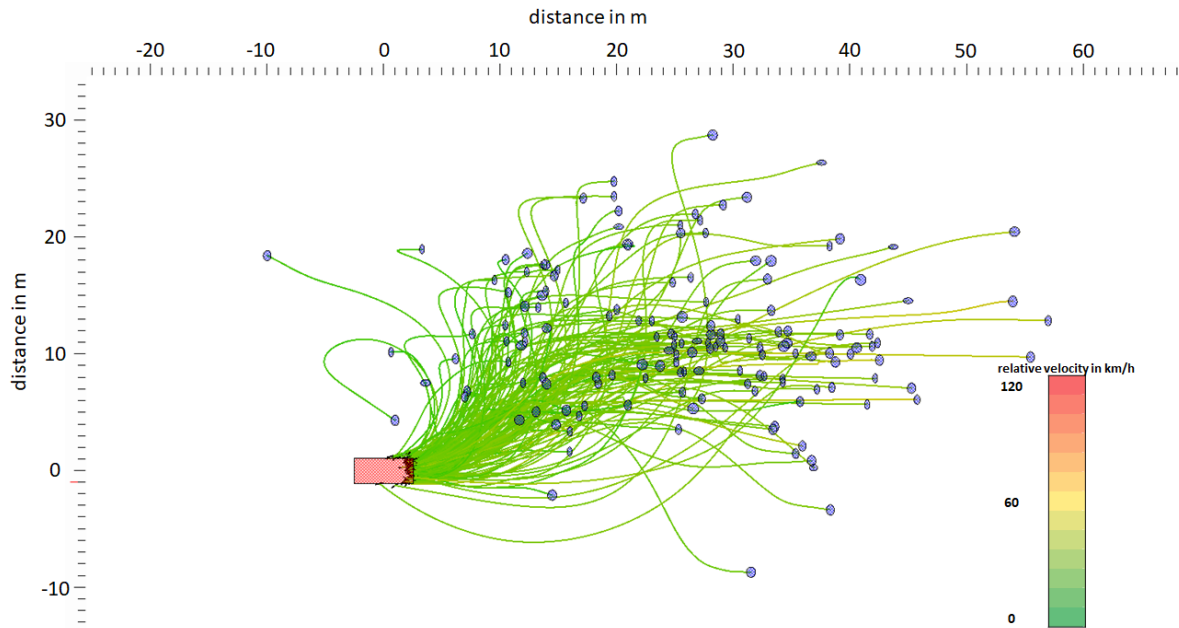


Figure 39 P-PCTurnL trajectories showing the relative motion of pedestrians w.r.t. the passenger car

Figure 40 below shows absolute trajectories.

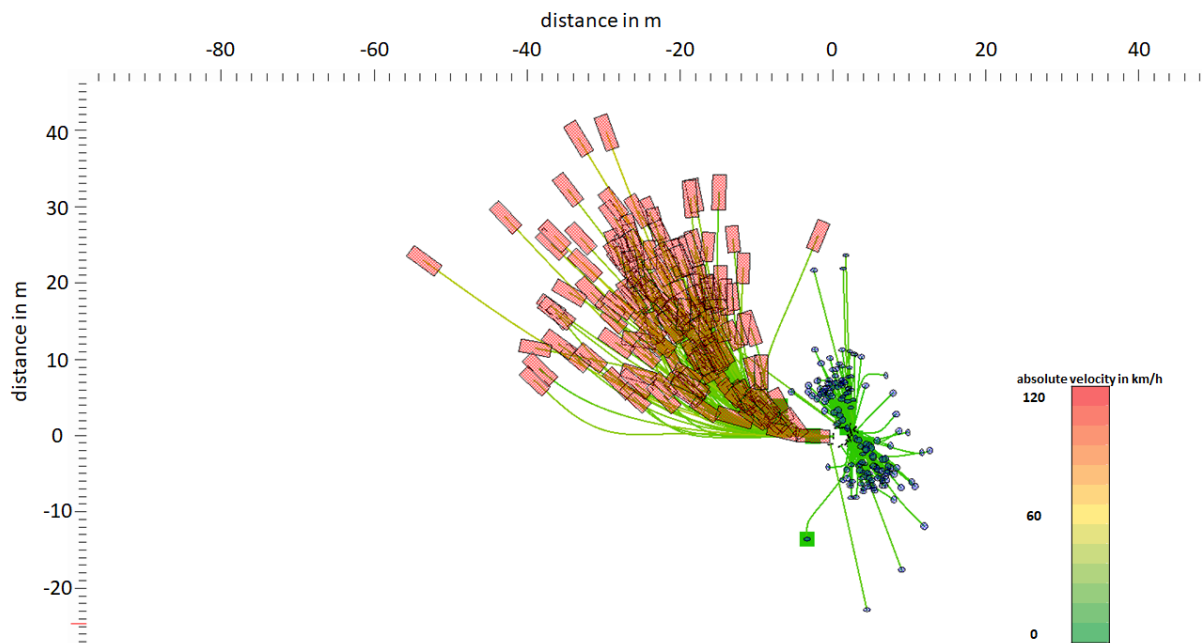


Figure 40 Trajectories of pedestrians - and passenger cars relative to the collision point in P-PCTurnL scenarios -passenger car heading east (to the right) at collision point.



4.3.1.2.8 Conflict scenario P-PCTurnR

An overview of C2P conflict scenario 8: Passenger car turning right (P-PCTurnR) is provided in Figure 41.

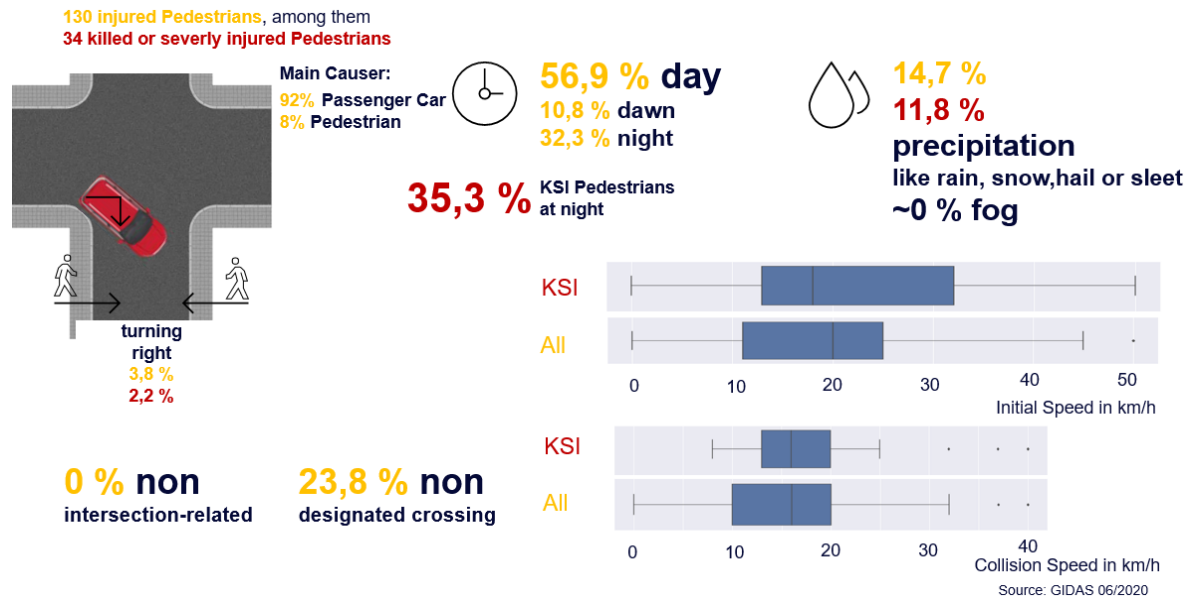


Figure 41 Results summary for C2P conflict scenario 8: P-PCTurnR

In total, there are 130 injured pedestrians in P-PCTurnR scenarios, among them 34 were killed or severely injured (KSI). As shown in Table 21, most of all injury and KSI cases are described by the conflict-based crash type 241: ‘Turning - right turning veh. and pedestrian in same direction’.

Table 21 Classification by crash type within P-PCTurnR

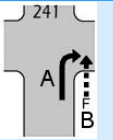
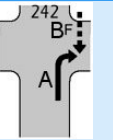

	UTYP 241	UTYP 242	UTYP 284
Pictogram			
Proportion of injured (all severities)	50.8%	44.6%	2.3%
Proportion of KSI	55.9%	38.2%	5.9%

Figure 42 shows the trajectories of 46 pedestrians including all severities identified based on the GIDAS-PCM 2020-1 dataset.



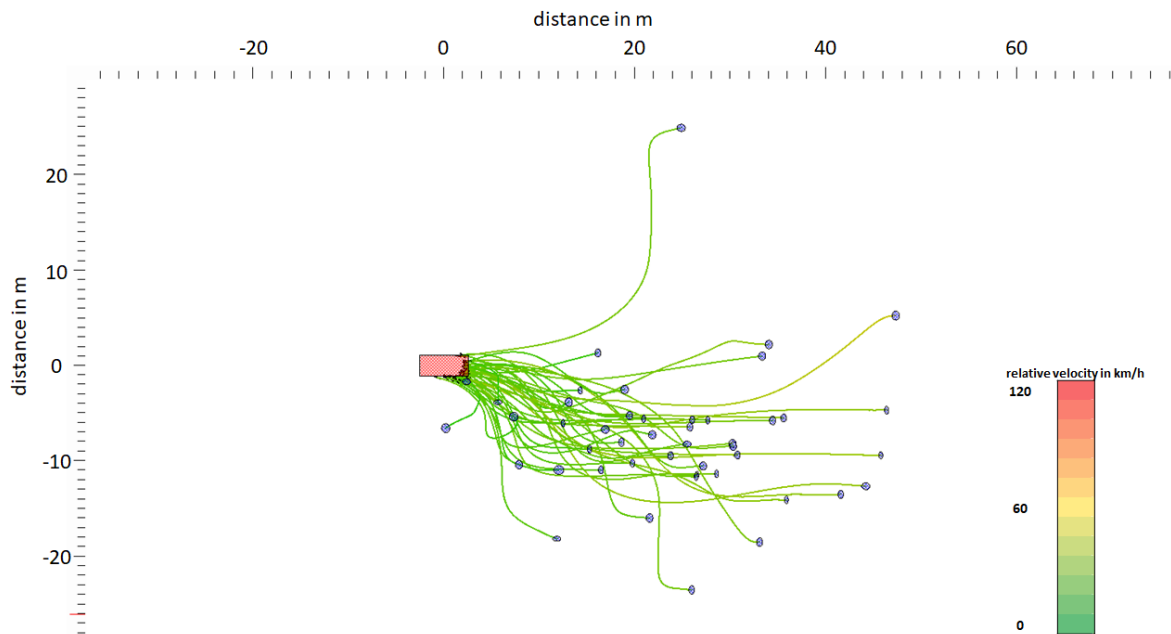


Figure 42 P-PCTurnR trajectories showing the relative motion of pedestrians w.r.t. the passenger car

Figure 43 below shows absolute trajectories.

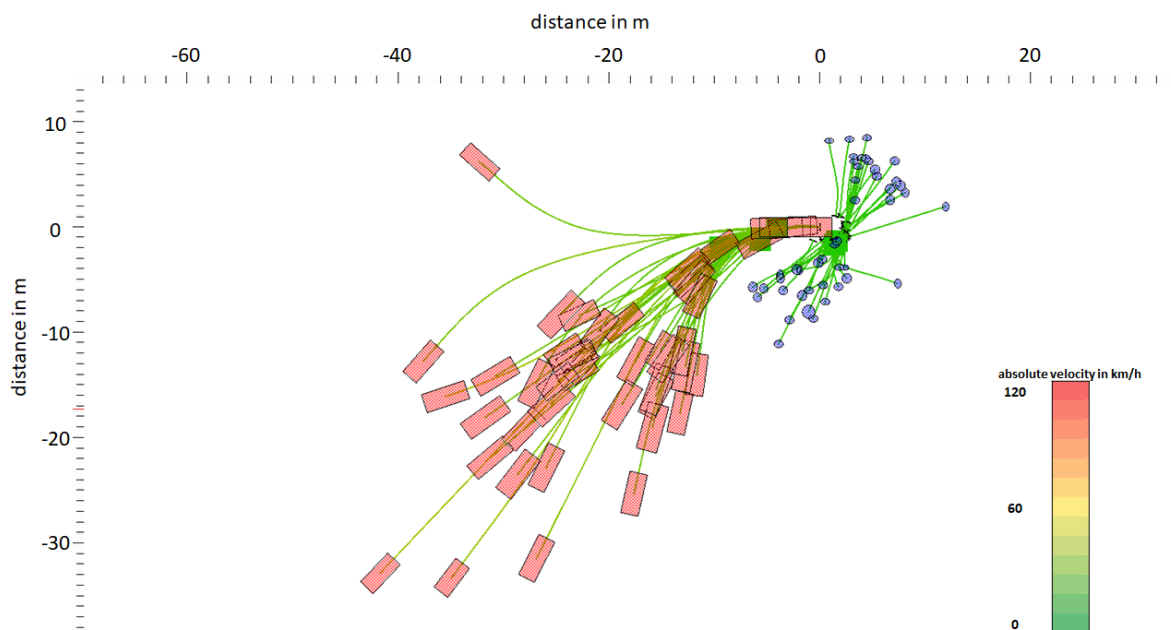


Figure 43 Trajectories of pedestrians - and passenger cars relative to the collision point in P-PCTurnR scenarios - passenger car heading east (to the right) at collision point.



4.3.1.3 Designated vs non-designated crossings of pedestrians

In Section 4.3.1.2, it was noted that a substantial share of KSI car-to-pedestrian crashes occurred at non-designated crossing locations. Therefore, the difference between designated and non-designated crossings of pedestrians is studied here and further details are described below.

The following research question forms the basis of the analysis: *What are the differences in car-to-pedestrian crashes between designated crossing and non-designated crossing scenarios with special focus on the interaction?*

For the assessment of car-to-pedestrian crashes and its interactions, naturalistic driving data (NDD) from JAAD and AMP (see sections 3.3.1 and 3.3.2) have been analyzed. Various information from the AMP database such as the driver state during a crash, emergency maneuvers from drivers or VRUs before the crash were used to depict the criticality of a scenario. Based on this, NDD hypotheses have been derived which were enriched by an in-depth accident analysis, with a special focus on behavioral causes of the GIDAS crashes.



Figure 44 Illustration of "designated" (source: JAAD) and "non-designated" (source: AMP) crossings

The JAAD database involves a category, which is called "designated crossing". This category has been used as the main filter in this analysis and can be defined as follows:

- Designated Crossing: The infrastructure provides dedicated roles, behaviors and obligations to the passenger car and the pedestrian. This includes roundabouts, signal lights and zebra crossings. The crossing of the pedestrian close to such infrastructure should be expected by the car driver.
- Non-Designated Crossing: The infrastructure does not additionally support the crossing of a pedestrian at this location. Examples are straight roads or junctions without a zebra crossing or a pedestrian ford (thin broken markings on the street which serve to guide the pedestrian. This type of infrastructure is predominantly available in Germany at traffic lights.)

In Figure 44 above, the left image shows an example of a designated crossing, where a group of pedestrians is waiting in front of a zebra crossing for the approaching car to stop. This behavior is good practice but also highly dependent on the region/country. The right image shows an example of a non-designated crossing, where two pedestrians are crossing

the street on a straight road without any road markings for pedestrians. In this case the crossing of the pedestrians could not be anticipated by the car driver.

In the AMP Portal, scenarios were filtered to form groups of crashes and near-crash cases with involvement of pedestrians. Reversing vehicles have not been considered.

Approximately 50 video snippets from both databases have been observed with special focus on environmental aspects which influence the driver and pedestrian behavior and the interaction between them. A summary of the key findings can be found in Table 22.

Table 22 Result summary of key findings from NDD analysis (JAAD and AMP) of pedestrians crossing at designated and non-designated locations

Constraints	Designated crossing	Non designated crossing
Daylight; No precipitation	Interaction between car driver and pedestrian present in most cases: head turn, eye contact, perception on vehicle speed reduction or complete stop	Interaction present, but not in all cases.
Night, No precipitation	When the vehicle is detected early, interaction trough body pose present.	Pedestrian seems to show running / hurrying behavior in some cases.
Bad weather (Rain, fog, snow and icy roads)	Interaction present, but not in all cases . Assumption: Pedestrians are in a hurry. Obstruction of direct communication observed (Jacket, hoodie, umbrella, windshield wipers etc.)	Interaction is present in a few cases only. Assumption: Pedestrians are in a hurry. Obstruction of direct communication observed (Jacket, hoodie, umbrella, windshield wipers etc.)
Behavior Driver	Aware of pedestrians standing in daylight. Slowing down/stopping and letting pedestrian pass.	Surprised in several cases, confused about the VRU behavior. Less driver-initiated maneuver observed.
Behavior VRU	Mostly aware of oncoming traffic, interaction present if the vehicle detected early. Waiting behavior.	Pedestrian show behavior change. (Due to the fact that they do not have priority?) Hurry up, running.



In the context of NDD analysis, an action initiated by either the pedestrian or the car driver and the consequent action(s) resulting from the initial action is defined as interaction. For example, a pedestrian waiting at a zebra crossing turns his or her head towards an approaching car (initial action), the car driver understanding the gesture and braking to bring the vehicle to stop are consequent actions. All these put together is defined as interaction.

With the findings of the NDD analysis of both databases, the following hypotheses have been created:

1. Planned interaction between a car driver and pedestrian is mostly present in a designated crossing.
2. Interaction in a non-designated crossing is poor or not present.
3. Interaction may not be present in the case of bad weather (rain, snow) or night due to obstruction of communication.
4. Pedestrians show hurried behavior in bad weather conditions.
5. Both pedestrians and car drivers are compelled to respect a traffic rule when present, involving pedestrians (Example: zebra crossing or a signal with lights).
6. Car drivers often do not expect a pedestrian crossing the road in a non-designated crossing. They are taken by surprise or are confused about pedestrians' intentions.

The presented findings from NDD cannot be interpreted as representative due to the low number of assessed and available video snippets. The GIDAS database has been used as a crash database with a large number of relevant cases to enrich the NDD analysis and to complement the key findings from the NDD. The used datasets and applied filters are shown in Figure 45. The results are unweighted, i.e., the GIDAS data have not been projected to national or EU level.

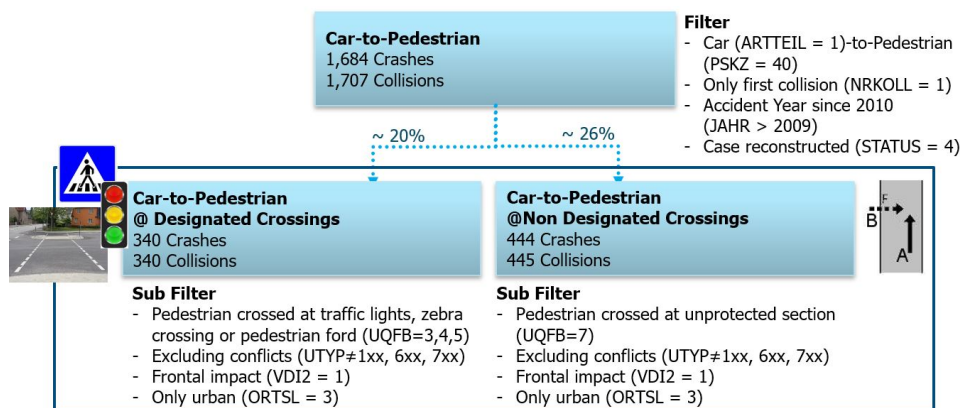


Figure 45 Description of the GIDAS analysis filters and sample sizes for designated and non-designated crossing

The analysis was based on the GIDAS dataset of July 2020 which was filtered for car-to-pedestrian collisions. This definition includes the assignment of an ego participant as a passenger car (ARTTEIL = 1) which collides in its first collision (NRKOLL = 1) with the bullet



participant - a pedestrian (PSKZ = 40). The data have been reduced to crash years since 2010, to ensure a good representation of current crash scenarios in terms of infrastructure as well as safety technologies available in the cars. The car-to-pedestrian dataset includes 1 684 crashes with 1 707 collisions (due to the involvement of more than one car in some of the crashes).

From the car-to-pedestrian dataset two sub-datasets were derived – one including scenarios with designated crossings and one including non-designated crossings. These sub-datasets include only urban scenarios (ORTSL = 3) and frontal car impacts (VDI2=1). Driving conflicts (UTYP starting with 1), longitudinal conflicts (UTYP starting with 6) and other conflicts (UTYP starting with 7) are excluded. The difference between the two sub-datasets is defined by the parameter UQFB which describes where the pedestrian crossed the street. Pedestrians crossing at traffic lights, zebra crossings or pedestrian fords are allocated to the designated crossing scenarios whereas pedestrians crossing at an unprotected section are assigned to the non-designated crossings. The former includes 340 crashes, the latter one 445 crashes.

Within the two created GIDAS datasets, it could be seen that non-designated crossings lead to slightly more severe injuries (55% KSI) compared to designated crossings (46% KSI). Further, designated crossings happen in most of the cases (81%) at a junction whereas non-designated crossings happen more frequently (58%) at a street without a junction.

Figure 46 and Figure 47 depict the main official crash cause within the two assessed datasets. Some of the crash causes indicate who of the participants is officially the main crash causer. Within the graph the causer is indicated with the pedestrian icon for the most frequent crash causes, as follows: green color – car driver is main causer, and red color – pedestrian is main causer. Nevertheless, the question about the fault is complex and would need further investigation.

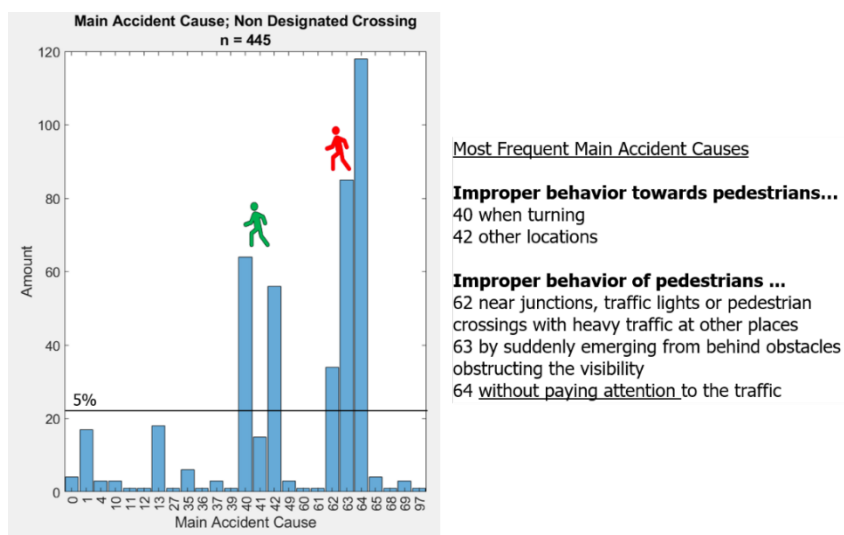


Figure 46 Overview of GIDAS Parameter "HURSU" and "HURSAU", stating the main crash cause in non-designated crossings; green pedestrian means the pedestrian behaved correct; red pedestrian means improper behavior by the pedestrian



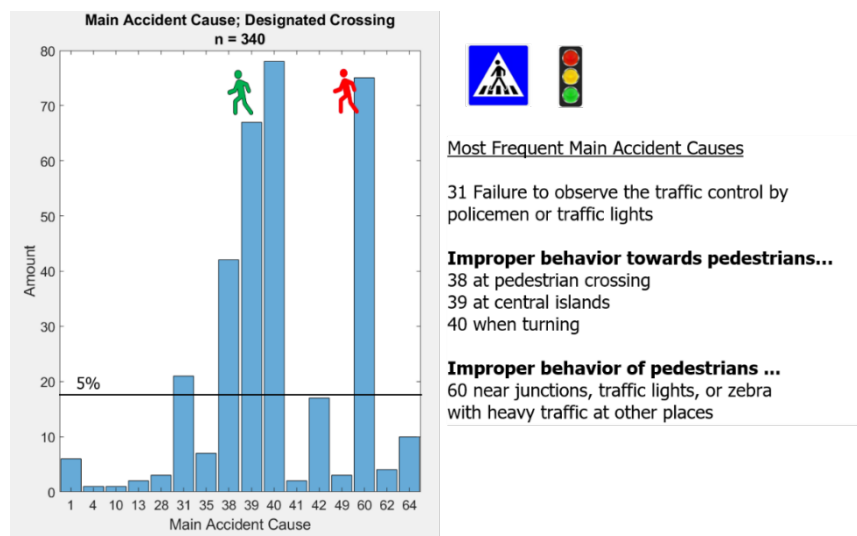


Figure 47 Overview of GIDAS Parameter "HURSU" and "HURSAU", stating the main crash cause in designated crossings; green pedestrian means the pedestrian behaved correct; red pedestrian means improper behavior by the pedestrian

The main official crash causes for crashes at designated crossings are due to failures of the driver to observe the traffic control by police officers or traffic lights, improper behavior of the car driver towards the pedestrians or vice versa. This analysis shows that in most of the cases, the car driver is not behaving properly.

The main crash causes for crashes at non designated crossings are either improper behavior of the driver towards the pedestrian or the other way round. These crashes show more frequently an improper behavior by the pedestrian.

Having a look at the crash descriptions (HERGANG) of the car driver in car-to-pedestrian crashes the situations can be typically described as one of the following alternatives:

- The driver did not see the pedestrian, due to e.g., sight obstruction, darkness;
- The driver overlooked the pedestrian;
- The driver did not see the traffic lights turning red (applicable to designated crossings).

Focusing on the pedestrian the following typical situations occur:

- Pedestrian crossed the street at a red traffic light or the traffic light became red while crossing (applicable to designated-crossing);
- Pedestrian did not see the car or underestimated the car's speed;
- Pedestrian was under the influence of alcohol;
- Pedestrian crossed the street in a hurry to reach the tram or bus;
- Pedestrian did not pay attention to the traffic;
- Child was running into the street.



4.3.1.4 Implications of the infrastructure-based analysis on safety measures

The NDD study based on a JAAD and AMP analysis implies that the interaction between a pedestrian and a car driver depends on whether the pedestrian crosses the street at a designated or a non-designated site; see Table 22. The GIDAS analysis complements this observation with the following, additional results.

It can be stated that the support by the infrastructure at designated crossing sites should ensure a safe crossing by the pedestrian if no violations are done by any participant. Infrastructure such as traffic lights can regulate the traffic to such an extent that no or little communication of the traffic participants would be needed. Nevertheless, a considerable number of crashes happen at traffic lights because of violations by the participants, e.g., pedestrians crossing at red traffic lights. These crashes may be prevented by road safety education. Other infrastructure measures such as zebra crossings solely indicate that the crossing of a pedestrian is likely. In these cases, a communication of both participants with each other would make the crossing of a pedestrian safer.

The non-designated crossing scenarios are characterized by not having infrastructural measures supporting and indicating the crossing of a pedestrian. Therefore, the crossing of the street needs to be well planned by the pedestrian. If the paths of a car and a pedestrian would meet, communication between the involved participants is essential. Crashes at non-designated crossings often are characterized by missing or failing interaction of both participants in regards of perception. These crashes tend to happen more frequently than crashes at designated crossings and seem to lead more often to severely or fatally injured pedestrians. In crossing scenarios of pedestrians where communication is needed, there is the opportunity for Cooperative Intelligent Transport Systems to provide a safety benefit.

4.3.2 Car-to-bicyclist crashes

While pedestrians were the most exposed VRU group to road fatalities in the EU (see Table 4), it is cyclists that are exposed to most injury crashes (Table 3). Notably, the same tables show that while most car-to-bicycles crashes occur in urban areas (90% of the affected cyclist suffer injuries in urban areas), the number of cyclist fatalities in car-to-bicycle crashes is only slightly larger in urban areas compared to the corresponding fatalities in rural areas (52% vs 47%, respectively). This result indicates that protecting bicyclists in fatal car-to-bicycle crashes may possibly require additional measures compared to those required to address the largest part of car-to-bicycle crashes. Section 4.3.2.1 contains an in-depth analysis of car-to-bicycle crashes of all injury levels as well as those with a serious or fatal outcome (i.e., KSI crashes), based on GIDAS data.

4.3.2.1 Filter criteria for the analysis of car-to-bicycle crashes in GIDAS

In the following paragraph, the assumptions and the results of the in-depth data analysis of car-to-bicycles crashes will be described. The focus of the analysis is on injured cyclists.



During the analysis, the conflicts that have led to a crash are in focus. They are described first, and in a later step, various aspects including the weather condition as well as sight obstructions regarding different injury severities of cyclists are investigated. The data analyzed is the GIDAS dataset (see section 3.2.2) from June 2020. The filter criteria shown in Table 23 have been used to identify the basic dataset.

Table 23 Criteria for the selection of car-to-bicycle crashes from the GIDAS database

Filter variable	Value	Explanation
STATUS	4	Cases with completed reconstruction
JAHR	>1999	Data are from the year 2000 or later
FART	3	Identification of passenger cars
FZART	<= 26 OR 56 OR 60-62	
FZGKLASS	< 15	
FAHRRAD record	Present	FAHRRAD Record needs to be present
UTYP, UTYPA, UTYPB	All	The crash type variables are considered to describe the conflict before the crash happens. The roles are used to identify the participants in conflict

A set of 7 877 crashes involving 8 036 passenger cars and 7 949 bicycles and 8 007 cyclists remain after filtering the GIDAS data. Of the identified crashes 97.5% happened in urban areas, 2.4% in rural areas and 0.01% on motorways.

The following stepwise approach was applied to identify the final GIDAS dataset:

1. Step: Assign the passenger car a role within the crash, which is causer (A) or non-causer (B) of the conflict.
2. Step: Include the following crashes:
 - a) Bicycle in their first collision in role A, B, or other (only with UTYP=1xx or UTYP=7xx) with passenger cars, which are in role A or B and its first collision;
 - b) Bicycles, which are in role A or B.
3. Step: Exclude the following crashes:
 - a) First collision of bicycle with another participant;
 - b) All others not matching the criteria above.

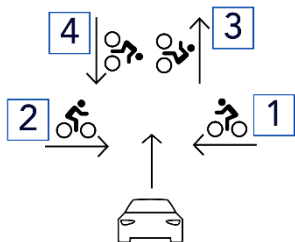

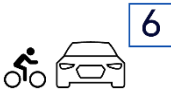
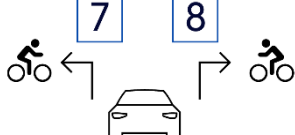


After the above stepwise approach, there remained data from 7 660 injured cyclists, thereof 99.6% riders, and 7 629 bicycles, thereof 2.3% pedelecs (electric bicycles). The remaining 7 660 cyclists in the dataset are the basis for the next steps.

4.3.2.2 Clustering of car-to-bicycle crashes

Based on the UTYP variable in GIDAS indicating the conflict situation that led to the crash, nine scenarios of conflicts between passenger cars (PC) and bicyclists (B) were defined, see Table 24 below.

Table 24 Scenario clustering in passenger car-to-bicycle crashes

Conflict scenario	Abbreviation	Schematic illustration
PC moves forward		
1. Bicyclist crossing from right	B-CR	
2. Bicyclist crossing from left	B-CL	
3. Bicyclist longitudinal same direction	B-LongSD	
4. Bicyclist longitudinal opposite direction	B-LongOD	
PC moves backwards		
5. Bicyclist in conflict with PC reversing	B-PCRev	
PC is stationary		
6. Bicyclist in conflict with stationary PC	B-PCStat	
PC turns		
7. Bicyclist in conflict with PC turning left	B-PCTurnL	
8. Bicyclist in conflict with PC turning right	B-PCTurnR	
PC in other crashes		
9. Bicyclist Other	B-Oth	

The clustered data results in a set of 7 660 cyclists in the 9 scenarios defined in Table 24, of which 1 567 got killed or severely injured (KSI). About 98% of the filtered conflict scenarios are crashes in urban areas; however, notably, about 20% of all longitudinal cases take place in rural areas. Approximately 58% of the injured cyclists are involved in crossing crashes. Regarding KSI cyclists, the share increases to approximately 63%.

It is notable that both crossing scenarios, i.e., ‘crossing left’ (22.4% of all cases) and ‘crossing right’ (35.2%) had a larger percentage when considering only cyclists with the



injury severity KSI (25.5% B-CL and 37.8% B-CR). The scenarios 'longitudinal same direction' (5.4% / 6.2% KSI) 'turning left' (9.3% / 10% KSI) had a slightly higher share within the KSI dataset while all the other scenarios have a lower KSI percentage compared to their overall prevalence.

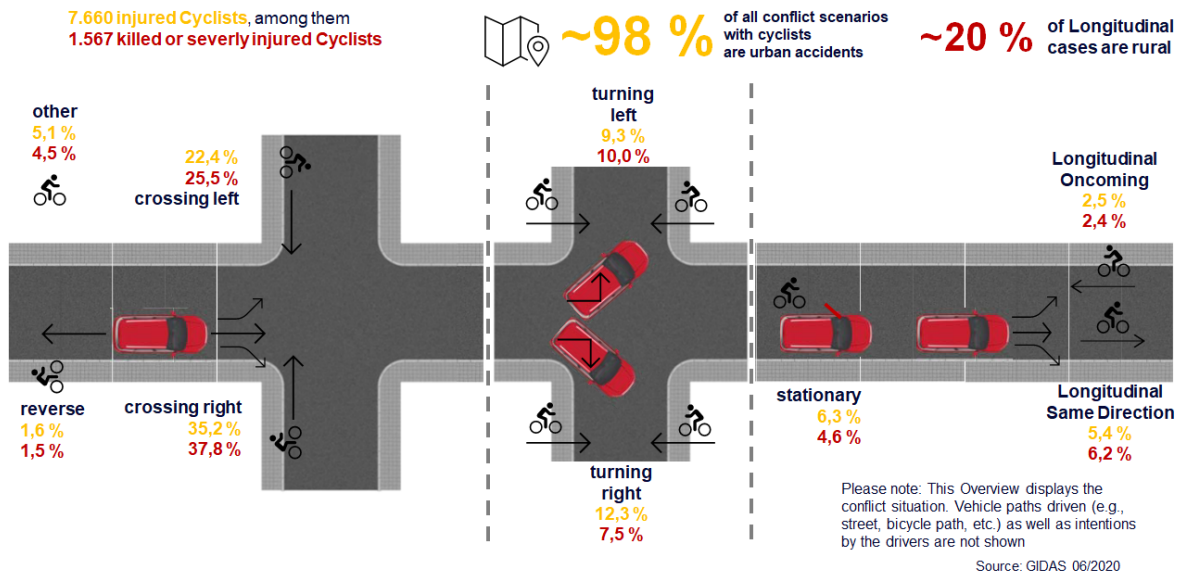


Figure 48 Overview of conflict scenarios for C2B crashes – schematic representation

The final dataset is analyzed regarding the following aspects:

- Relation to junction;
- Availability and usage of bicycle path;
- Passenger car speed distribution (initial / collision);
- Cyclist speed distribution (initial / collision);
- Time of day;
- Sight obstruction;
- Weather conditions that adversely affect sensor performance: precipitation (aggregates the following weather conditions: rain, snow, hail and sleet) and fog;
- Crash type using the UTYP classification in GIDAS (GDV, 2016);
- Pre-crash trajectories;
- Crash causes.

In the following paragraphs the conflict scenarios defined in Table 24 are summarized with the results of all aspects mentioned above. As the cluster “9-Other” includes a wide variety of situations without clear common characteristics, it is not analyzed here.

A summary of the eight C2B conflict scenarios with an additional overview of crash causes for participants of car-to-bicycle crashes is given in Table 53 and Table 54 in the Appendix.



4.3.2.2.1 Conflict scenario B-CR

An overview of C2B conflict scenario 1: Bicyclist crossing from right while PC moves forward (B-CR) is provided in Figure 49.

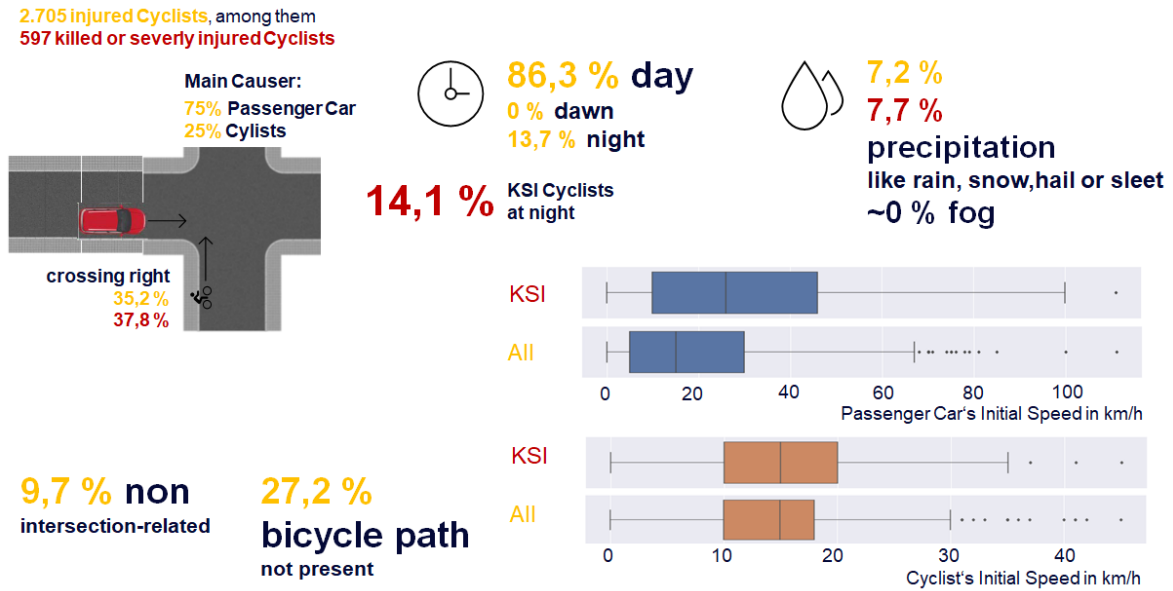


Figure 49 Results summary for C2B conflict scenario 1: B-CR

In total, there were 2 705 injured cyclists in B-CR scenarios. Among them, 597 were killed or severely injured (KSI). As shown in Table 25, most of all injury and KSI cases are described by the crash type with the number 342: ‘crossing - bicycle with right of way from bicycle lane right and straight’.

Table 25 Classification by crash type within B-CR

	UTYP 342	UTYP 371	UTYP 301
Pictogram			
Proportion of injured (all severities)	62.0%	12.5%	7.6%
Proportion of KSI	43.0%	19.1%	13.4%

Figure 50 shows the trajectories of 1 142 cyclists including all severities identified based on the GIDAS-PCM 2020-1 dataset.

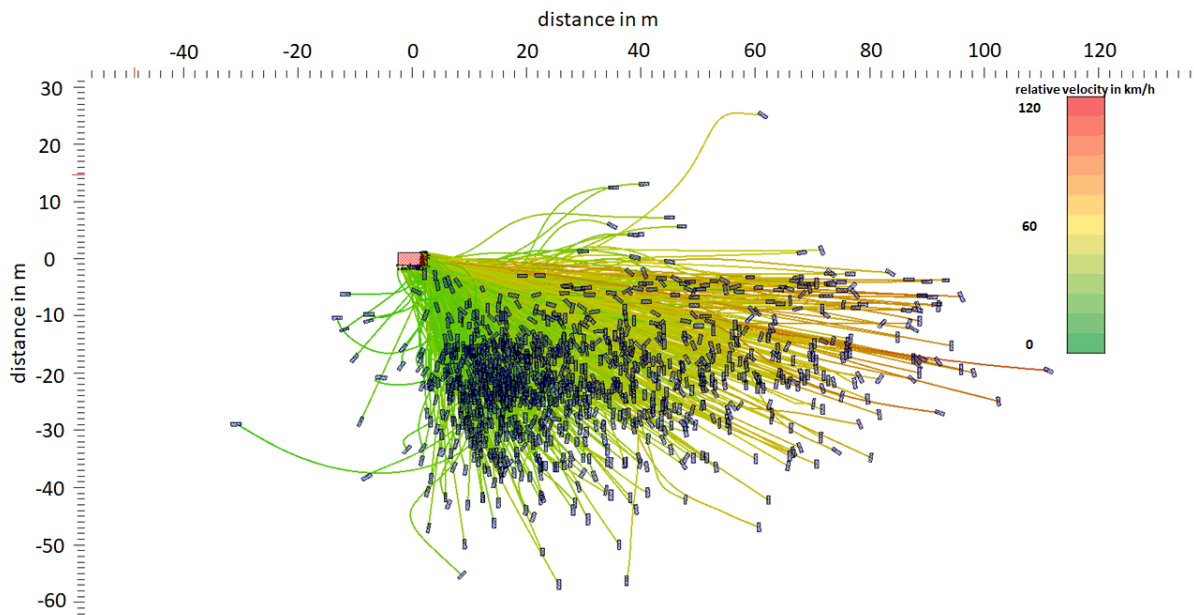


Figure 50 B-CR trajectories showing the relative motion of bicyclists w.r.t. the passenger car

Figure 51 below shows absolute trajectories.

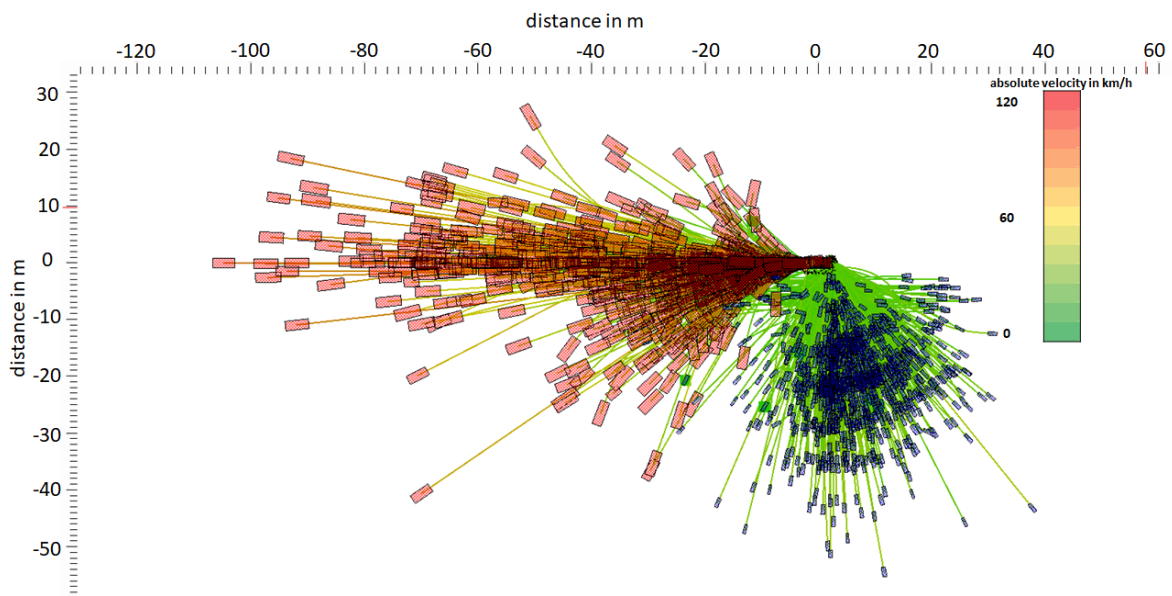


Figure 51 Trajectories of bicyclists - and passenger cars relative to the collision point in B-CR scenarios -passenger car heading east (to the right) at collision point.



4.3.2.2.2 Conflict scenario B-CL

An overview of C2B conflict scenario 2: Bicyclist crossing from left while PC moves forward (B-CL) is provided in Figure 52.

1.707 injured Cyclists, among them 397 killed or severely injured Cyclists

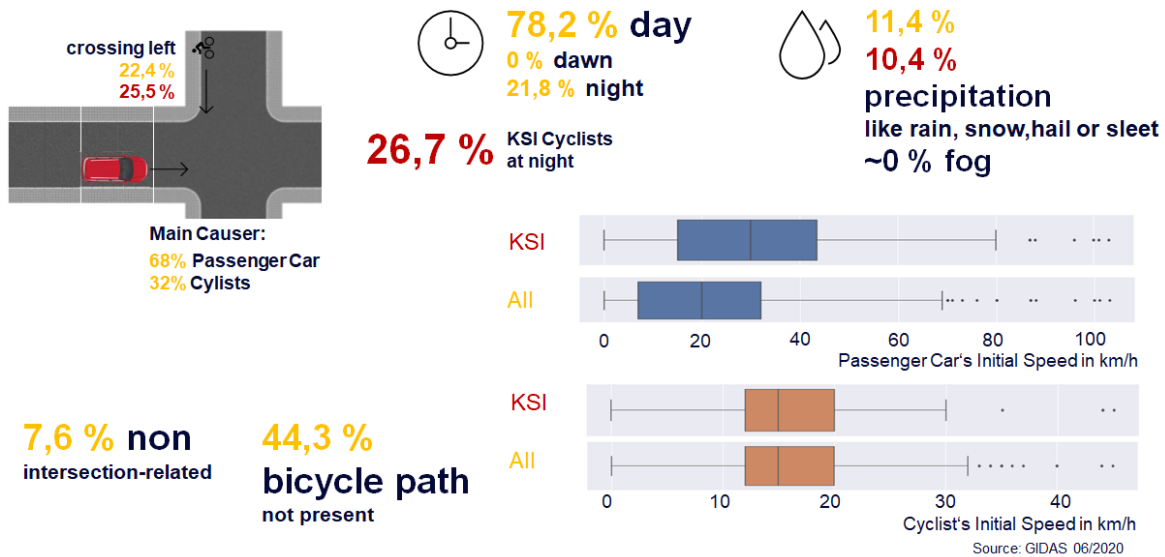


Figure 52 Results summary for C2B conflict scenario 2: B-CL

In total, there are 1 707 injured cyclists in B-CL scenarios. Among them, 397 were killed or severely injured (KSI). As shown in Table 26, most of all injury and KSI cases are described by the crash type with the number 341: 'Crossing - bicycle with right of way from bicycle lane left and straight'.

Table 26 Classification by crash type within B-CL

	UTYP 341	UTYP 321	UTYP 372
Pictogram			
Proportion of injured (all severities)	38.1%	18.4%	10.4%
Proportion of KSI	27.7%	28.0%	14.4%



Figure 53 shows the trajectories of 788 cyclists including all severities identified based on the GIDAS-PCM 2020-1 dataset.

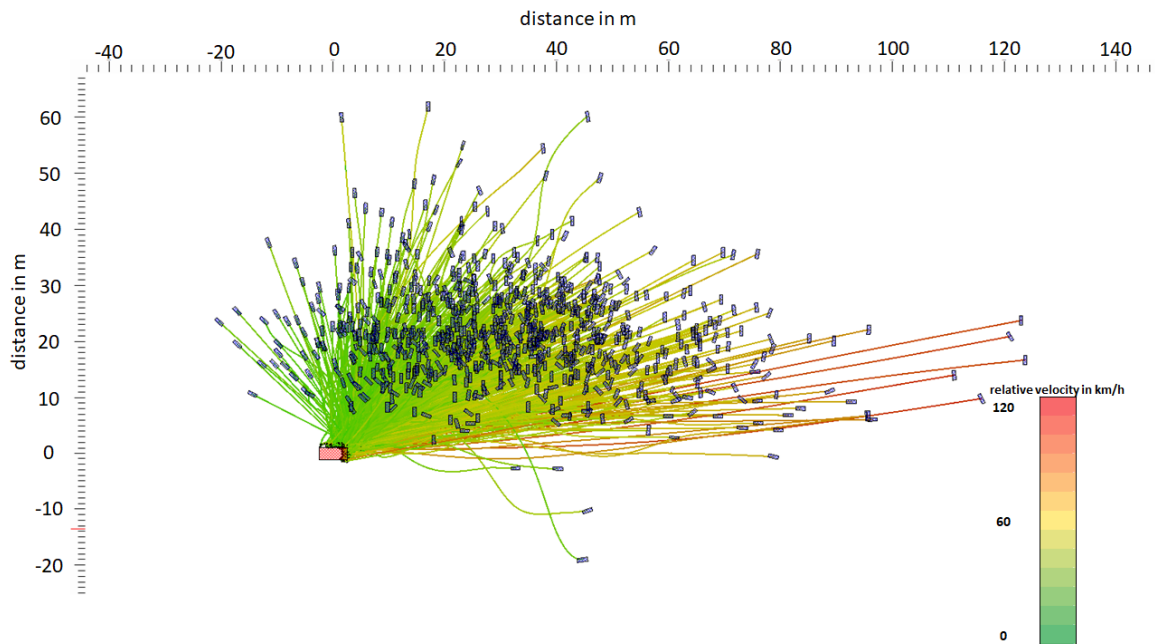


Figure 53 B-CL trajectories showing the relative motion of bicyclists w.r.t. the passenger car

Figure 54 below shows absolute trajectories.

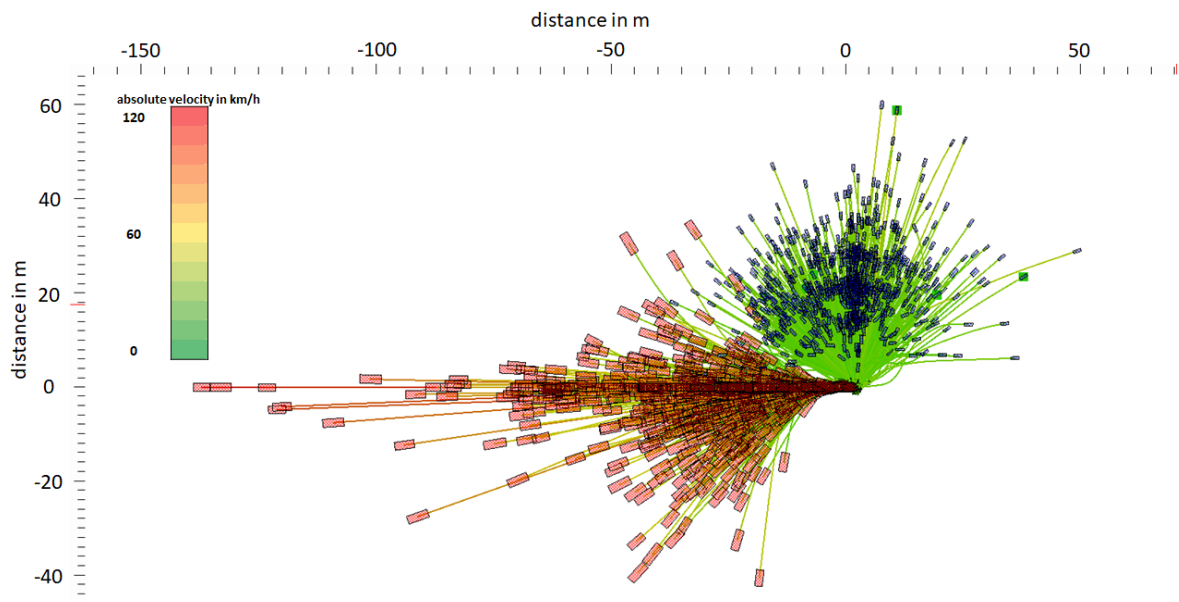


Figure 54 Trajectories of bicyclists - and passenger cars relative to the collision point in B-CL scenarios -passenger car heading east (to the right) at collision point.



4.3.2.2.3 Conflict scenario B-LongSD

An overview of C2B conflict scenario 3: Bicyclist longitudinal same direction while PC moves forward (B-LongSD) is provided in Figure 55.

412 injured Cyclists, among them
98 killed or severely injured Cyclists

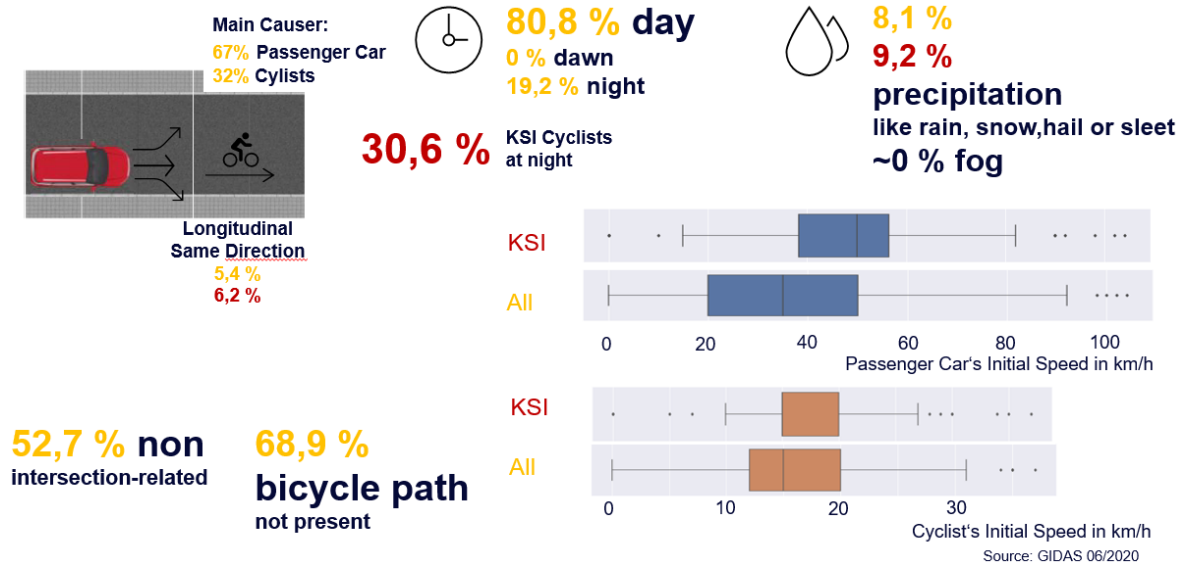


Figure 55 Results summary for C2B conflict scenario 3: B-LongSD

In total, there are 412 injured cyclists in B-LongSD scenarios. Among them, 98 were killed or severely injured (KSI).

As shown in Table 27, most of all injury cases are described by the crash type with the number 651: 'Longitudinal Traffic - parallel driving in same direction'. The crash type 601: 'Longitudinal Traffic - vehicle and follower in one lane' is included in Table 27 instead of the slightly more common crash type 551: 'Resting Traffic – starting or parking out longitudinal on the right, same direction' (which has a share of 10.0% among all injured, but only 2.0% among KSI) because UTYP 601 has the highest share for KSI cyclists within B-LongSD among all crash types.

Table 27 Classification by crash type within B-LongSD

	UTYP 651	UTYP 202	UTYP 601
Pictogram			
Proportion of injured (all severities)	18.2%	11.9%	9.5%
Proportion of KSI	14.3%	14.3%	19.4%



Figure 56 shows the trajectories of 167 cyclists including all severities identified based on the GIDAS-PCM 2020-1 dataset.

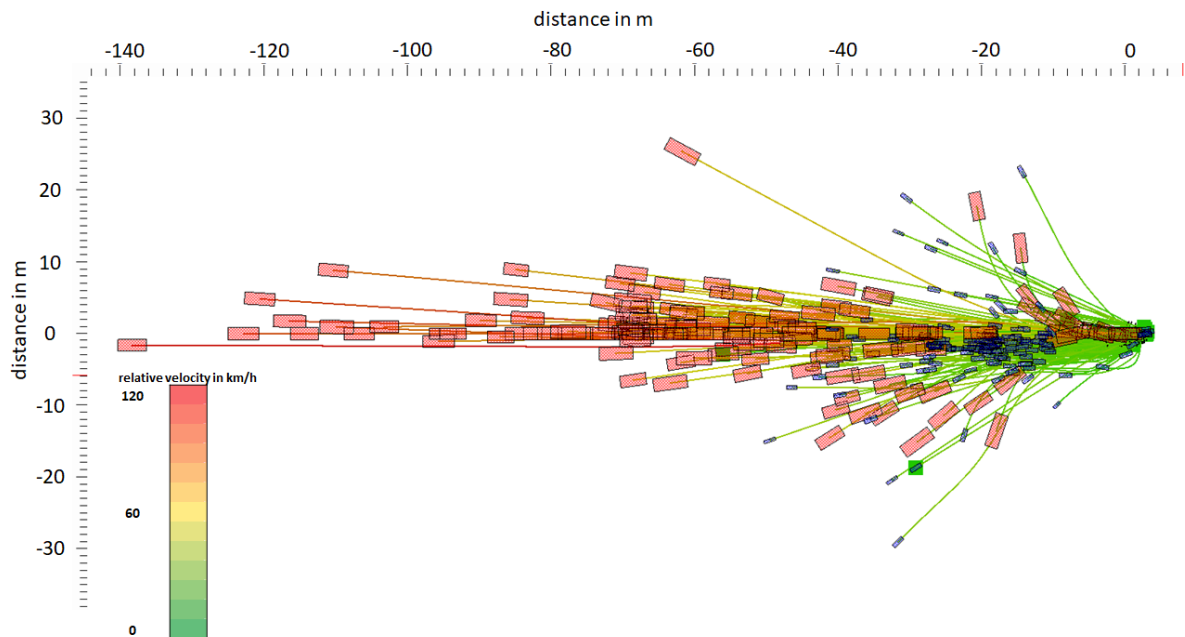


Figure 56 B-LongSD trajectories showing the relative motion of bicyclists w.r.t. the passenger car

Figure 57 below shows absolute trajectories.

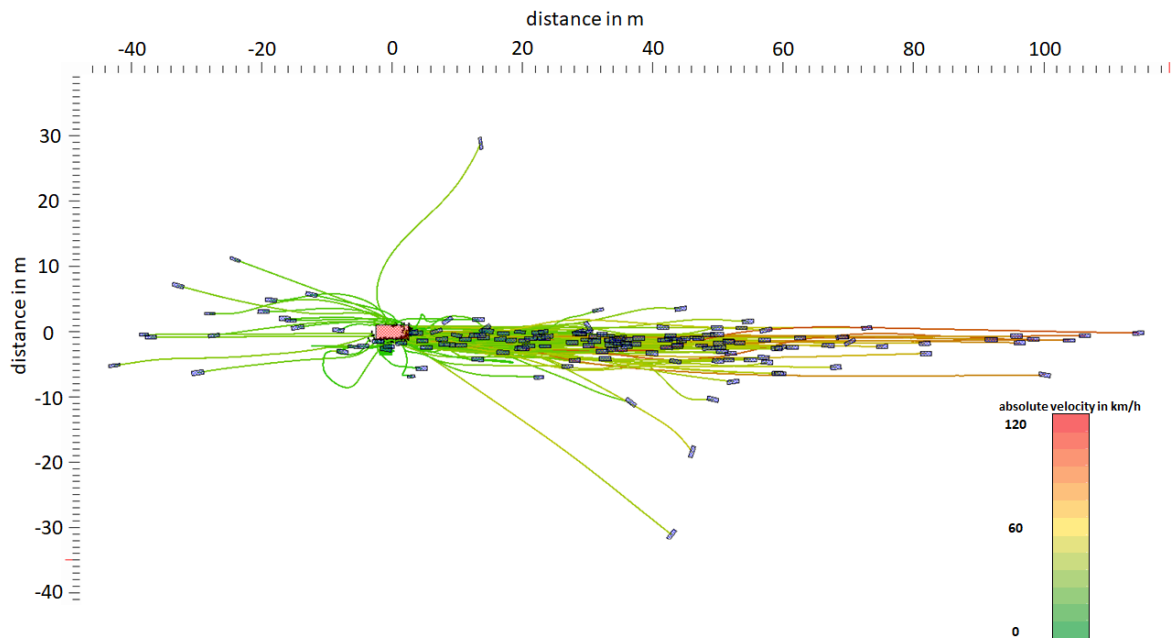


Figure 57 Trajectories of bicyclists - and passenger cars relative to the collision point in B-LongSD scenarios -passenger car heading east (to the right) at collision point.



4.3.2.2.4 Conflict scenario B-LongOD

An overview of C2B conflict scenario 4: Cyclist longitudinal opposite direction while PC moves forward (B-LongOD) is provided in Figure 58.

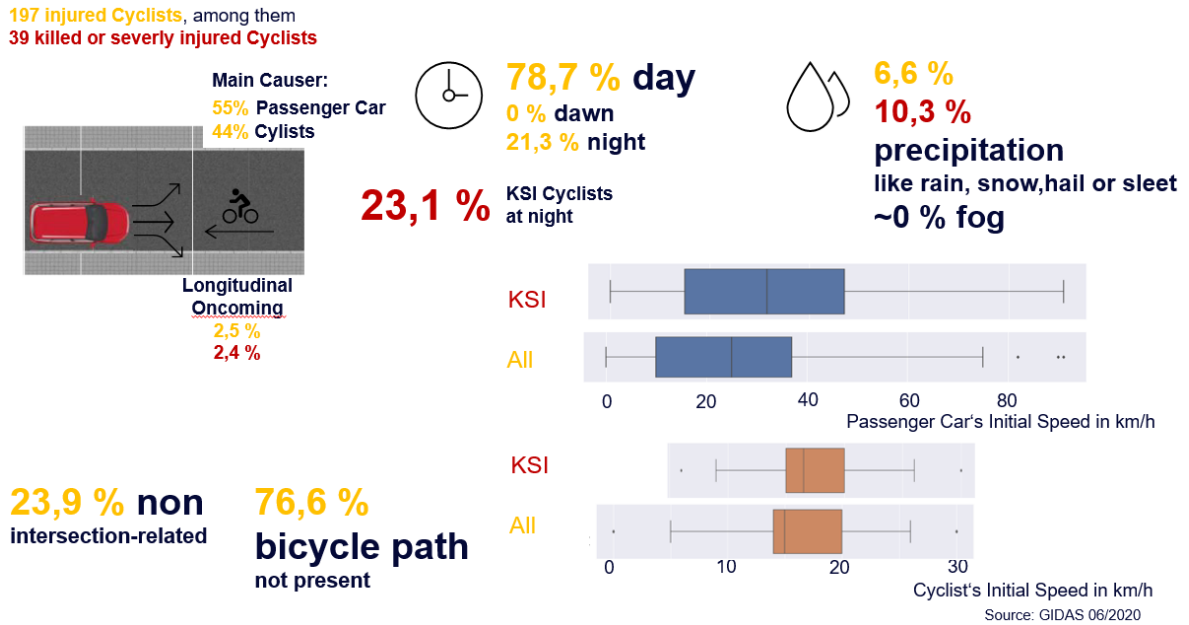


Figure 58 Results summary for C2B conflict scenario 4: B-LongOD

In total, there were 197 injured cyclists in B-LongOD scenarios. Among them, 39 were killed or severely injured (KSI).

As shown in Table 28, most of all injury cases are described by the crash type with the number 681: 'Longitudinal Traffic - encountering vehicles on straight'. The crash type 211: 'Turning - left turning vehicle and oncoming traffic in lane, straight' has the highest share for KSI cyclists.

Table 28 Classification by crash type within B-LongOD

	UTYP 681	UTYP 211	UTYP 351
Pictogram			
Proportion of injured (all severities)	27.4%	20.8%	18.3%
Proportion of KSI	25.6%	28.2%	12.8%



Figure 59 shows the trajectories of 70 cyclists including all severities identified based on the GIDAS-PCM 2020-1 dataset.

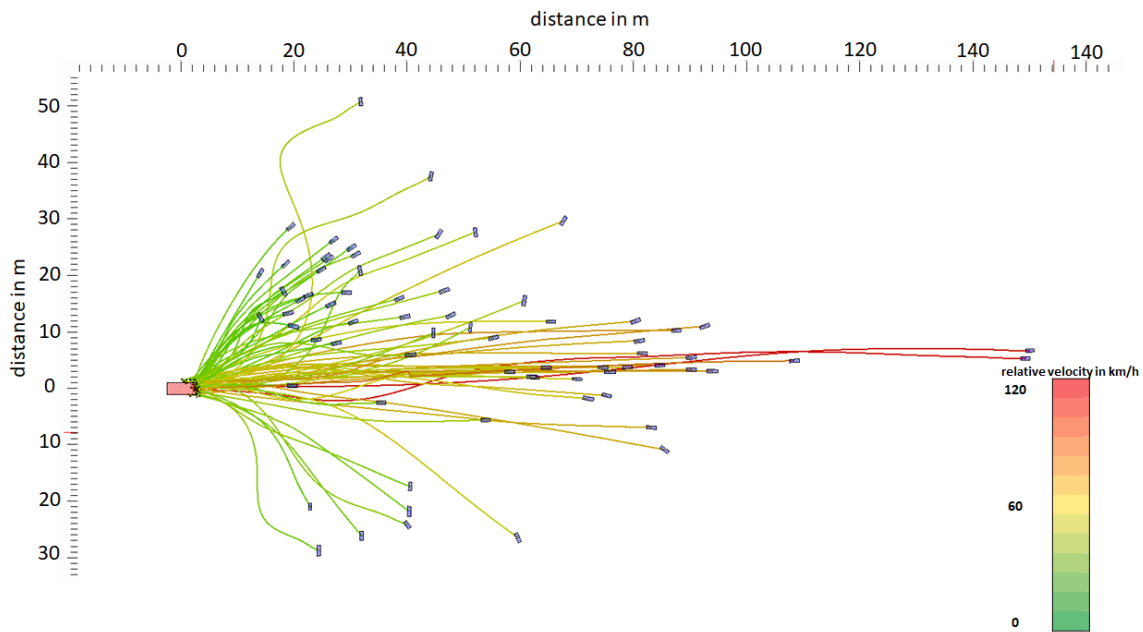


Figure 59 B-LongOD trajectories showing the relative motion of bicyclists w.r.t. the passenger car

Figure 60 below shows the absolute trajectories.

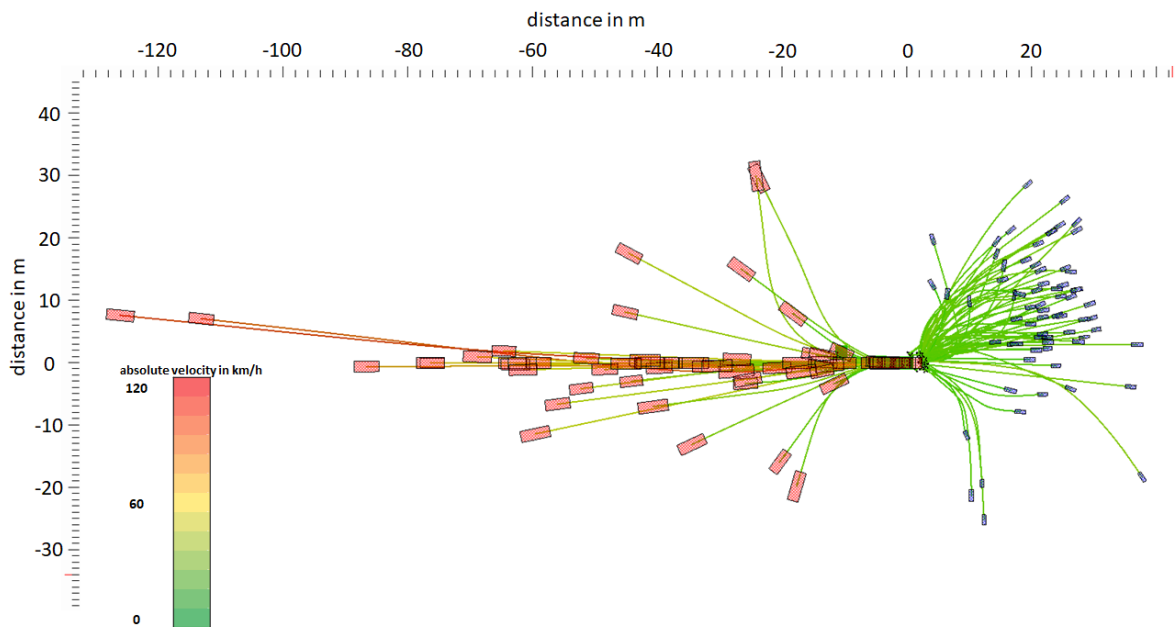


Figure 60 Trajectories of bicyclists - and passenger cars relative to the collision point in B-LongOD scenarios -passenger car heading east (to the right) at collision point.



4.3.2.2.5 Conflict scenario B-PCRev

An overview of C2B conflict scenario 5: Bicyclist in conflict with PC reversing (B-PCRev) is provided in Figure 61.

121 injured Cyclists, among them
23 killed or severely injured Cyclists

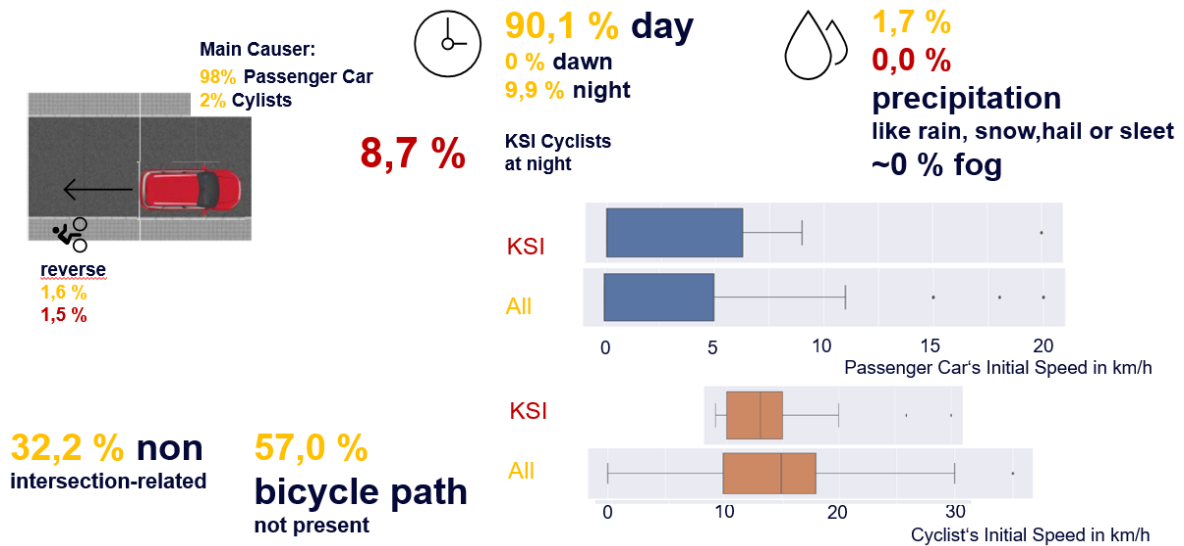


Figure 61 Results summary for C2B conflict scenario 5: B-PCRev

In total, there are 121 injured cyclists in B-PCRev scenarios. Among them, 23 were killed or severely injured (KSI).

As shown in Table 29, most of all injury and KSI cases are described by the crash type with the number 571: 'Resting Traffic - parking out backward from perpendicular position on the right'. The crash type 711: 'Others - vehicle backing up by driving and parker behind' is included in Table 27 instead of the slightly more common crash type 715: 'Others - vehicle backing out from the left side and crossing traffic on the road' (which has a share of 16.5% among all injured, but only 8.7% among KSI) because UTYP 711 has a substantially higher share of KSI cyclists within B-PCRev (21.7%).

Table 29 Classification by crash type within B-PCRev

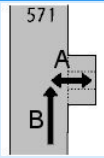
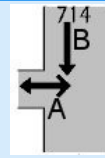
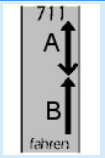
	UTYP 571	UTYP 714	UTYP 711
Pictogram			
Proportion of injured (all severities)	28.1%	23.1%	14.9%
Proportion of KSI	34.8%	21.7%	21.7%



Figure 62 shows the trajectories of 24 cyclists including all severities identified based on the GIDAS-PCM 2020-1 dataset.

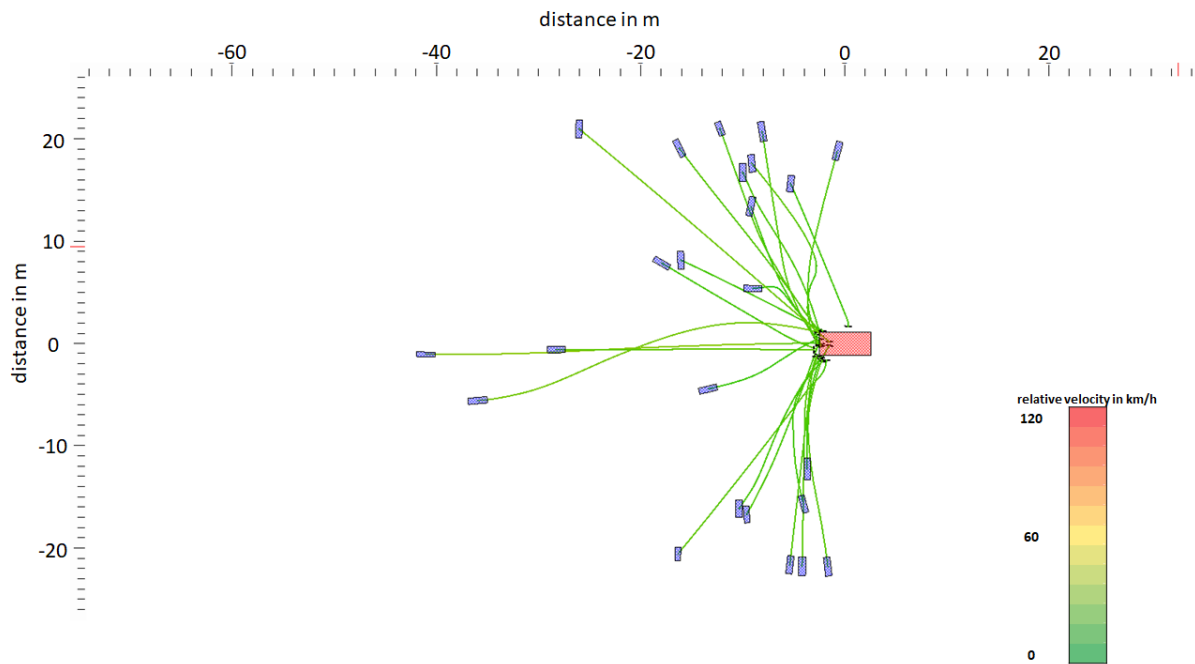


Figure 62 B-PCRev trajectories showing the relative motion of bicyclists w.r.t. the passenger car

Figure 63 below shows the absolute trajectories.

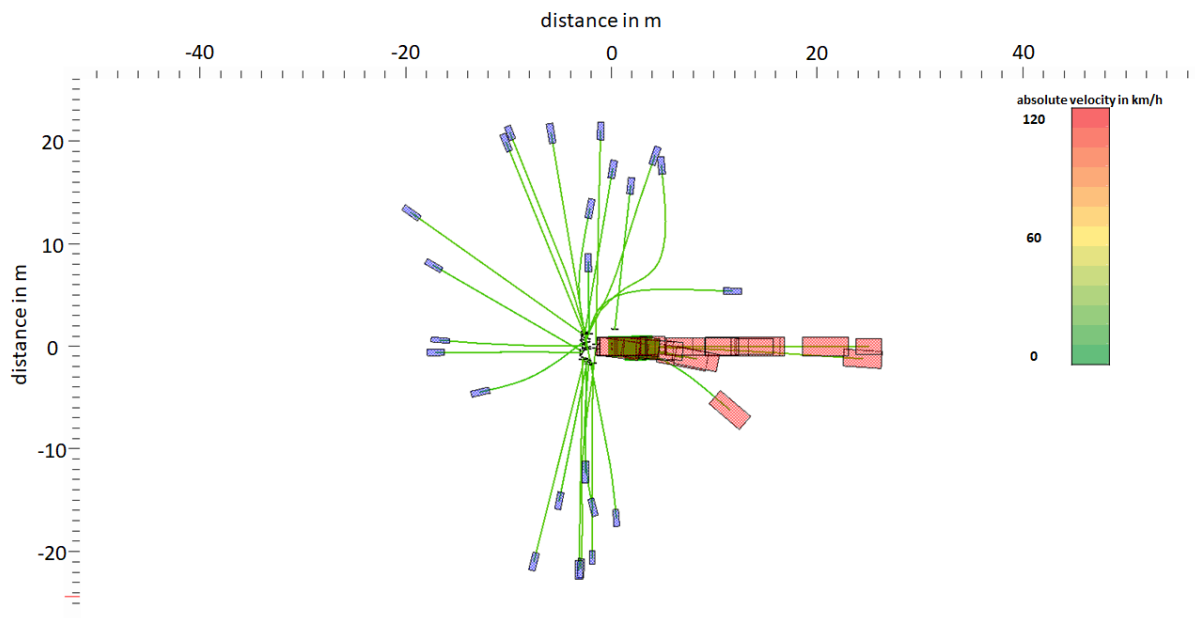


Figure 63 T Trajectories of bicyclists - and passenger cars relative to the collision point in B-PCRev scenarios -passenger car heading east (to the right) at collision point.



4.3.2.2.6 Conflict scenario B-PCStat

An overview of C2B conflict scenario 6: Bicyclist in conflict with stationary PC (B-PCStat) is provided in Figure 64.

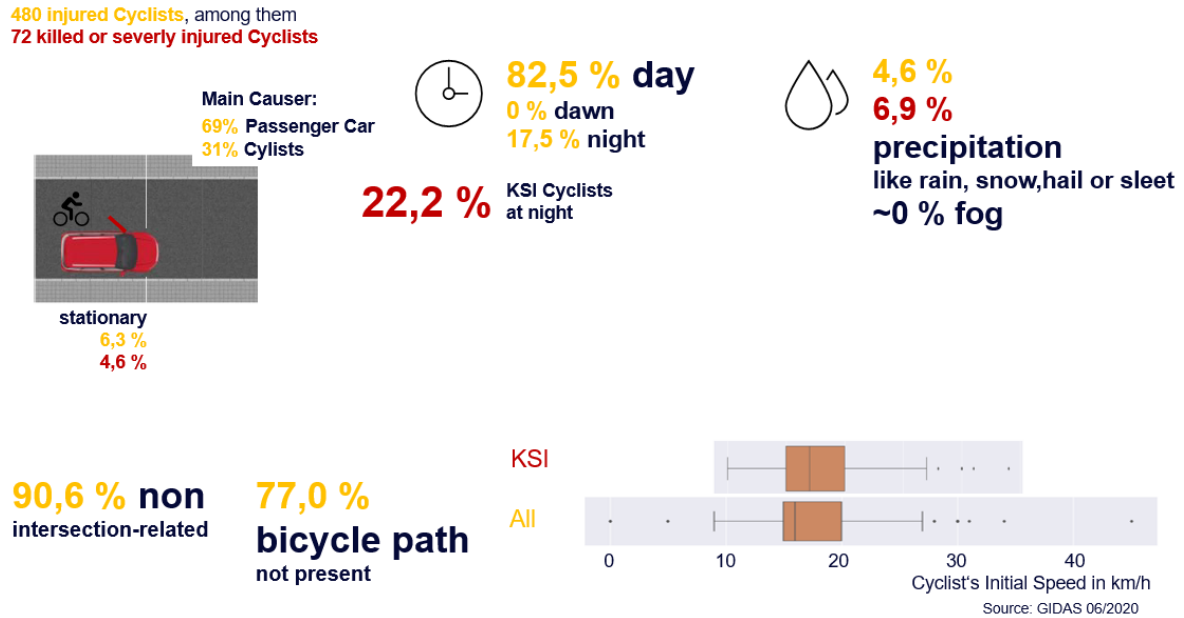


Figure 64 Results summary for C2B conflict scenario 6: B-PCStat

In total, there are 480 injured cyclists in B-PCStat scenarios. Among them, 72 were killed or severely injured (KSI). IAs shown in Table 30, most of all injury and KSI cases are described by the crash type with the number 581: 'Resting Traffic - door opening while getting in or out on the right'.

Table 30 Classification by crash type within B-PCStat

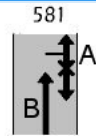
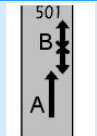
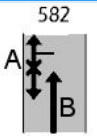
	UTYP 581	UTYP 501	UTYP 582
Pictogram			
Proportion of injured (all severities)	60.4%	21.9%	8.8%
Proportion of KSI	63.9%	20.8%	2.8%

Figure 65 shows the trajectories of 35 cyclists including all severities identified based on the GIDAS-PCM 2020-1 dataset.

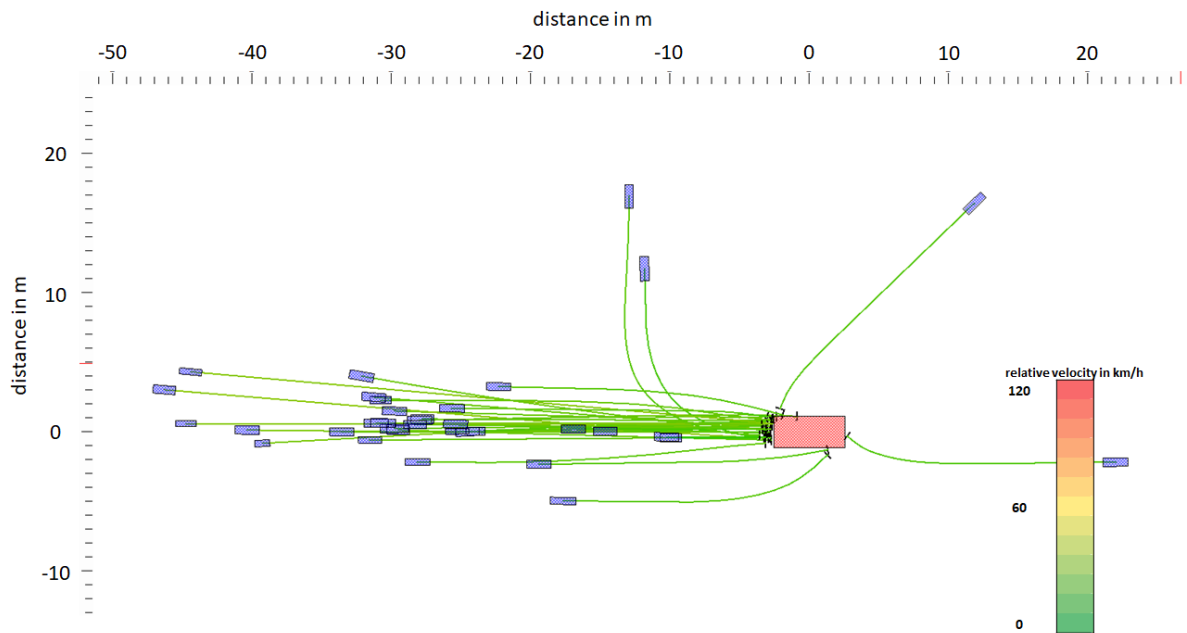


Figure 65 B-PCStat trajectories showing the relative motion of bicyclists w.r.t. the passenger car

Figure 66 below shows absolute trajectories.

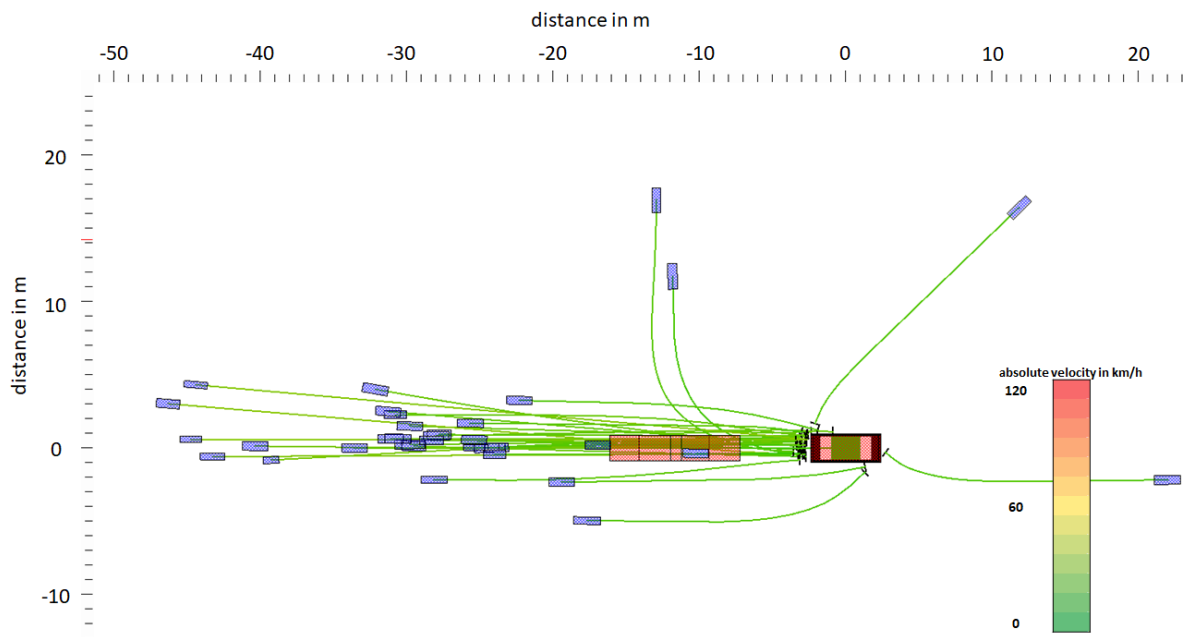


Figure 66 Trajectories of bicyclists - and passenger cars relative to the collision point in B-PCStat scenarios -passenger car heading east (to the right) at collision point.



4.3.2.2.7 Conflict scenario B-PCTurnL

An overview of C2B conflict scenario 7: Bicyclist in conflict with PC turning left (B-PCTurnL) is provided in Figure 67.

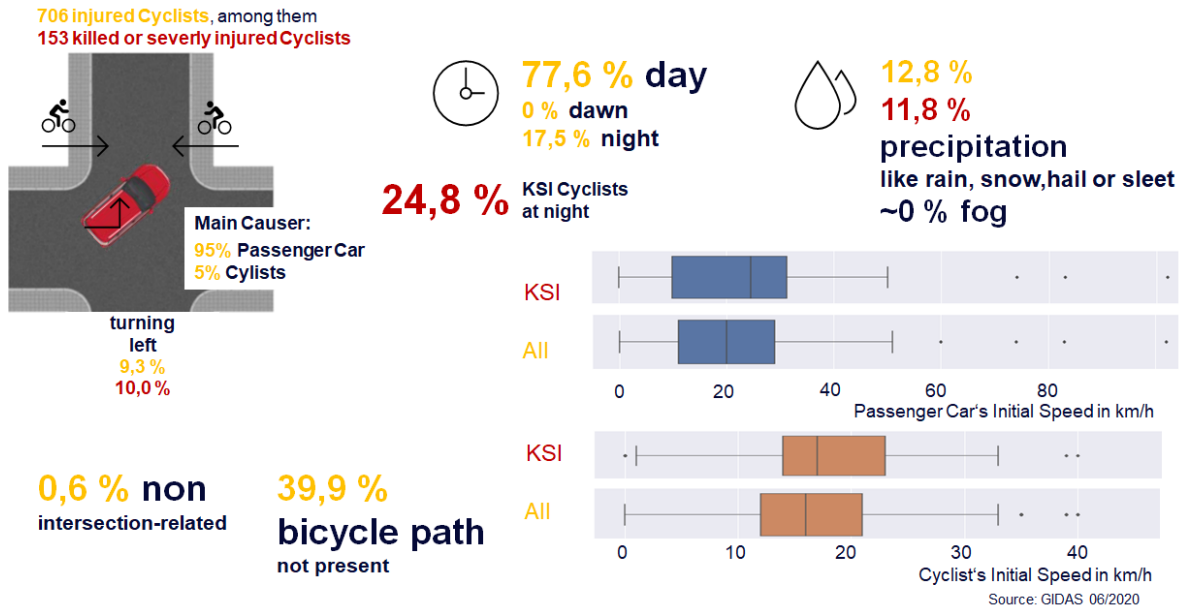


Figure 67 Results summary for C2B conflict scenario 7: B-PCTurnL

In total, there are 706 injured cyclists in B-PCTurnL scenarios, among them 153 were killed or severely injured (KSI). As shown in Table 31, the most common of all injury and KSI cases is described by the conflict UTYP 224: 'Turning - left turning vehicle and cyclist from bicycle lane in opposite direction'.

Table 31 Classification by crash type within B-PCTurnL

	UTYP 224	UTYP 211	UTYP 223
Pictogram			
Proportion of injured (all severities)	41.2%	34.8%	16.6%
Proportion of KSI	39.9%	35.9%	17.0%



Figure 68 shows the trajectories of 278 cyclists including all severities, based on the GIDAS-PCM 2020-1 dataset.

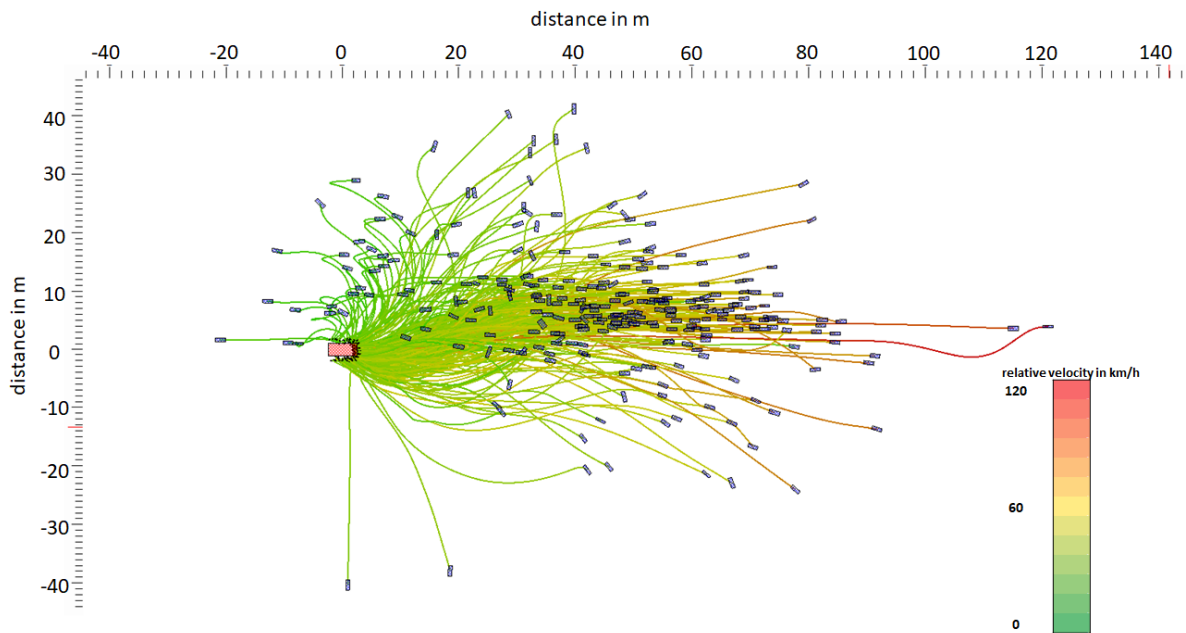


Figure 68 B-PCTurnL trajectories showing the relative motion of bicyclists w.r.t. the passenger car

Figure 69 shows absolute trajectories.

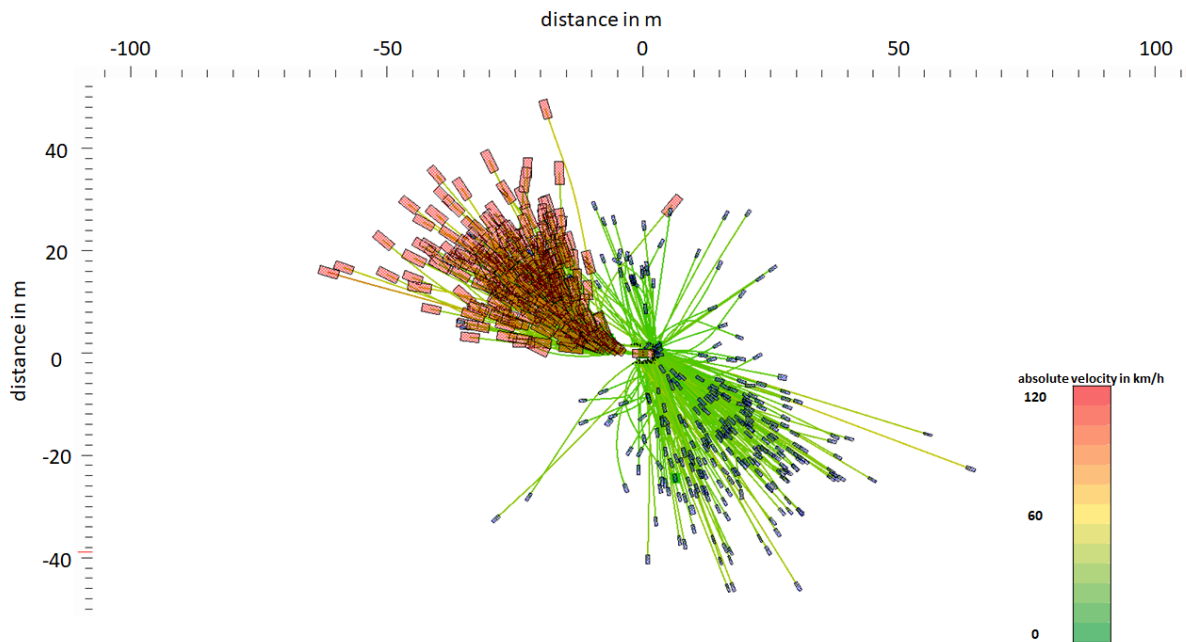


Figure 69 Trajectories of bicyclists - and passenger cars relative to the collision point in B-PCTurnL scenarios -passenger car heading east (to the right) at collision point.



4.3.2.2.8 Conflict scenario B-PCTurnR

An overview of C2B conflict scenario 8: Bicyclist in conflict with PC turning right (B-PCTurnR) is provided in Figure 70.

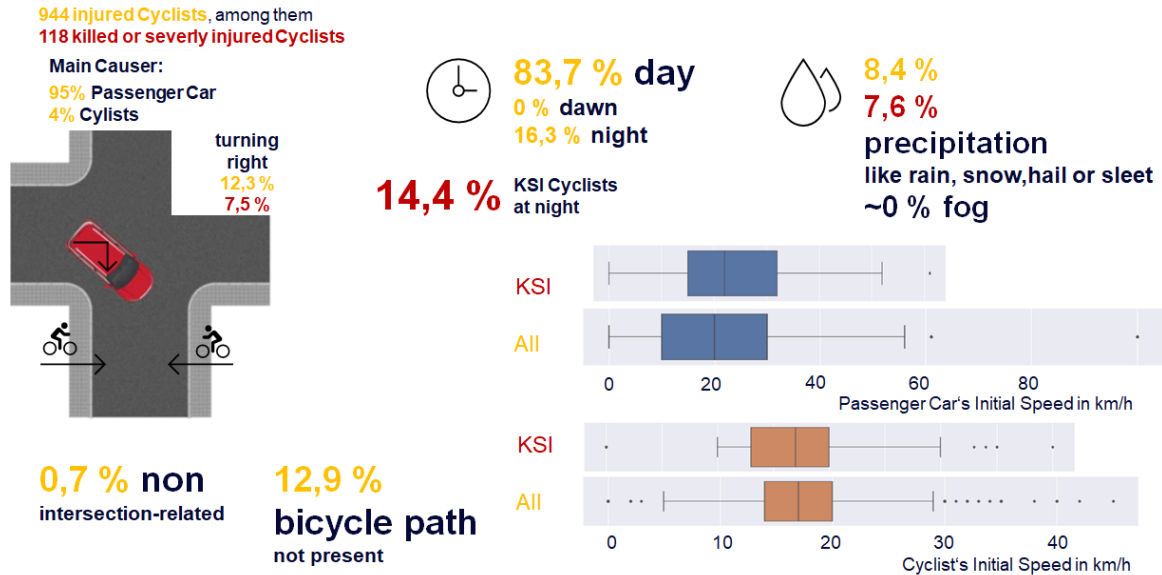


Figure 70 Results summary for C2B conflict scenario 8: B-PCTurnR

In total, there are 944 injured cyclists in B-PCTurnR scenarios. Among them, 118 were killed or severely injured (KSI).

As shown in Table 32, the most common of all injury and KSI cases is described by the conflict UTP 243: 'Turning - right turning veh. and cyclist from bicycle lane in same direction'.

Table 32 Classification by crash type within B-PCTurnR

	UTYP 243	UTYP 244	UTYP 232
Pictogram			
Proportion of injured (all severities)	54.6%	31.7%	8.2%
Proportion of KSI	47.5%	32.2%	13.6%



Figure 71 shows the trajectories of 338 cyclists including all severities based on the GIDAS-PCM 2020-1 dataset.

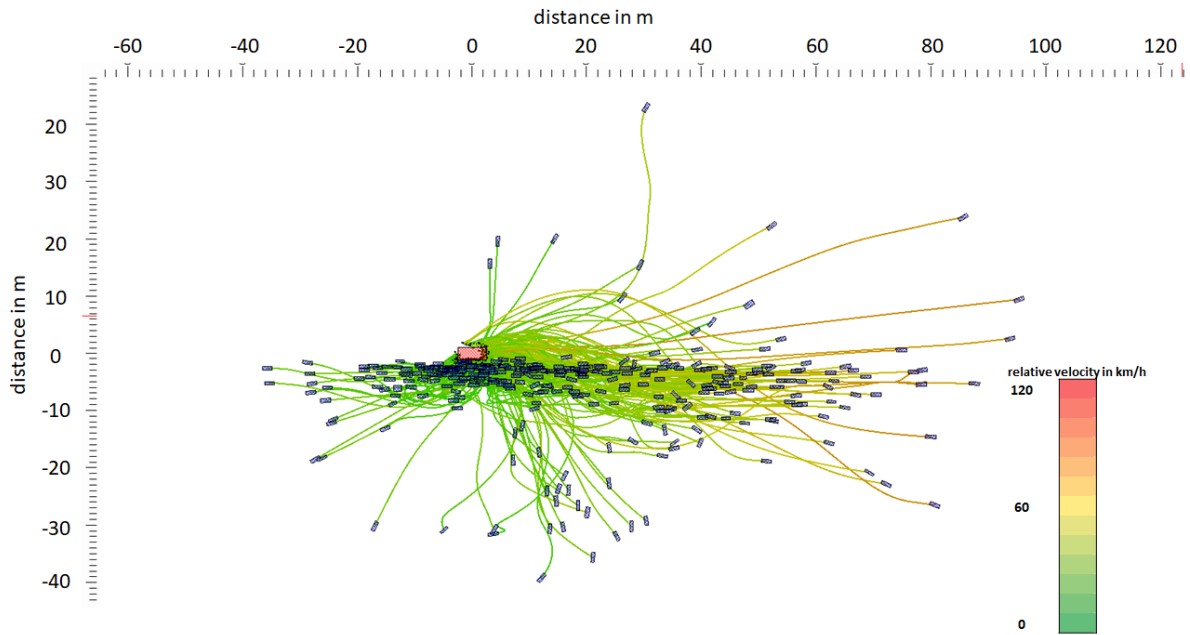


Figure 71 B-PCTurnR trajectories showing the relative motion of bicyclists w.r.t. the passenger car

Figure 72 below shows absolute trajectories.

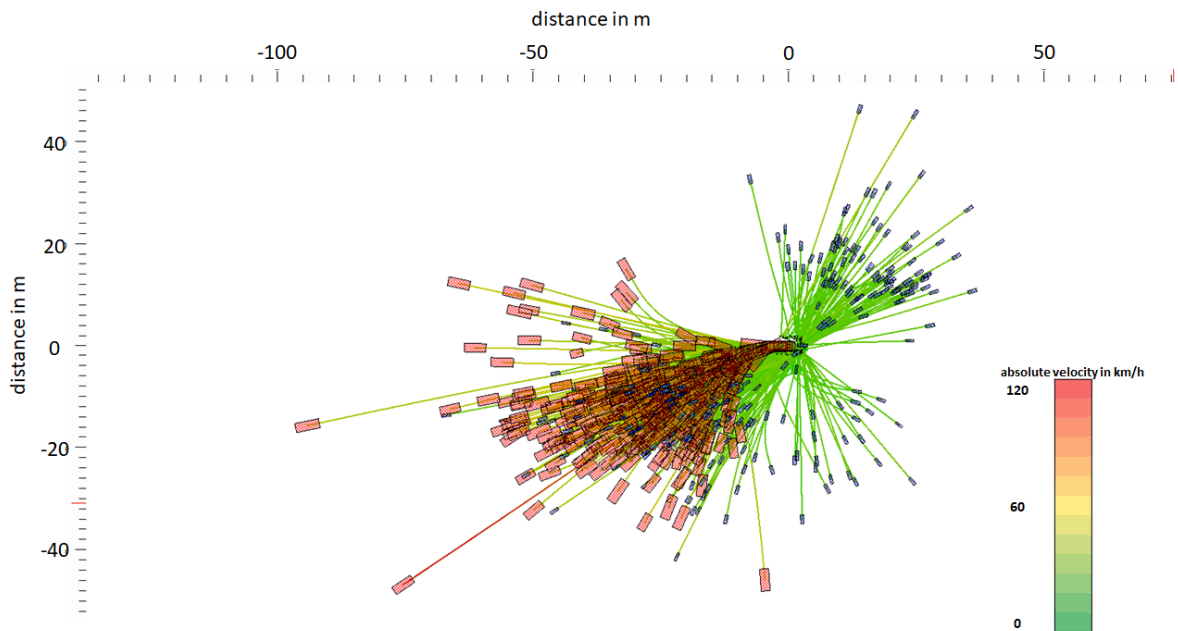


Figure 72 Trajectories of bicyclists - and passenger cars relative to the collision point in B-PCTurnR scenarios -passenger car heading east (to the right) at collision point.



4.3.3 Powered two-wheelers

The third largest group of unprotected road users is powered two-wheeler (PTW) riders, of motorcycles as well as mopeds. According to Table 3 and Table 4, riders of these two vehicle types together made up 12.5% of all injured and 11.5% of all fatalities in car-involved crashes in the EU in 2018, highlighting the importance of addressing crashes with PTW involvement. While PTW riders are not the main target group for the SAFE-UP safety systems, sections 4.3.3.1 - 4.3.3.5 provide detailed analyses of car-to-PTW crashes based on in-depth crash data from GIDAS as well as an additional study of crash causation based on new analyses of the data from the Motorcycle Accidents In-Depth Study (MAIDS) project and recently collected naturalistic riding data within the 2BeSafe project.

4.3.3.1 Car-to-PTW crashes

In the following paragraph the assumptions and the results of the in-depth data analysis of car-to-PTW (C2PTW) crashes are described. The focus of the analysis is on injured PTW riders.

Cases selected for the analysis were identified by conflicts types that resulted in crashes. The data analyzed was the GIDAS dataset (see section 3.2.2) from December 2020. The filter criteria to identify the basic dataset are Table 33. Importantly, the analysis will differentiate between small PTWs (≤ 50 ccm) and large PTWs (> 50 ccm) for which the corresponding crashes were expected to have different characteristics.

The following stepwise approach was used to identify the final GIDAS dataset:

1. Assign the passenger car a role within the crash, which is causer (A) or non-causer (B) of the conflict.
2. Include the following crashes:
 - a) PTW in their first collision in role A, B, or other (only with UTYP=1xx or UTYP=7xx) with passenger cars, which are in role A or B and its first collision;
 - b) PTWs which are in role A or B.
3. Exclude the following crashes:
 - a) First collision of PTW with another participant;
 - b) All others not matching the criteria above.



Table 33 Criteria for the selection of car-to-PTW crashes from the GIDAS database

Filter variable	Value	Explanation
STATUS	4	Cases with completed reconstruction
JAHR	>1999	Data for the year 2000 and later
FART	3	Identification of passenger cars
FZART	<= 26 OR 56 OR 60-62	
FZGKLASS	< 15	
FART	11	Identification of small PTW (<=50 ccm)
FZART	37 OR 38	
FART	11	Identification of large PTW (>50 ccm)
FZART	35 OR 40	
UTYP, UTYPA, UTYPB	All	The crash type variable UTYP is considered to describe the conflict before the crash happens. The role-specific variables UTYPA and UTYPB are used to identify the participants in conflict

A set of 2 317 crashes including 891 small PTWs with 956 riders and 1 426 large PTWs with 1 519 riders remained after filtering the GIDAS data. Figure 73 shows distributions for crash sites and injury severities of riders of small and large PTWs. Most of PC vs. PTW crashes occurred in urban locations. Specifically, 94 % of share crashes with small PTWs and PCs happened in urban areas. For large PTWs, the share of rural and motorway crashes is higher (13.7 % rural and 1.6 % motorway). This is one effect which potentially leads to a higher share of killed and severely injured riders of large PTWs (39.0 % - large PTW rider vs. 29.1 % - small PTW riders).

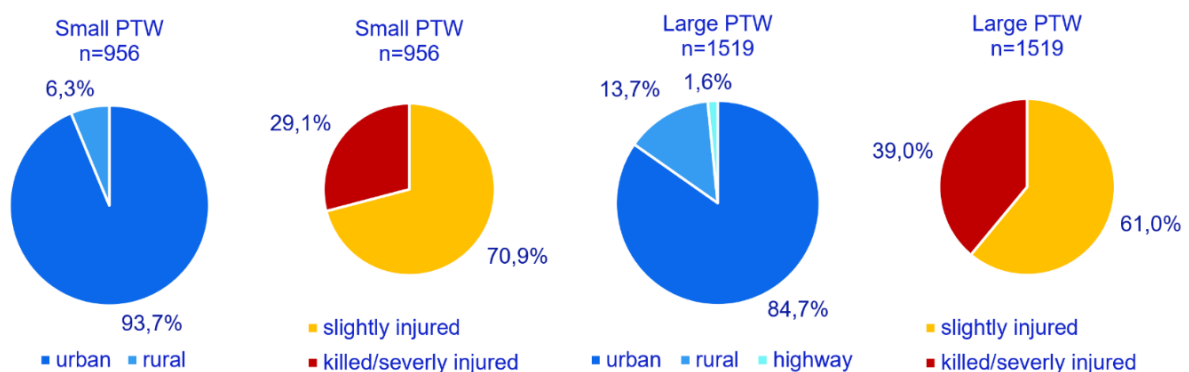


Figure 73 Distribution of crash site and injury severity for small and large PTW in GIDAS

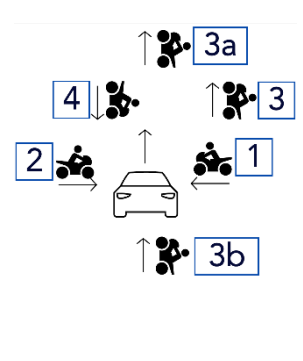


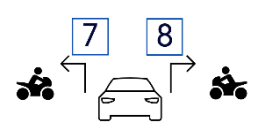


The next section defines a clustering of car-to-PTW crashes based on the moving direction of vehicles in the conflict situation.

4.3.3.2 Clustering of Car-to-PTW crashes

The following nine conflict scenarios between passenger cars and PTWs were defined based on the UTYPs (see Table 34).

Table 34 Scenario clustering in passenger car-to-PTW crashes

Scenario	Abbreviation	Schematic illustration
PC moves forward		
1. PTW crossing from right	PTW-CR	
2. PTW crossing from left	PTW-CL	
3. PTW longitudinal same direction	PTW-LongSD	
a. PTW ahead longitudinal same direction	PTW-AheadLongSD	
b. PTW following longitudinal same direction	PTW-FollowLongSD	
4. PTW longitudinal opposite direction	PTW-LongOn	
PC moves backwards		
5. PTW PC reverse	PTW-PCRev	
PC is stationary		
6. PTW in conflict with stationary PC	PTW-PCStat	
PC turns		
7. PTW in conflict with PC turning left	PTW-PCTL	
8. PTW in conflict with PC turning right	PTW-PCTR	
PC in other crashes		
9. PTW Other	PTW-Oth	

The data clustering yielded a set of 2 475 cases spanning the 9 scenarios depicted above. In 870 of cases the riders were killed or severely injured (KSI). The cases involving small versus large PTWs were analyzed separately with the results presented in separate sections below.

4.3.3.3 Small PTW vs. PC crashes

About 94% of the filtered conflict scenarios were crashes in urban areas. Approximately 37% of the injured PTW riders were involved in crossing crashes. There were more ‘crossing left’ crashes than ‘crossing right’ crashes. Among KSI cases, the share of crossing crashes increased. Figure 74 shows frequencies of injured as well as KSI riders for each scenario.

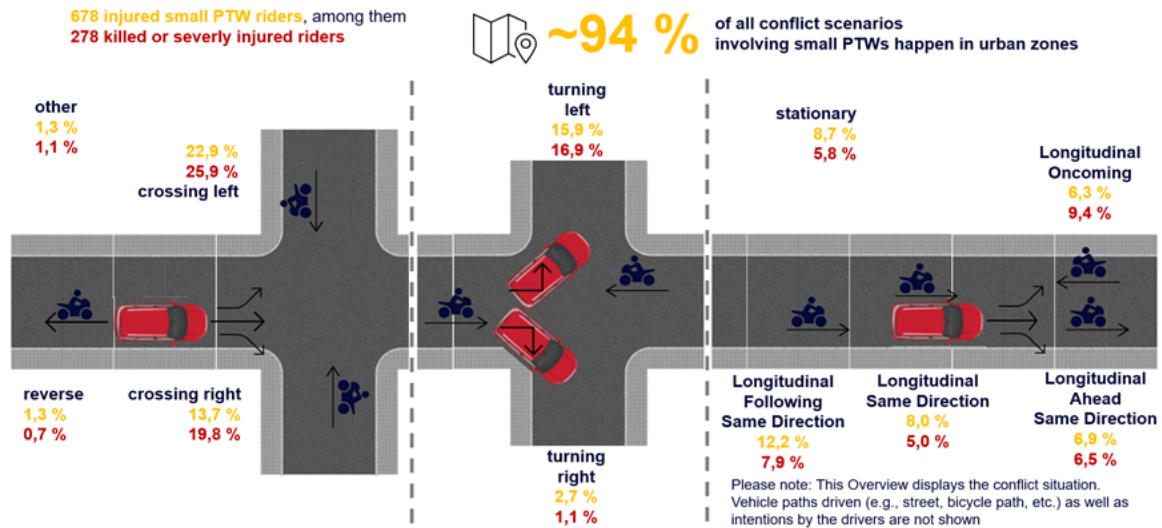


Figure 74 Overview of conflict scenarios for car-to-small PTW crashes – schematic representation

4.3.3.4 Large PTW vs. PC crashes

Crashes in urban areas made up about 85% of the conflict scenarios involving for large PTWs. In contrast, nearly 30 % of all longitudinal oncoming cases with KSI riders were rural crashes. Figure 75 shows all scenarios with their share of all injured riders and KSI riders.

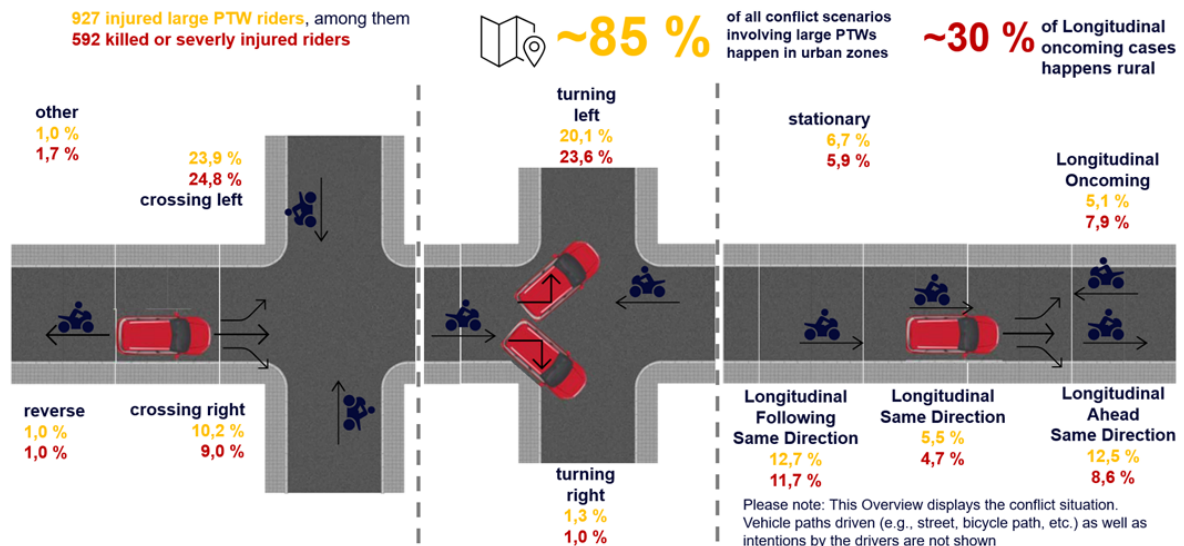


Figure 75 Overview of conflict scenarios for car-to-large PTW crashes – schematic representation



According to UTYP clustering, approximately 34.1% of the injured PTW riders were involved in crossing crashes. There are more 'crossing left' than 'crossing right' crashes in the data. The KSI share of crossing crashes is slightly lower at 33.8%.

Figure 75 The scenarios 'crossing left' (24.8% of all cases), 'turning left' (20.1% of all cases) and 'longitudinal oncoming' (5.1% of all cases) had larger percentages when only the KSI cases are considered (24.8% PTW-CL, 23.6% PTW-PCTL, 7.9% PTW-LongOn, respectively) compared to their overall prevalence. However, the scenario 'longitudinal following same direction' (12.7% / 11.7% KSI), 'longitudinal same direction' (5.5% / 4.7% KSI) and 'longitudinal ahead same direction' (12.5% / 8.6% KSI) show a slightly lower share within the KSI subset. Less common crash scenarios were 'Turning right' (1.3% of all, 1.0% of KSI), and 'stationary' (6.7% of all, 5.9% of KSI). Reversing scenarios were the least common crashes happening in 1.0% of all cases and in 1.0% of KSI.

4.3.3.5 PTW crash contributing factors from MAIDS data and naturalistic riding data



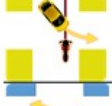
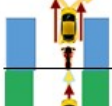



The next sections investigate crash data and naturalistic riding data for a better understanding of crash contributing factors, PTW rider behavior, and the interaction between the PTW rider and other traffic participants.

4.3.3.5.1 In-depth crash data involving PTWs

This section includes a brief summary of previous work (Huertas-Leyva, Baldanzini, Savino, & Pierini, 2021) which defined a methodology that uses in-depth data to identify the skills needed by PTW riders to reduce casualty rates. This methodology provides new insights related to the highest risk crash configurations involving PTWs and other vehicles (mostly passenger cars). The study used the raw (i.e., unweighted) in-depth data from the MAIDS project. The original dataset of 921 cases was reduced to 803 after excluding crashes for which the primary contributing factor was rider impairment or mechanical problems (i.e., rider or PTW were not in a riding condition). The crashes were grouped into seven conflict configurations (Table 35), which were defined by the trajectories and interactions of the road users involved. This resulted in four multi-vehicle configurations crossing path crash at junctions; two multi-vehicle collisions not related to junctions; and one single vehicle crash category covering cases of the PTW falling or running off the roadway with no other vehicle (OV) involvement. The remaining configurations were categorized as 'Other' (138 cases). Table 35 shows the frequency distributions for crash configurations considered. The four configurations that grouped the multi-vehicle crossing path crashes at junctions (SCP/LD, TIP/LD, TAP/OD and TAP/SD) altogether represented around 58% of all the cases analyzed. The crash data were mainly collected in urban areas with a high proportion of mopeds, so the crash prevalence of the configurations may be influenced by exposure.

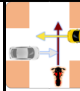
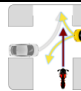








Table 35 Definition of the seven merged crash configurations selected and frequency distribution (Huertas-Leyva, Baldanzini, Savino, & Pierini, 2021)

		Total (N=803)	Severe Injury (N=182)
INTERSECTION ≈ 58%		SCP/LD: Straight Crossing Paths /Lateral Direction	16.9%
		TIP/LD: Turn Into same or oppose Path /Lateral Direction	12.5%
		TAP/OD: Turn Across Path /Opposing Direction	11.8%
		TAP/SD: Turn Across Path /Same Direction	16.7%
		RE/SD: Rear-End, PTW striking /Same Direction	6.5%
		HS/OD: Head-on or Sideswipe /Opposing Direction	7.3%
		SV: Single Vehicle crash (no other involved vehicles)	11.1%
OTHER		17.2%	17.0%
TOTAL		100%	100%

As evidenced by the results summarized in Table 36, for the crash configurations related to junctions, the main contributing factor was a failure of the driver of the other vehicle (mostly cars). Of the identified types of failures, driver error in detecting the PTW was the most common in each of the four crash configurations related to junctions. *Adverse weather* was rarely the main contributing factor, while *view obstruction* was a frequent contributor to TIP/LD crashes. In terms of relevance to future scenarios with autonomous vehicles, the results suggest that PTW detection at junctions represents a key intervention for improved PTW rider safety, with significant scope for reducing the number of current crashes by means of optimal detection systems, but also with a high risk of PTW-collision if the AV's detection system performs poorly.

Table 36 Relation between primary crash contributing factor and configuration. PTW: PTW rider; OV: Other Vehicle driver. Adapted from Huertas-Leyva, et al. (2021)

		INTERSECTIONS						
		Total						
	detection	40,8%	47,8%	56,0%	67,4%	50,0%	21,2%	13,6%
	decision	12,2%	12,5%	16,0%	15,8%	15,7%	9,6%	11,9%
	compreh.+ exec.	1,7%	1,5%	0,0%	2,1%	3,0%	1,9%	3,4%
	PTW	32,0%	26,5%	14,0%	9,5%	29,1%	50,0%	49,2%
	view							
	obstruction	4,4%	4,4%	12,0%	4,2%	0,7%	1,9%	6,8%
	adverse weather	1,2%	0,0%	0,0%	0,0%	0,0%	0,0%	1,7%
	other	8,0%	7,3%	2,0%	1,1%	1,4%	15,3%	13,6%

4.3.3.5.2 Analysis of Naturalistic Riding Data

A preliminary analysis was performed on the naturalistic riding data collected in the EU project 2-wheeler Behavior and Safety (2BeSafe, 2021). During the project an instrumented scooter was ridden by five volunteers. Each volunteer rode the scooter every day for one month. Trip purpose was mostly commuting, so the data were collected primarily in urban or peri-urban scenarios. Several on-board sensors enabled collection of acceleration (both rotational and translational), speed, braking pressure, and steering angle. Additionally, two cameras were mounted on the scooter to record both the surrounding environment and the rider.

The results reported in the present deliverable represent a preliminary analysis and thus carries certain limitations. For example, the data analyzed is from only one of the volunteers and traffic conflicts were identified based only on braking maneuvers. Nevertheless, the maneuvers analyzed are relevant to safety-critical scenarios (Davoodi & Hamid, 2013); indeed, braking maneuvers have been widely studied to determine different patterns or styles of braking performance and to better understand what riders do in different conditions (Attal, Boubezul, Oukhellou, & Espié, 2013; Attal, Boubezul, Oukhellou, & Espié, 2015; Baldanzini, Huertas-Leyva, Savino, & Pierini, 2016).

Thus, a screening of the data based on braking actions (identified as changes in braking pressure and speed) was performed to identify traffic conflicts. Then, a review of the collected videos was performed and information about the surrounding environment was encoded for later analysis. The resulting dataset is comprised of 1358 braking events. The maximum deceleration for each event ranges from 0.1 to 8.5 m/s². The dataset includes different levels of the braking maneuver, some very mild and other ones more brusque; see the distribution of the level of braking maneuvers in Figure 76 below.



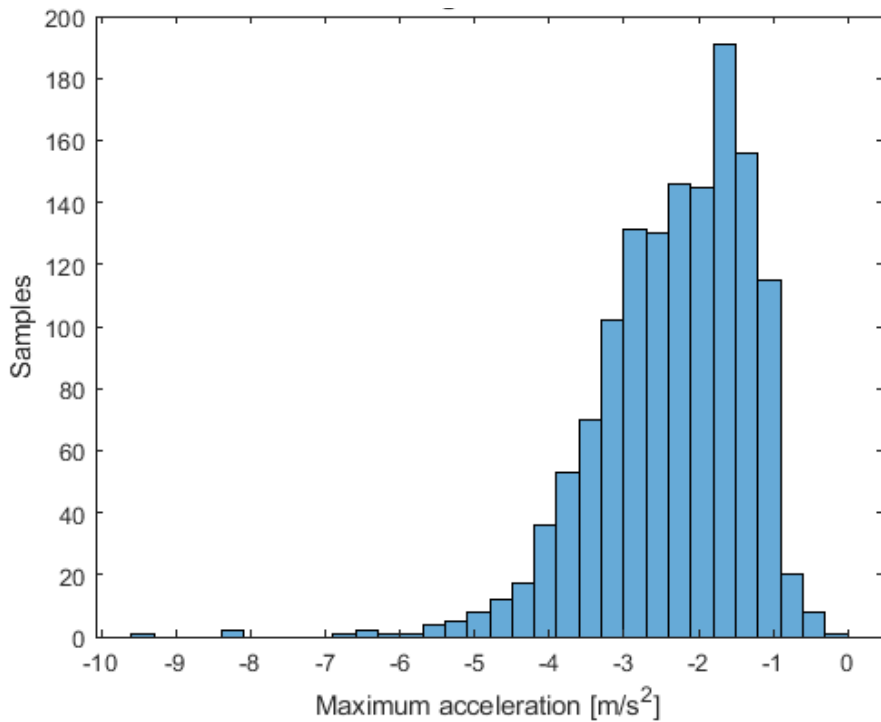


Figure 76 Maximum longitudinal deceleration in braking maneuvers of the PTW

For this reason, the dataset is quite heterogenous despite its small size. Figure 77 summarizes the results from braking events according to three aspects of the scenarios: the: infrastructural context, the main opponent users by type and specific interaction, and the lead vehicle type. In 53% of the cases, the rider braked at a junction (including roundabouts), highlighting the importance of this infrastructure and in interacted with leading vehicle. Thus, in most cases, the rider performed a braking maneuver in a car-following situation. Among the 1 358 events, in the majority of the cases (46%), the lead vehicle was a car. Thus, from these first results, it appears that the rider tended to brake close to junctions, in a car following scenario with a car is leading.

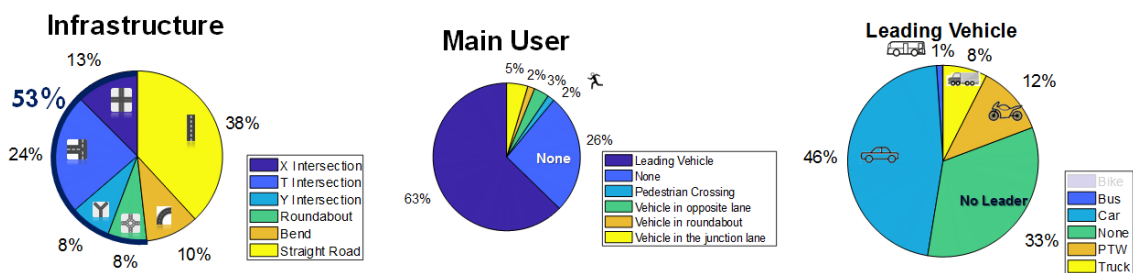


Figure 77 Road infrastructure, interaction type, and lead vehicle in braking maneuvers from naturalistic PTW riding (data from a single volunteer)

In the 26% of the cases, braking events did not involve other road users, i.e., there were no interactions. Consequently, they were removed from the dataset and the analysis was repeated. The new dataset contained 1 005 braking events. Results of their analysis are



shown in Figure 78. In each event, the maximum deceleration was found to fall within the same range reported in the previous analysis, i.e., considering the whole dataset as reported above. Considering only braking maneuvers for which the rider interacted with other road users, junctions showed a lower proportionate share than in the previous analysis (48% vs. 53%). However, they are still identifiable as the most typical scenario in which the rider responded in interactions with other users by braking. Additionally, the proportion of braking events in straight road sections outside of junctions increased from 38% to 44%.

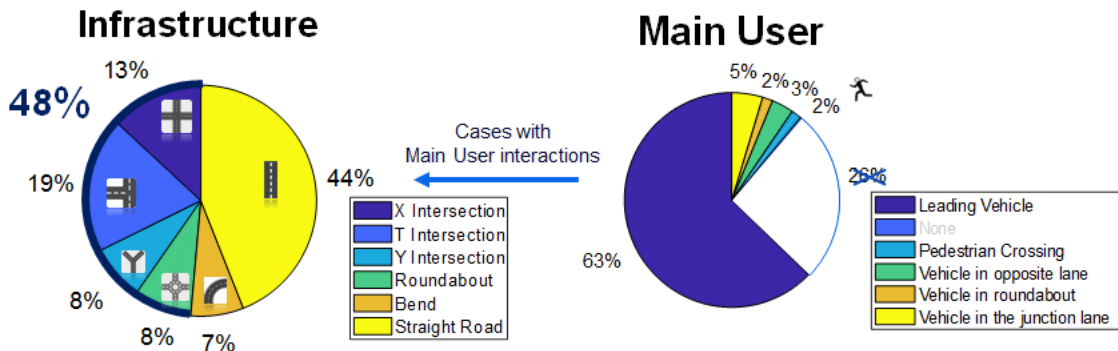


Figure 78 Infrastructure context and type of lead vehicle in braking events from naturalistic riding after excluding braking events without interaction

Initially all braking maneuvers were analyzed together without distinguishing by level of criticality. To analyze the safety-critical cases more specifically, a subset of the 100 most abrupt maneuvers were selected and reanalyzed. Results are reported in the following figure. In each event the maximum deceleration ranged from 3.5 m/s² to 8.5 m/s². In 61% of the cases, the riders performed a sudden abrupt maneuver close to a junction. In all cases, the rider interacted with another road user, and in most of these (74%) the other user was the lead vehicle. In 60% of cases the lead vehicle was a car. These results confirm what was stated above: the most critical scenarios for a PTW rider are a car-following situation close to a junction, with the PTW following the car. Of the 100 events identified by reviewing the recorded video, 7 were classified as near-misses. The criteria used for the identification were the same as applied in Dingus, et al. (2006).

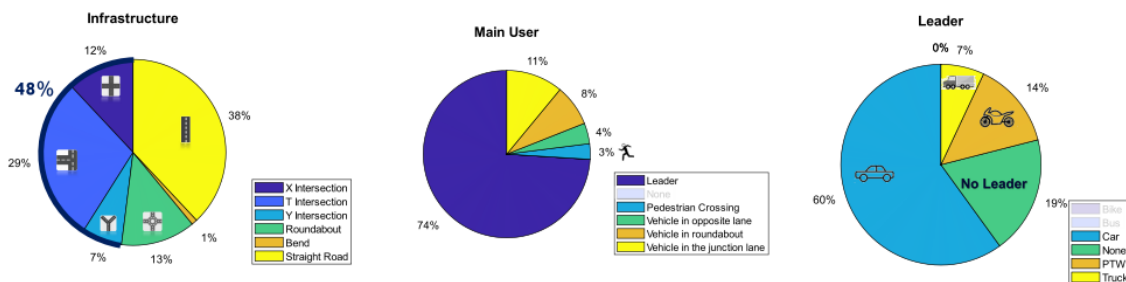


Figure 79 Infrastructure, interaction type, and type of lead vehicle for the 100 sharpest braking maneuvers



4.3.4 VRU crashes in adverse weather conditions

In contrast to common passive safety systems such as airbags or seat belts, active safety systems provide the potential not only to mitigate the crash severity, but also to prevent crashes entirely. As many active safety systems like Autonomous Emergency Braking (AEB), Autonomous Emergency Steering (AES) or Lane Departure Warning Systems (LDWS) rely on information from sensors, their functionality under various environmental conditions is essential. Their effectiveness under adverse weather and poor lighting conditions is particularly important because human drivers' vision is reduced in poor visibility conditions, which increases the risk of a crash involvement (WHO, 2004).

Since the analysis of Sections 4.1 and 0-4.3.2 shows that precipitation is significantly more prevalent in crashes with VRUs than fog, the use cases are selected based on precipitation evaluations. Therefore, this section derives a precipitation baseline for the crash analysis and a method for inferring objective precipitation amounts, before selecting use cases for car-to-VRU crashes in bad weather.

4.3.4.1 Databases and variables for the analysis of weather conditions

To analyze the effect of weather conditions on the crash situation, variables of the GIDAS database (see Section 3.2.2) and the database of the German Meteorological Service (Deutscher Wetterdienst, DWD) are investigated.

4.3.4.1.1 Variables in GIDAS

For the precipitation analysis, the variables on the type of precipitation (NIED) and the precipitation rate (NIEDR) are of importance besides the case number and the information on the crash time. The type of precipitation is classified as “no precipitation”, “precipitation without further details”, “rain”, “hail”, “snow” and “freezing rain”. The precipitation rate is coded categorically as “no precipitation”, “light”, “moderate”, “heavy” and “not determinable”.

4.3.4.1.2 Variables in the DWD database

The DWD offers with the Climate Data Center a download archive for current as well as historical climate and weather data of its weather stations in Germany (DWD, 2020). For the evaluations in this work the 10-minute precipitation amount (RWS_10), the 10-minute precipitation duration (RWS_DAU_10), and the 10-minute temperature information at 2m altitude (TT_10) are relevant. As the information of the DWD needs to be linked to the GIDAS data, five weather stations of the DWD for each of the data collection areas Dresden and Hanover are investigated, which are shown in Figure 80 and Figure 81.



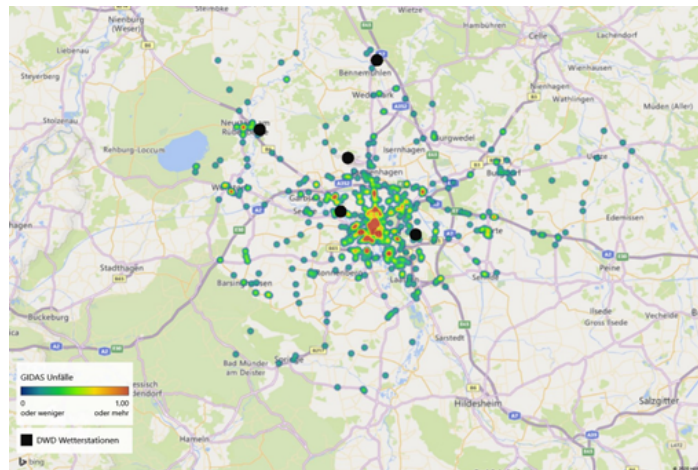


Figure 80 Heat Map of GIDAS crashes with rain (Hanover, 2010-2017) (blue-green-red) and considered DWD weather stations (black dots). Data from GIDAS and DWD Climate Data Center (DWD, 2020)

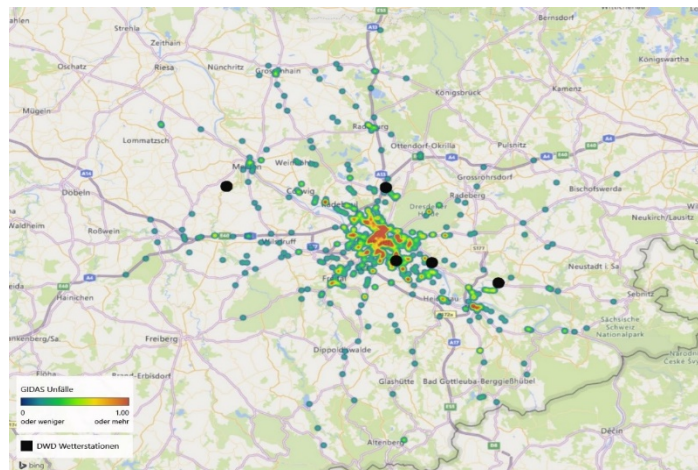


Figure 81 GIDAS crashes with rain (Dresden, 2010-2017) and considered DWD weather stations. Data from GIDAS and DWD Climate Data Center (DWD, 2020)

4.3.4.2 Linkage of DWD and GIDAS data

The aim of linking the GIDAS crash data to the data of the DWD is to generate a precipitation baseline for the crash analysis and to determine objective precipitation amounts.

Although fog is also a weather condition, which needs to be analyzed in the crash analysis and can be simulated in the test hall, the focus in the following is on precipitation. The reason therefore is that the occurrences of VRU crashes in fog are relatively rare and the information of the DWD for fog is not as detailed as in GIDAS. For example, the variable that shows if fog was present is coded in the DWD weather phenomenon section, which is only available on a daily basis. In the 10-minute data for the air-temperature, a variable on the relative humidity at 2m height (RF_10) is included, but even 100% relative humidity does not guarantee fog. Exemplarily, also cloud condensation nuclei (CCN) are required in the air, which are aerosols capable of forming droplets, see the deliverable DENSE D2.1 (DENSE,



2017a). This report also contains a detailed physical specification of the formation of different fog types.

4.3.4.2.1 Precipitation baseline

To analyze whether crashes occur more often during precipitation, a baseline that describes the general frequency of precipitation is necessary. By comparing the occurrence of precipitation in the baseline and in the crash data, it is possible to draw conclusions about the risk of the weather conditions if an unchanged traffic participation can be assumed or knowledge thereof is available.

As for the investigated GIDAS database, crashes in the regions around Dresden and Hanover are collected. These locations are also considered for the calculation of the baseline. Since the stations at the airports have recorded the data usually for the longest time and include only few missing data values, the stations with the numbers 1048 (Dresden airport) and 2014 (Hanover airport) were used to calculate the baseline (DWD, 2020). The 10-minute precipitation data contain a variable, which describes the duration of precipitation in minutes (RWS_DAU_10). As this variable is only recorded from July 2009, the calculation of the baseline is limited to the 10 years from the beginning of 2010 to the end of 2019. For this period, the total time in minutes is calculated first and then the minutes with precipitation per weather station. Missing values in the weather station data are excluded for both calculations such that the ratio of both values is maintained.

With this approach, the share of time with precipitation in Dresden and Hanover can be determined. To specify the type of precipitation, the measured temperature in 2m height in the 10-minute slot of the weather stations is used (TT_10), because there is no variable in the 10-minute data that describes the type of precipitation. For this purpose, it is simply assumed that there was rain if the temperature at 2m height was higher than 0°C and snow if the temperature was lower than or equal to 0°C. The resulting baselines are shown in Figure 82 for Dresden and Hanover. In Dresden in the period from 2010 to 2019, the relative frequency of rain was 10.01% and of snow 2.43%. In Hanover, these values were 10.34% and 1.12% respectively. To get a combined baseline, the shares can be averaged, which would result in a total precipitation share of 11.95%.

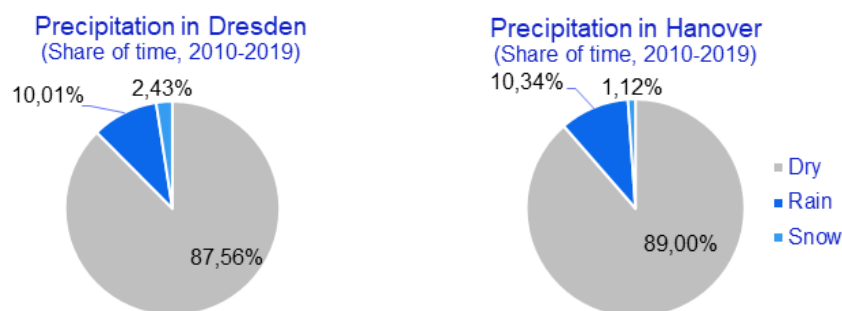


Figure 82 Precipitation baselines for Dresden and Hanover (2010-2019). Data from the DWD Climate Data Center



For more insights into the precipitation types rain and snow, the frequency of occurrence of the intensity ranges light, moderate, and heavy was analyzed. Therefore, the precipitation duration (RWS_DAU_10) and the precipitation height (RWS_10) of the 10-minute slot at the weather station and the ranges defined by the DWD for the rain and snow intensity values are used. The precipitation height in the 10min slot is divided by the precipitation duration in the respective slot to get an amount in mm per min. The intensity ranges defined by the DWD are given in mm/h (Table 37), which is why they are divided by 60 before being compared to the precipitation height at the weather stations. Thereby, the share of time with light, moderate, and heavy rain and snow can be calculated.

Table 37 Intensity ranges defined by the DWD for rain and snow (DWD, 2020b)

Intensity	Rain [mm/h]	Snow [mm/h]
Light	$i < 2.5$	$i < 1$
Moderate	$2.5 \leq i < 10$	$1 \leq i < 5$
Heavy	$i \geq 10$	$i \geq 5$

Figure 83 shows the distribution for the three intensity ranges for rain and snow in Dresden and Hanover from 2010 to 2019.

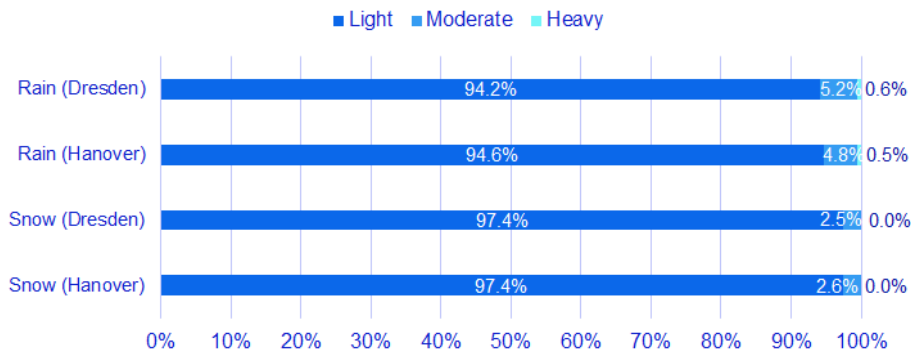


Figure 83 Rain and snow intensity shares in Dresden and Hanover based on the intensity ranges defined by the DWD (2010-2019). Data from the DWD Climate Data Center (DWD, 2020).

When rain or snow was falling, most of the time the precipitation amount recorded at the weather station is grouped as light according to the definition of the DWD. Moreover, it is interesting that in Dresden 47% of the time with rain and in Hanover in 48% of the time with rain the amount was too small to be measured by the weather station. This means that the precipitation height (RWS_10) is given as 0 despite the precipitation duration (RWS_DAU_10) being larger than 0. For snow, these shares are even higher with 71% in Dresden and Hanover. These results lead to the assumption that according to the definition and recordings of the DWD, precipitation is mostly present in a light intensity.



4.3.4.2.2 Objective rainfall amounts

An objective of the crash analysis in the SAFE-UP project is to determine scenarios that are influenced by environmental conditions and have an increased risk under these conditions. Scenarios with rain can be recreated with the rain simulator in the test hall and influences on the sensors can be evaluated. For recreating the scenarios, it is not only essential whether it was raining at the time of the crash, but also information of the fallen amount of rain is important. In GIDAS, the precipitation rate can be specified on the basis of a subjective assessment in the three intensity levels light, moderate, and heavy.

By linking the GIDAS data to the DWD weather stations, the subjective rainfall amounts light, moderate, and heavy can be deduced to objective rainfall amounts, which can be tested in the test hall. The methodology is summarized in Figure 84.

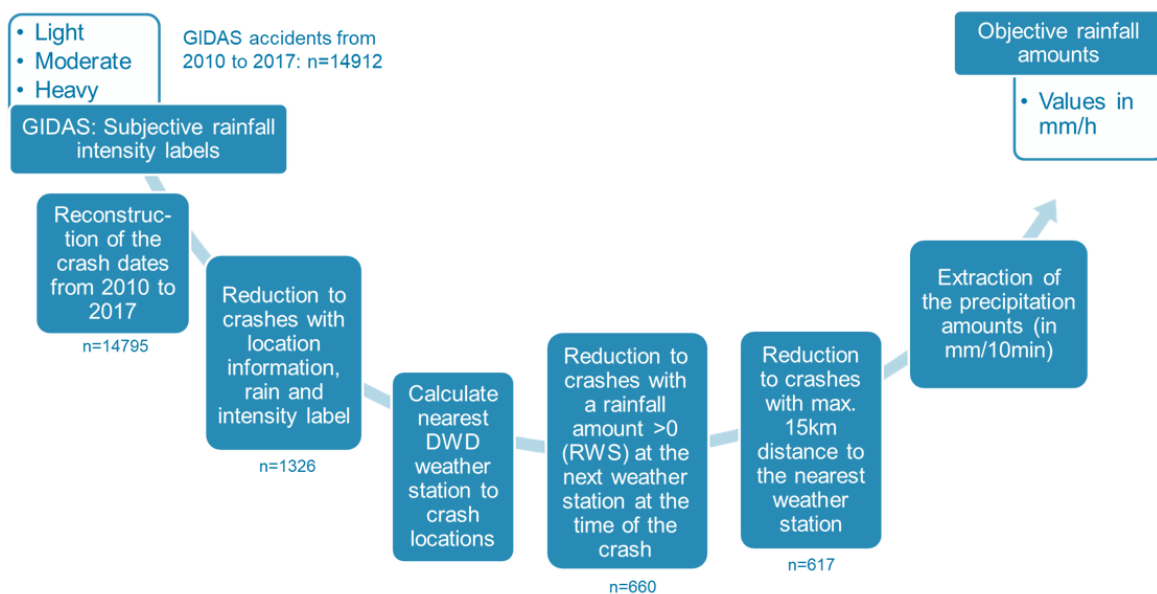


Figure 84 Methodology for extracting objective rainfall amounts of the DWD data for the intensity labels in GIDAS

First, the dates of the crashes are reconstructed using the case number and the included time information. Afterward, the nearest weather station of the considered DWD weather stations (see Figure 80 and Figure 81) is calculated for the crashes in GIDAS, which have a location information and are coded with rain and a corresponding intensity label. The locations of the crashes as well as the weather stations is given in latitude (lat.) and longitude (lon.). With the following formula for calculating the distance d between two points A and B on a spherical surface, and using $R = 6378.388$ km, the distance of the crash to the weather stations in kilometers can be determined and the nearest station selected (Kompf, 2020):

$$d = R * \text{acos}(\sin(\text{lat}_A) * \sin(\text{lat}_B) + \cos(\text{lat}_A) * \cos(\text{lat}_B) * \cos(\text{lat}_B - \text{lon}_A)).$$

Especially the distance to the weather station, inaccuracies in determining the crash time in GIDAS and the measuring period of the weather station can lead to different precipitation data in the databases. There are also cases where the index in the DWD data



(RWS_IND_10) indicates that precipitation has fallen, but no precipitation amount (RWS_10) was measured. For these reasons, the objective rainfall amount determination is limited to crashes, which are labelled with rain and a rainfall intensity in GIDAS and for which the DWD has recorded a precipitation amount in the corresponding 10-min slot. The intention is that under these circumstances the amounts should be comparable. In addition, crashes that occurred more than 15km away from the nearest weather station are excluded to reduce the inaccuracies due to high distances. This distance value was chosen because above this value all cases in the box plot (Figure 85) are classified as outliers.

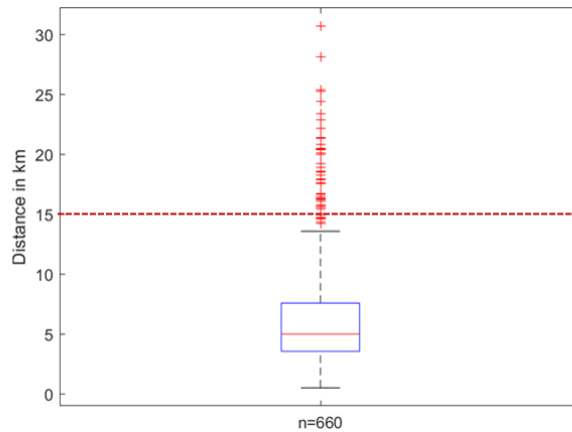


Figure 85 Box plot for the distance between GIDAS crashes with rain (2010-2017) to the nearest considered weather station. Data from GIDAS and DWD Climate Data Center (DWD, 2020)

The 10-min time stamp in the data of the weather station is given in the UTC and marks the end of the interval. However, the measuring instruments of the DWD show an average time delay of 5 minutes (DWD, 2020). Figure 86 shows the DWD timestamps at the outer circle on which the crashes in the corresponding 10-minute periods needs to be projected.

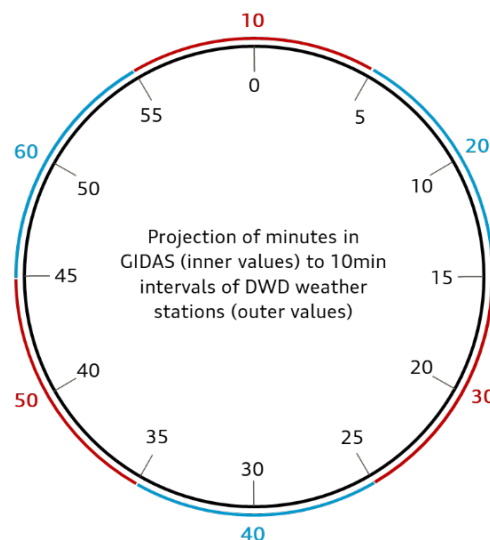


Figure 86 Projection of the minutes of the crash time in GIDAS to the 10-minute interval of the DWD according to the description in (DWD, 2020).



The hour information in GIDAS, which is given in CET or CEST depending on the time of the year, needs to be converted to the time zone UTC, because the data of the weather stations are given in this time zone. Afterwards, the corresponding precipitation amounts in mm per 10min can be extracted from the variable “RWS_10” of the weather stations. For the three precipitation intensity levels the rain amounts are shown as cumulative distribution functions in Figure 87 and as box plots in Figure 88.

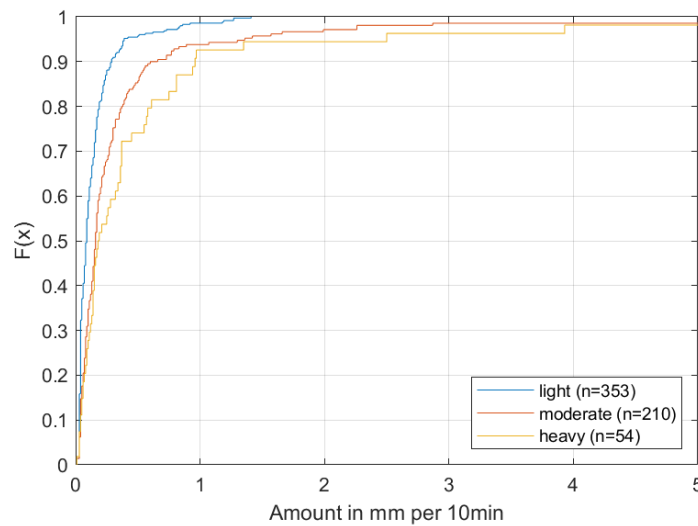


Figure 87 Cumulative distribution functions for rain amount recorded by the DWD at different rain intensity labels in GIDAS (2010-2017, max. 15 km distance to weather station). Data from GIDAS and DWD Climate Data Center (DWD, 2020), x-axis is limited to the interval [0,5] mm per 10 min.

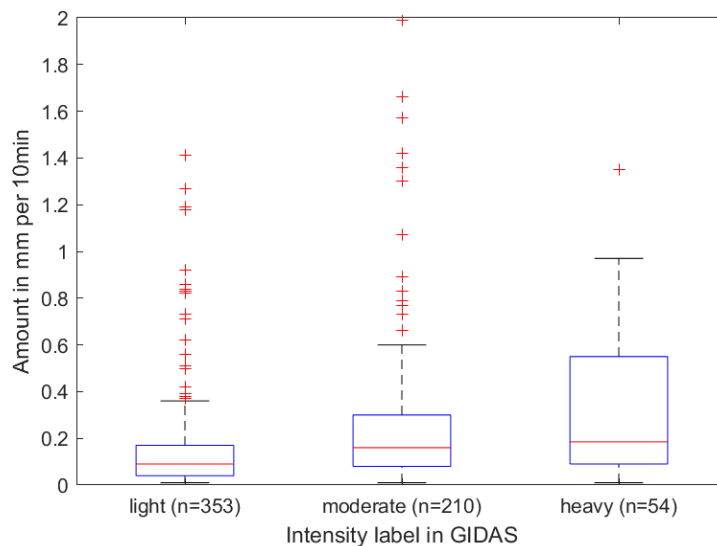


Figure 88 Box plots for the amount of rain recorded by the DWD at different rain intensity labels in GIDAS (2010-2017, max. 15km distance to weather station). Data from GIDAS and DWD Climate Data Center (DWD, 2020), y-axis is limited to the interval [0,2] mm per 10 min.



Additionally, some relevant statistical measures are given in Table 38. It is noticeable that the arithmetic mean value for the intensity level “heavy” and the medians for the intensity levels “moderate” and “heavy” are clearly below the ranges defined by the DWD for the intensity values (DWD, 2020b). With the extracted values it is possible to assign an objective rain amount to the crashes in GIDAS with rain intensity labels “light”, “moderate” and “heavy” and to adjust the rain quantity in the test hall accordingly for the tested scenarios.

Table 38 Comparison of the extracted values to the ranges defined by the DWD for the intensity labels. Data from GIDAS, DWD Climate Data Center (DWD, 2020), and (DWD, 2020b).

Rain intensity (i) label	Range by DWD [mm/h]	Median in GIDAS crashes [mm/h]	Mean in GIDAS crashes [mm/h]	90 th percentile in GIDAS crashes [mm/h]
Light	$i < 2.5$	0.54	0.87	1.7
Moderate	$2.5 \leq i < 10$	0.96	2.7	3.6
Heavy	$i \geq 10$	1.1	3.1	5.7

As in many cases the nearest weather station has not recorded a precipitation amount in the corresponding 10-min time slot, the filter criteria are extended such that information of the next three weather stations are considered if they have a maximum distance of 15km to the crash location. If only one of those stations has recorded a precipitation amount, this value is used. If two or three stations have recorded a precipitation amount, the values are weighted based on the stations’ distances to the crash. Therefore, the amounts are multiplied with the inverse of the distance and a correction term such that the sum of all weights is 1 to get an unbiased result. The amount is calculated according to following formula if two stations with distances d_i recorded precipitation amounts:

$$weighted_{amount} = \frac{1}{d_1} * \frac{d_1 d_2}{d_1 + d_2} * a_1 + \frac{1}{d_2} * \frac{d_1 d_2}{d_1 + d_2} * a_2.$$

If three stations recorded precipitation amounts, it is calculated as follows:

$$weighted_{amount} = \frac{1}{d_1} * \gamma * a_1 + \frac{1}{d_2} * \gamma * a_2 + \frac{1}{d_3} * \gamma * a_3,$$

with the following correction term:

$$\gamma = \frac{d_1 d_2 d_3}{d_1 d_2 + d_1 d_3 + d_2 d_3}.$$

The resulting rain amounts are shown as cumulative distribution functions in Figure 89, as boxplots in Figure 90, and the corresponding relevant statistics are given in Table 39.



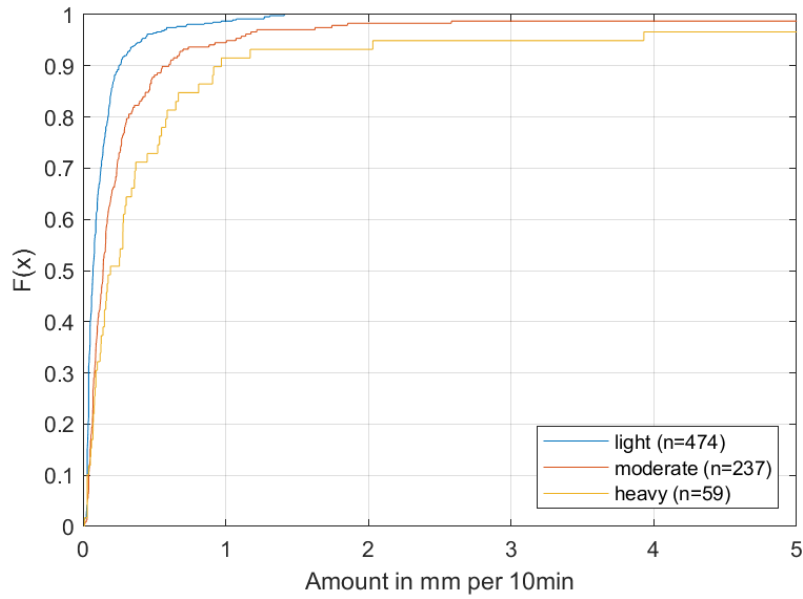


Figure 89 Cumulative distribution functions for the amount of rain recorded by the DWD at different rain intensity labels in GIDAS (2010-2017, up to three stations with max. 15 km distance to weather station). Data from GIDAS and DWD Climate Data Center (DWD, 2020), x-axis is limited to the interval [0,5] mm per 10 min

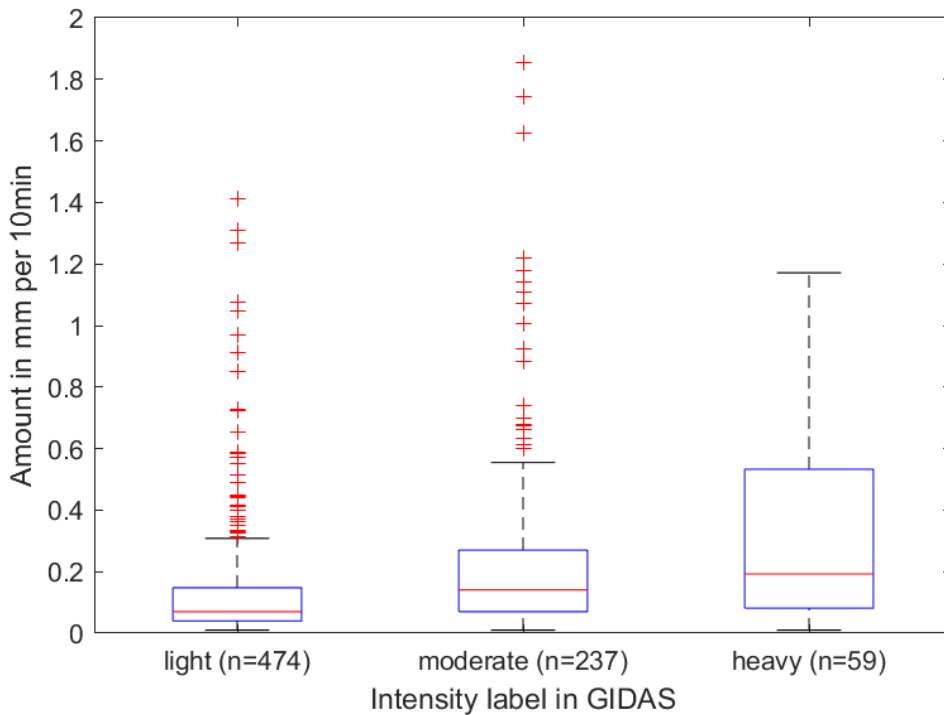


Figure 90 Box plots for the amount of rain recorded by the DWD at different rain intensity labels in GIDAS (2010-2017, up to three stations with max. 15km distance to weather station). Data from GIDAS and DWD Climate Data Center (DWD, 2020), y-axis is limited to the interval [0,2] mm per 10 min



Table 39 Comparison of the extracted weighted values to the ranges defined by the DWD for the intensity labels. Data from GIDAS, DWD Climate Data Center (DWD, 2020), and (DWD, 2020b).

Rain intensity (i) label	Range by DWD [mm/h]	Median in GIDAS crashes [mm/h]	Mean in GIDAS crashes [mm/h]	90 th percentile in GIDAS crashes [mm/h]
Light	$i < 2.5$	0.42	0.77	1.5
Moderate	$2.5 \leq i < 10$	0.84	2.2	3.6
Heavy	$i \geq 10$	1.2	3.4	5.8

Note that the extracted values for the intensities “light” and “moderate” are equal or smaller when up to three stations are considered instead of one station, while for the intensity “heavy”, the values are greater. However, both approaches lead to similar values with the highest difference of 0.5mm/h (mean of intensity “moderate”).

4.3.4.3 Use cases for car-to-VRU-crashes with precipitation

For deriving use cases for car-to-VRU-crashes with precipitation, the related results from the pedestrian crash analysis of section 4.3.1.1 are summarized in Table 40, and the related results from the cyclist crash analysis of section 4.3.1.2 are summarized in Table 41. In addition to the occurrence share of each conflict scenario and the share of crashes with precipitation within these conflict scenarios, the multiplication thereof is given. Therefore, conflict scenarios with a high relative occurrence of precipitation as well as conflict scenarios with a high absolute occurrence of precipitation can be extracted.

For the precipitation shares within the conflict scenarios, values above the baseline value 11.95% are written in bold in Table 40 and Table 41. As the share of pedestrians does not increase in rain (which is the prevalent type of precipitation in Germany) compared to dry conditions (BMVBW, 2002), it can be assumed that there is an increased risk of a crash involvement in conflict scenarios with a precipitation share above the baseline. The shares of precipitation in the conflict scenarios between passenger cars and cyclists are, except for one evaluation, below the baseline. However, this does not directly indicate that precipitation is connected with a decreased risk for cyclists as bicycles are less used under precipitation (BMVBW, 2002).



Table 40 Precipitation shares within the C2P conflict scenarios (with values above the precipitation baseline of 11.95% written in bold) and the total precipitation shares within car-to-pedestrian cases.

C2P conflict scenario	Prevalence of precipitation within conflict scenario, all injured	Prevalence of precipitation within conflict scenario, KSI	Share of cases in conflict scenario with precipitation with respect to C2P, all injured	Share of cases in conflict scenario with precipitation with respect to C2P, KSI
P-CLwoSO	21.5%	23.0%	3.3%	4.6%
P-CLwSO	12.3%	13.4%	1.5%	1.9%
P-CRwoSO	13.4%	14.5%	3.0%	3.3%
P-CRwSO	12.3%	12.8%	2.1%	2.4%
P-Long	19.8%	23.3%	0.7%	0.7%
P-PCRev	5.5%	4.9%	0.4%	0.3%
P-PCTurnL	25.3%	23.2%	2.8%	2.1%
P-PCTurnR	14.7%	11.8%	0.6%	0.3%

Table 41 Precipitation shares within the C2B conflict scenarios (with values above the precipitation baseline of 11.95% written in bold) and the total precipitation shares within car-to-bicycle cases.

C2B conflict scenario	Prevalence of precipitation within conflict scenario, all injured	Prevalence of precipitation within conflict scenario, KSI	Share of cases in conflict scenario with precipitation with respect to C2B, all injured	Share of cases in conflict scenario with precipitation with respect to C2B, KSI
B-CR	7.2%	7.7%	2.5%	2.9%
B-CL	11.4%	10.4%	2.9%	2.3%
B-LongSD	8.1%	9.2%	0.4%	0.6%
B-LongOD	6.6%	10.3%	0.2%	0.2%
B-PCRev	1.7%	0.0%	0.0%	0.0%
B-PCStat	4.6%	6.9%	0.3%	0.3%
B-PCTurnL	12.8%	11.8%	1.2%	1.2%
B-PCTurnR	8.4%	7.6%	1.0%	0.6%



The use cases selected for car-to-pedestrian crashes in bad weather are the conflict scenarios P-CLwoSO (Pedestrian crossing left without sight obstruction) and P-PCTurnL (Passenger car turning left). The results in Table 40 show that the highest absolute occurrence of crashes with precipitation is in the conflict scenario P-CLwoSO for the group of injured (3.3%) as well as for the group of killed and severely injured pedestrians (4.6%). The highest relative share of precipitation within one conflict scenario is in the conflict scenario P-PCTurnL, where 25.3% of the crashes in the group of injured pedestrians are with precipitation. This value is significantly above the baseline value of 11.95% (time with precipitation).

For the car-to-bicycle crashes in bad weather, the conflict scenarios B-CR (Cyclist crossing from right while PC moves forward) and B-PCTurnL (Cyclist in conflict with PC turning left) are selected as use cases. The results in Table 41 show that the highest absolute occurrence of crashes with precipitation is in conflict scenario B-CR for killed and severely injured cyclists (2.9%) and in conflict scenario B-CL for the group of all injured cyclists (2.9%). As the conflict scenario B-CR also has a relatively high share of all injured cyclists (2.5%), it is chosen as a use case. The highest relative share of precipitation within one conflict scenario is in conflict scenario B-PCTurnL, where 12.8% of the injured cyclist cases are with precipitation. This value is slightly above the baseline value of 11.95% although cyclists are less frequent under precipitation (BMVBW, 2002).

Figure 91 shows for the selected use cases the share of “light”, “moderate”, and “heavy” precipitation intensity in the crashes with precipitation. It is apparent that for all use cases, the share of the intensity “light” is highest and the share of the intensity “heavy” is lowest among the known intensity types. The subjective intensity labels can be mapped to concrete rainfall amounts according to Table 39. For example, the subjective intensity label “light” can be mapped to the median value of 0.42 mm/h, “moderate” to the median value of 0.84 mm/h, and “heavy” to the median value of 1.2 mm/h.

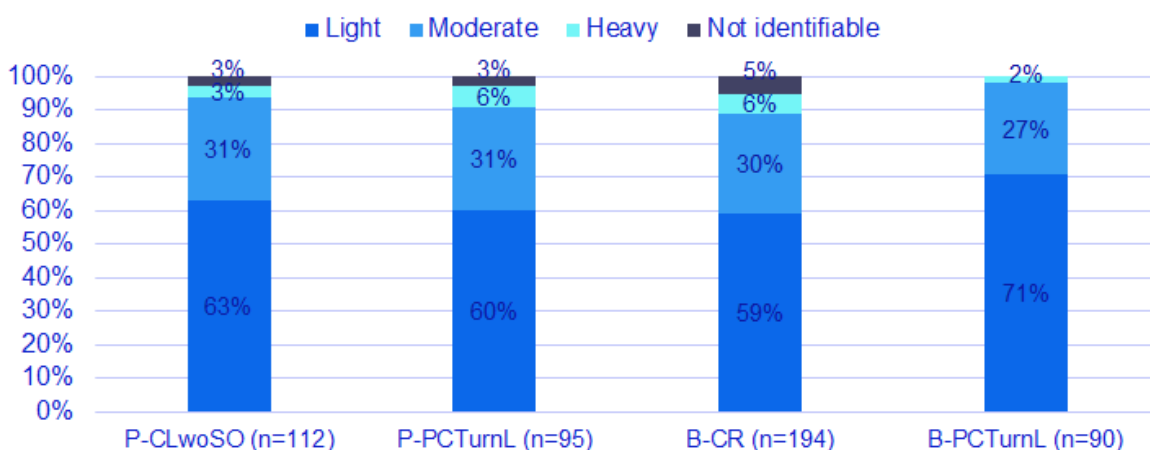


Figure 91 Precipitation intensity shares for SAFE UP use cases in adverse weather conditions



4.4 Future crash scenario outlook in IGLAD

With the introduction of more and more advanced active safety systems and automated driving functions, the crash scenarios currently observed might be different in the future. Such changes will be investigated in SAFE-UP WP2 using the Aimsun Next traffic simulator. The following analysis aims to provide a first overview of how these future situations might look like; specifically, it is investigated how the current distribution of crash types may change as a result from widespread usage of active safety systems. The methodology for this analysis is based on the work done in Östling, Jeppsson, & Lübbe (2019) and Östling, Lübbe, Jeppsson, & Puthan (2019) and has been adapted for using the IGLAD database (see section 3.2.3) as a source. This study will also complement the corresponding part of OSCCAR D1.1 (Dobberstein, Lich, & Schmidt, 2019) where IGLAD data are used for identification of future scenarios based on an analysis of crash contributing factors.

From this database, the crashes in European countries (namely Austria, Czech Republic, Germany, France, Italy, Sweden and Spain) are extracted and their information analyzed. This data serves as a baseline, i.e., to understand the current situation. In a second step, generic active safety systems that are expected to have a widespread implementation in the coming years, are applied to this dataset to identify which crashes would be avoided by the systems. Table 42 shows a short overview of the systems that were applied to the IGLAD database for car-involved crashes.

These systems were applied to the individual crashes in the IGLAD database. If the properties of a crash (e.g., no inclement weather or of a certain crash type configuration) satisfy the working conditions set by one of the active safety systems, it is assumed that the corresponding system would avoid this crash in the future, i.e., the situation would no longer result in a crash. This procedure is done for all the different systems. The identified crashes are then removed from the database, resulting in an updated version that is aimed to mimic a future crash database. In the last step, the original baseline database can be compared to the resulting future database, to draw conclusions about how the crash distribution changes and how parameters such as impact speed and injuries are impacted.

The original database, that contains the collected crashes until the end of 2020, contains 7 055 cases worldwide, out of which 3 110 originate from the European countries of the database (Austria, Czech Republic, Germany, France, Italy, Sweden and Spain). The original sample contains 671 cases with a fatal outcome, i.e., at least one involved person sustained fatal injuries. The previously described systems address 992 of these crashes, leaving the future database with 2 118 cases remaining (about 68.1 % of the original database), out of which 510 are fatal (about 76.0 % of the original database). The generic active safety systems used show a tendency of being less effective towards fatal crashes, as their reduction is lower compared to the overall reduction of crashes. The observed reduction of crashes of 31.9% is similar to what had been identified in previous research, e.g., results from OSCCAR (Dobberstein, Lich, & Schmidt, 2019) where around 28% of crashes were identified as inherently avoided by automated vehicles.



Table 42. Systems implemented in IGLAD for car-involved crashes

System	Typical scenarios avoided
Advanced Front Lighting System	Single vehicle crashes at night
Driver Drowsiness/Distraction Monitoring	Crashes where the drivers were drowsy or distracted
Alcohol Interlock	Crashes where the driver was driving under the influence of alcohol
Intelligent Speed adaptation	Crashes where the main cause is speeding
Autonomous Emergency Braking rear-end	Rear-end crashes with vehicles in the same lane
Autonomous Emergency Braking crossing	Crashes at crossings and junctions
Autonomous Emergency Braking reversing	Crashes when reversing
Emergency steering	Head-on crashes where the driver did not perform any maneuver
Traffic Jam Assist	Low speed rear-end and sideswipe crashes
Highway Assist	High speed rear-end crashes
Lane Keep Assist	Crashes during lane change maneuvers and drifting into oncoming vehicles
Blind Spot Detection	Side swipes when changing lane or merging
Blind Spot Detection VRU	Side swipes of Vulnerable Road Users (VRU) when lane changing
Side Guard Warning	Crashes with Vulnerable Road Users during turning maneuvers
Autonomous Emergency Braking VRU	Crashes with Vulnerable Road Users in front of the vehicle
Dooring Prevention Assist	Crashes between cyclists and opened car doors

Figure 92 shows the number of cases within the 7 main crash type categories between the baseline and future database. With the systems implemented, crash categories 2 (turning scenarios) and 3 (crossing scenarios) show the largest proportional reduction in the number of crashes by 40.2% and 36.2% respectively, while category 4 (crossing pedestrians) shows the lowest reduction with 19.4%.



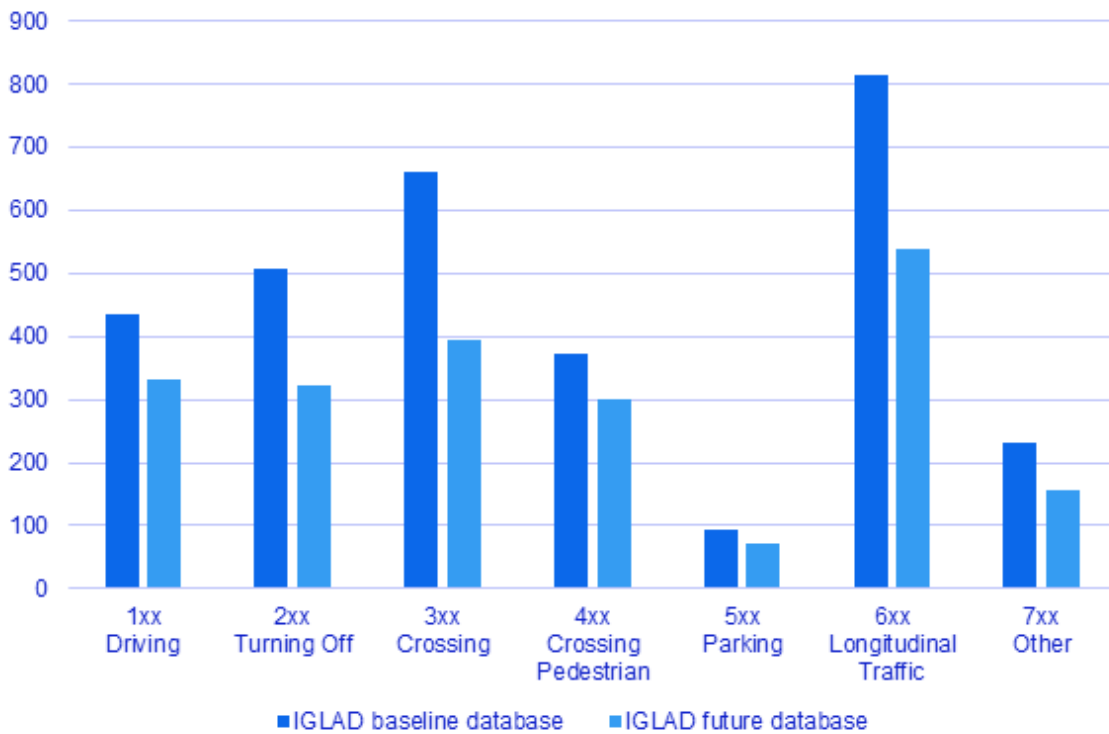



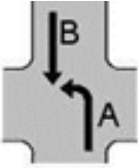
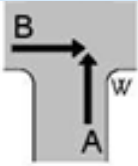
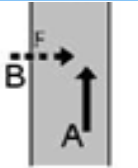
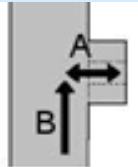

Figure 92. Crash distributions for the main crash type categories

Table 43 shows a more detailed overview over the main crash categories. It is notable that crossing scenarios have a reduced share among all crashes in the future database (2.6 points less compared to the baseline database), whereas single vehicle crashes and pedestrian crossing crashes have an increased share in the future (by 1.6 and 2.2 points respectively).

Note that Figure 92 and Table 43 represent the effect of safety systems on crashes in the IGLAD database and are not necessarily representative of road crashes in Europe in general. In SAFE-UP WP5, further analysis will be conducted based on this study to understand how different weighting methods affect the conclusions drawn from this study, and the final, weighted results are expected to be published in SAFE-UP deliverable D5.8. The current results are intended to provide an initial outlook into how the share of crash configurations are expected to change in the future, while the final results will give a more precise description of the expected crashes with the given method and data.



Table 43. Overview of different crash types and the expected changes in the crash type distribution based on an analysis of IGLAD data

Main crash type	Illustration	Number of crashes in IGLAD sample	Share among crashes	Reduction	Share among future crashes	Change in share
1: Driving		434	14.0 %	23.7 %	15.6 %	+1.6%
2: Turning Off		506	16.3 %	36.2 %	15.3 %	-1.0%
3: Crossing		660	21.2 %	40.2 %	18.6 %	-2.6%
4: Crossing Pedestrian		371	12.0 %	19.1 %	14.2 %	+2.2%
5: Parking		94	3.0 %	23.4 %	3.4 %	+0.4%
6: Longitudinal Traffic		813	26.1 %	33.6 %	25.5 %	-0.6%
7: Other crash type	N/A	232	7.5 %	32.3 %	7.4 %	-0.1%
SUM	N/A	3110	100 %	31.9 %	100 %	N/A



4.5 Summary

The previous sections described various analyses of field data to derive initial safety-critical scenarios that further SAFE-UP work related to safety systems can consider until the final scenarios are available. These use cases were in the form of crash scenarios with pre-crash information for the active safety systems for VRU protection and crash configurations (including, e.g., velocities and angles at the time of impact) for car occupant protection. These are briefly summarized below. Note that the use cases are only recommendations to serve as starting points; detailed data about additional parameters and additional scenarios are provided in this deliverable, which allows the selection of additional scenarios or the replacement of certain recommended scenarios.

4.5.1 Use cases for car occupant protection

For the avoidance of AV occupant fatalities in mixed traffic, it was identified that future work in SAFE-UP (related to Demonstrator 1) should focus on car-to-car (C2C) and car-to-heavy goods vehicle (C2HGV) crash scenarios. Due to project timing, much of the corresponding work was reported in SAFE-UP deliverables D4.1 and further developed in D4.2. In SAFE-UP D4.1, a target population of fatalities in modern cars (with registration year 2000 or later) in C2C and C2HGV crashes, excluding crashes with parking vehicles, was defined; according to CARE analysis, there were 2 085 such fatalities in 2018 in the EU. The scenarios that were selected for further analysis were the crash types identified as the most frequent ones in specific traffic environments, as follows:

- a) C2C head-on and C2HGV head-on crashes (covering 11.1-25.0% and 5.2%-11.9% of the target population, mainly relevant for fatal crashes away from junctions in rural areas);
- b) C2C crossing or turning and C2HGV crossing or turning crashes (covering 0.2-4.4% and 0.1%-1.8% of the target population, mainly relevant for crashes at a junction in rural areas);
- c) C2C rear-end and C2HGV rear-end crashes (covering 1.1-2.2% and 1.2%-2.2% of the target population, mainly relevant for fatal crashes on motorways away from junctions).

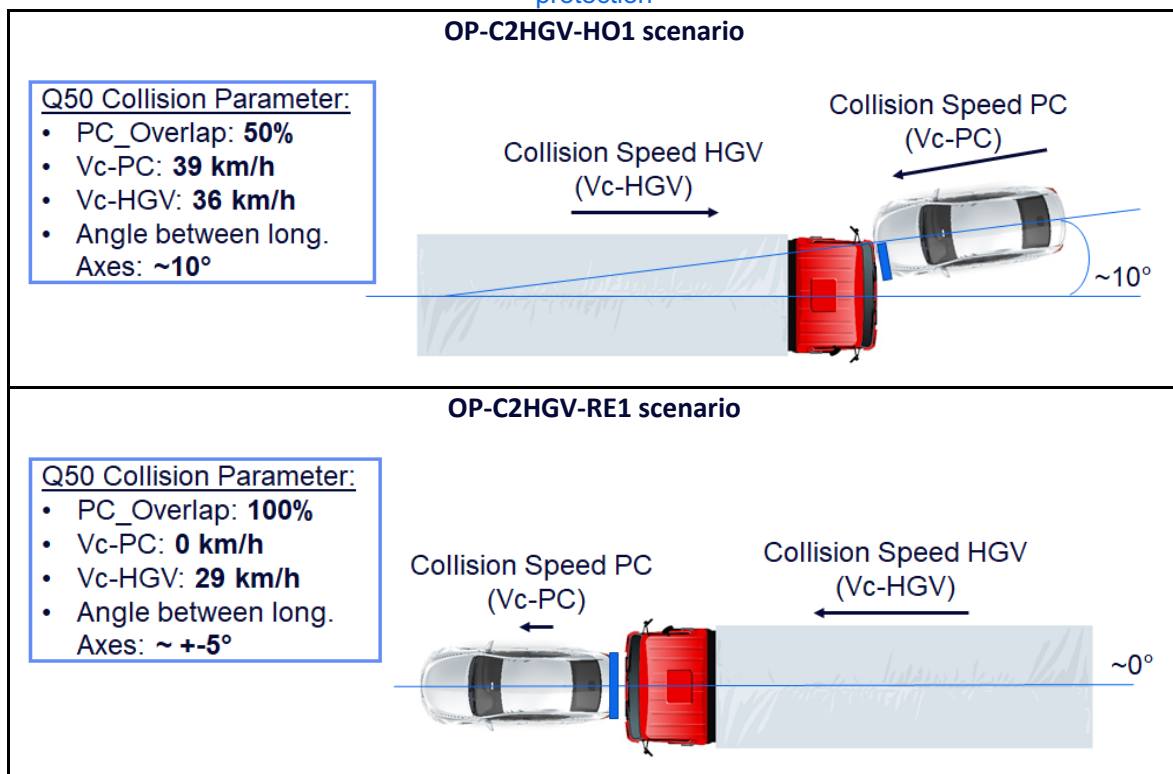
Further work with occupant protection (OP) requires the specification of crash configurations (e.g., kinematic parameters, angles, and other relevant parameters describing the moment of impact) within the above crash scenarios. Publications in the field of traffic safety as well as previous project results will be used in WP4 to specify relevant crash configurations for C2C crashes. As such results are not available for C2HGV crashes, C2HGV head-on and C2HGV rear-end crashes were analyzed further in GIDAS data, and the following crash configurations were identified as starting points for further analysis:



- a) OP-C2HGV-HO1: head-on collision in which the front of a passenger car of weight 1.5-2.5t at a speed 39 km/h collides with the front of a heavy goods vehicle of weight 10-18t having collision velocity 36 km/h, at an angle of 10°, with 50% overlap;
- b) OP-C2HGV-RE1: rear-end collision in which the front of a heavy goods vehicle of weight 10-18t having collision velocity 29 km/h, at an angle close to 0°, with 100% overlap, strikes the rear-end of a passenger car of weight 1.5-2.5t that is standing at the moment of collision.

These crash configurations are illustrated in Figure 16 and Figure 18 above; these figures are reproduced in Table 44 below for more convenient access.

Table 44 Car-to-HGV crash configurations recommended for further consideration for car occupant protection



The above crash configurations are very specific and, depending on the outcome of finite element simulations, may need to be modified to get relevant results. To facilitate this process, the distributions of relevant kinematic parameters (collision speed of car and HGV, relative speed, impact angle, hit point, weight) are described in this report so that appropriate parameter ranges can be considered, see Table 10 and Table 11.

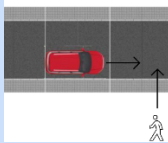
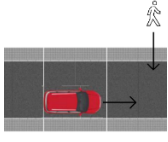
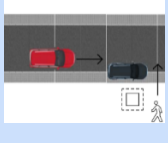

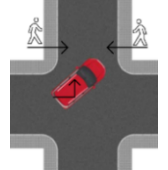
4.5.2 Use cases for advanced intervention functions and CITS

The recommended use cases for advanced intervention functions and Cooperative Intelligent Transport Systems (CITS), considered in Demonstrators 3 and 4 within SAFE-UP, are primarily based on the frequency of car-to-VRU scenarios. Section 4.3.1 indicates the most common car-to-pedestrian scenarios while the most common car-to-bicycle scenarios are addressed in section 4.3.2.

4.5.2.1 Most common car-to-pedestrian crashes

Table 45 below summarizes the most common car-to-pedestrian crash scenarios, indicating the share of injured and KSI pedestrians in the corresponding scenario (relative to the total numbers in car-to-pedestrian crashes) with the specification of initial speed, relation to junction and whether the infrastructure at the crash site supported the crossing of the pedestrian. Those scenarios are listed in which >10% of all injured or KSI suffer their injuries.

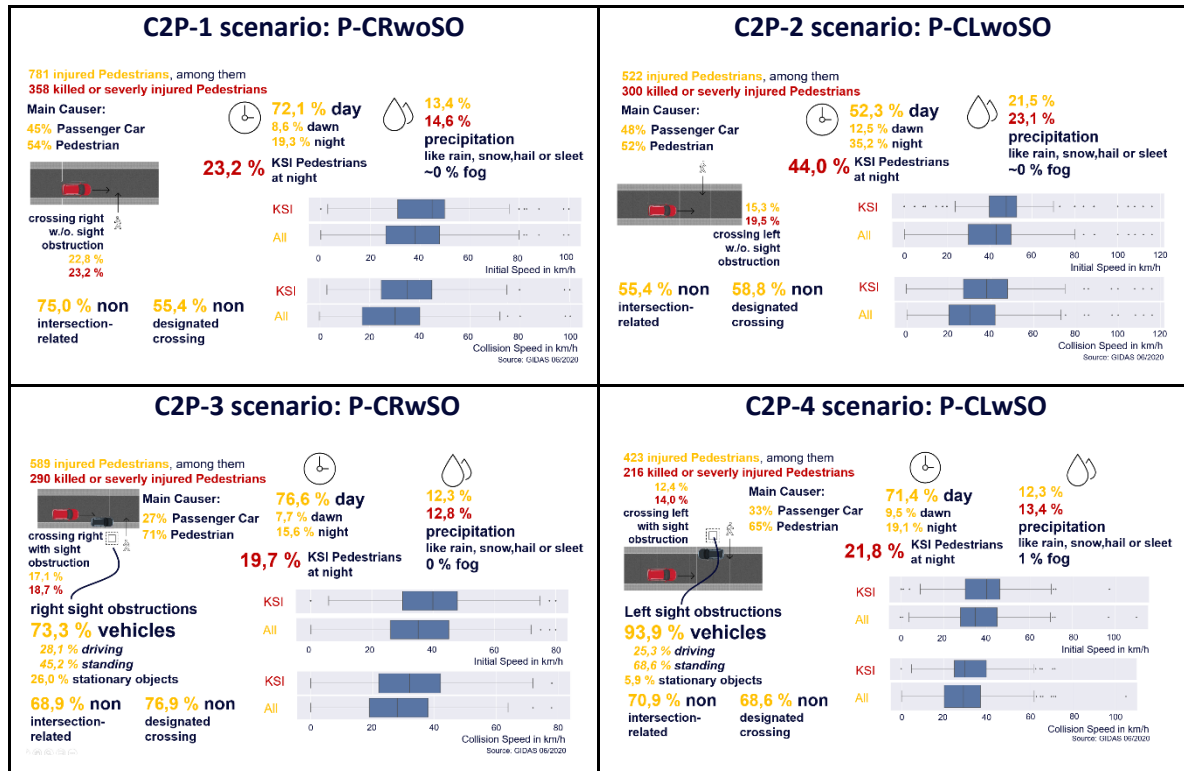
Table 45 Most common car-to-pedestrian crashes and corresponding use cases

Scenario name	Schematic illustration of conflict situation	% all injured	% KSI	Initial speed of car (IQR)	Typical infrastructural environment	Infrastructural support of crossing
P-CRwoSO Pedestrian crossing from right without sight obstruction		22.8%	23.2%	26-48 km/h	Away from junction (75%)	Non-designated (55.4%)
P-CLwoSO Pedestrian crossing from left without sight obstruction		15.3%	19.5%	30-50 km/h	Away from junction (55.4%)	Non-designated (58.8%)
P-CRwSO Pedestrian crossing from right with sight obstruction		17.1%	18.7%	26-45 km/h	Away from junction (68.9%)	Non-designated (76.9%)
P-CLwSO Pedestrian crossing from left with sight obstruction		12.4%	14.0%	28-45 km/h	Away from junction (70.9%)	Non-designated (68.6%)
P-PCTurnL Passenger car turning left		11.1%	9.2%	10-28 km/h	Junction (97.6%)	Designated (63.6%)



The first four scenarios in Table 45 above have common characteristics in that each of these scenarios occurs primarily away from junctions (which is in line with the CARE-based results on EU level in Figure 11 and the crossing of pedestrians is not supported by the infrastructure. Further features of these scenarios are described in section 4.3.1.2; for easier access, the four overview slides from that section are provided below in Table 46.

Table 46 Overview of the most frequent car-to-pedestrian scenarios, recommended for consideration for CITS



The fifth most common car-to-pedestrian scenario, P-PCTurnL, has different features compared to the ones in Table 46. Additionally, the P-PCTurnL scenario has high relevance for pedestrian scenarios in adverse weather conditions (see section 4.5.3 below), hence it will be considered for Demonstrators 2 and 3. Therefore, it is recommended that the work related to CITS for pedestrian protection is primarily focused on the first four scenarios (named as C2P scenarios 1-4 in Table 46 above).

Table 46 above indicates that C2P scenarios 1-4 include both designated and non-designated crossings of pedestrians, with most occurring during pedestrians crossing at non-designated locations. Therefore, it is important to understand how behavioral aspects and crash causation differs depending on whether the crossing is supported by the infrastructure. A study of road user behavior in NDD (see section 4.3.1.3) indicates that interaction between a car driver and pedestrian is mostly present in a designated crossing while it is poor or absent in non-designated crossings (especially at night or in case of bad weather, when pedestrians may be in a hurry). In case of non-designated crossings, car drivers are often taken by surprise or are confused about pedestrians' intentions. A more

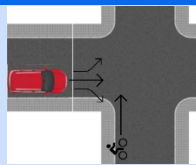
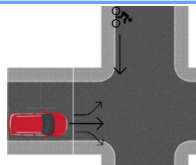
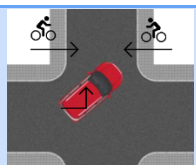
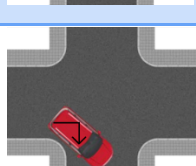


detailed summary of the key findings regarding behavioral aspects in designated and non-designated crossings from NDD analysis can be found in Table 22, while section 4.3.1.4 gives further details of crash causation based on analysis of GIDAS data.

4.5.2.2 Most common car-to-bicycle crashes

Table 47 below summarizes the most common car-to-bicycle crash scenarios, indicating the share of injured and KSI cyclists in the corresponding scenario (relative to the total numbers in car-to-bicycle crashes) with the specification of initial speed for both car and cyclist, and relation to junction. Those scenarios are listed that have relative frequency >10% with respect to all injured or KSI.

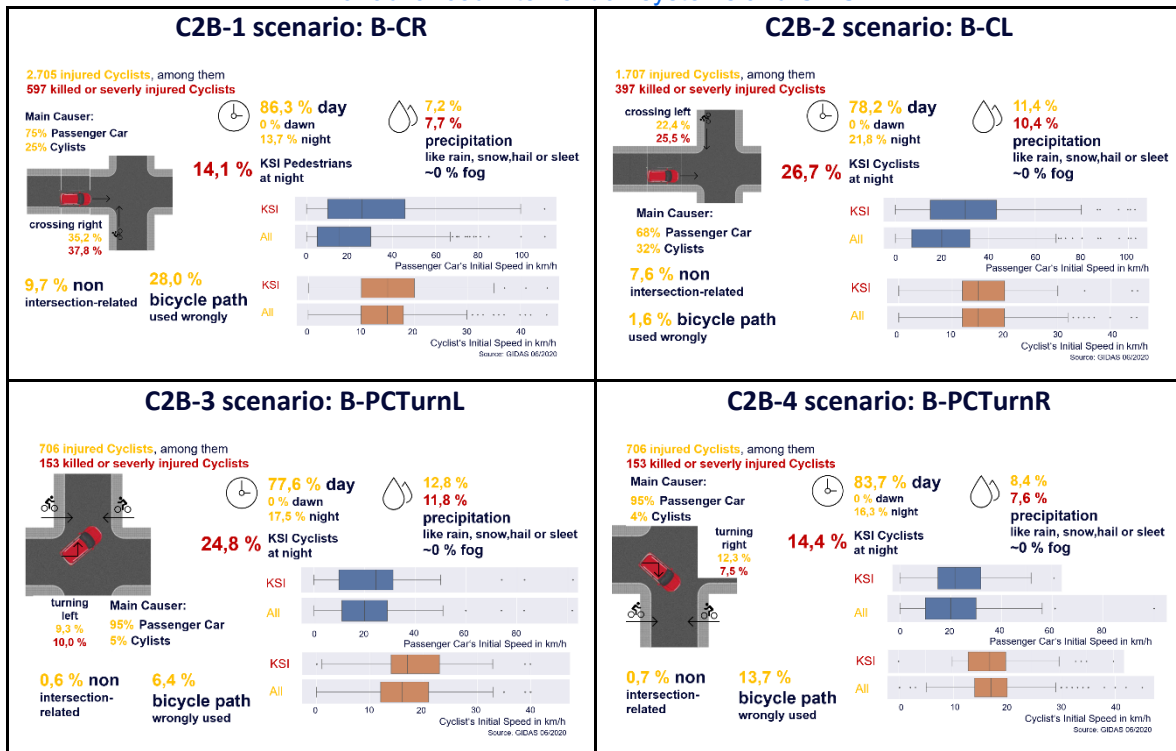
Table 47 Most common car-to-bicycle crashes and corresponding use cases

Scenario name	Schematic illustration of the conflict situation	% all injured	% KSI	Initial speed of car (IQR)	Initial speed of bicycle (IQR)	Typical infrastructural environment
B-CR Bicyclist crossing from right while PC moves forward		35.2%	37.8%	5-30 km/h	10-18 km/h	Junction (90.3%)
B-CL Bicyclist crossing from left while PC moves forward		22.4%	25.5%	7-32 km/h	12-20 km/h	Junction (92.4%)
B-PCTurnL Bicyclist in conflict with PC turning left		17.1%	10.0%	11-29 km/h	12-21 km/h	Junction (99.4%)
B-PCTurnR Bicyclist in conflict with PC turning right		12.3%	7.5%	10-30 km/h	14-20 km/h	Junction (99.3%)

As Table 47 shows, junction-related scenarios are substantially more common for car-to-bicycle crashes compared to car-to-pedestrian crashes. This, again, is in line with EU level results in Figure 10. Placing an infrastructure-based CITS in the junction may contribute to a substantial reduction of the relevant cases. Further details of the car-to-bicycle scenarios for advanced intervention systems and CITS, given in section 4.3.2.2, are reproduced for easier access in Table 48 below.



Table 48 Overview of the most frequent car-to-bicyclist scenarios, recommended for consideration for advanced intervention systems and CITS



4.5.3 Use cases for car-to-VRU crashes in adverse weather conditions

The use cases for car-to-VRU crashes in adverse weather conditions (AWC) are those scenarios with a larger-than-average prevalence of precipitation like rain, snow, hail or sleet. Fog was found to be less relevant as it is present in 0-1% of crashes. The use cases that are recommended to be addressed by safety systems with improved performance in weather conditions that could adversely affect sensor performance (addressed in SAFE-UP Demonstrators 2 and 3) include the following scenarios, shown in Table 49 below:

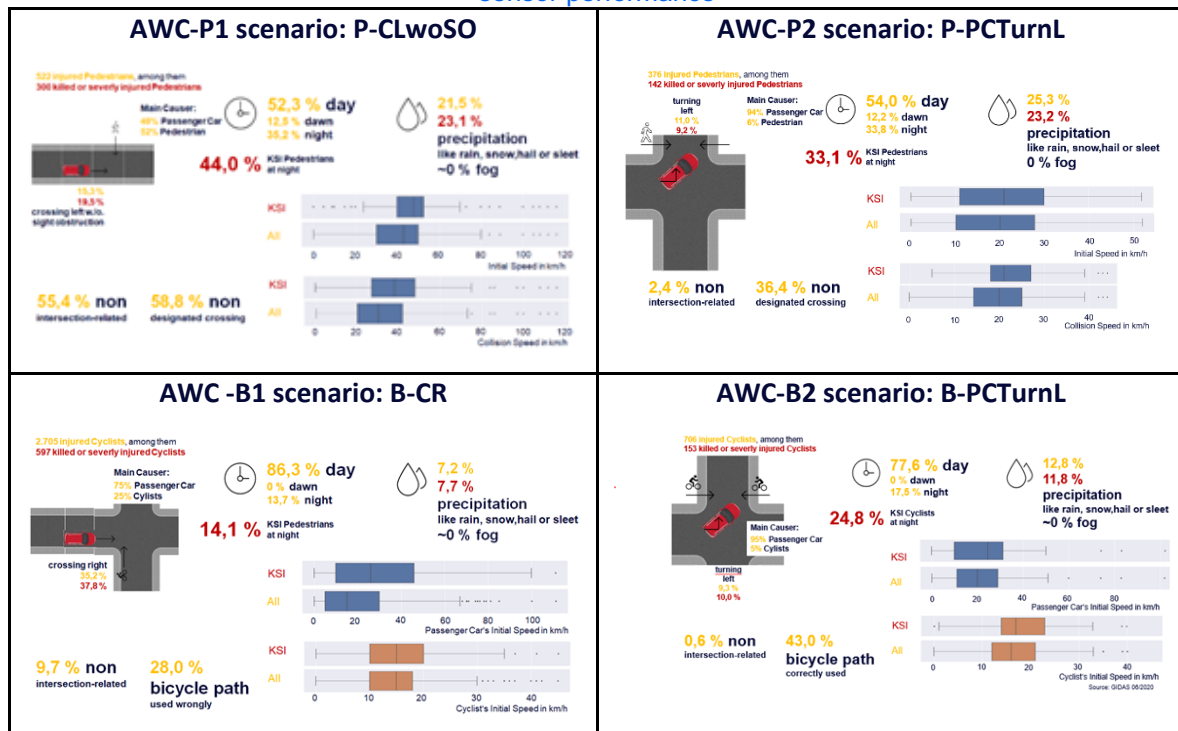
- a) AWC-P1, identical to C2P-2: Pedestrian crossing from left, without sight obstruction (P-CLwoSO, 19.5% of KSI, 15.3% of all injured within C2P), with typical initial speeds of 30-50 km/h for the passenger car. 23.1% of KSI and 21.5% of all injuries within this scenario occur in weather conditions with precipitation. The intensity of precipitation in the corresponding crashes is 63% “light”, 31% “moderate”, 3% “heavy” and 3% “not identifiable”.
- b) AWC-P2: Pedestrian in conflict with passenger car turning left (P-PCTurnL, 9.2% of KSI, 11.1% of all injured within C2P), with typical initial speeds of 10-28 km/h for the passenger car. 23.2% of KSI and 25.3% of all injuries within this scenario occur in weather conditions with



precipitation. The intensity of precipitation in the corresponding crashes is 60% “light”, 31% “moderate”, 6% “heavy” and 3% “not identifiable”.

- c) AWC-B1, identical to CITS-B1: Bicyclist crossing from right while passenger car moves forward (B-CR, 37.8% of KSI, 35.2% of all injured within C2B), with typical initial speeds of 5-30 km/h for the passenger car and 10-18 km/h for the cyclist. 7.7% of KSI and 7.2% of all injuries within this scenario occur in weather conditions with precipitation. The intensity of precipitation in the corresponding crashes is 59% “light”, 30% “moderate”, 6% “heavy” and 5% “not identifiable”.
- d) AWC-B2, identical to CITS-B3: Bicyclist in conflict with passenger car turning left (B-PCTurnL, 10.0% of KSI, 17.1% of all injured within C2B), with typical initial speeds of 11-29 km/h for the passenger car and 12-21 km/h for the cyclist. 11.8% of KSI and 12.8% of all injuries within this scenario occur in weather conditions with precipitation. The intensity of precipitation in the corresponding crashes is 71% “light”, 27% “moderate”, and 2% “heavy”.

Table 49 Car-to-VRU scenarios recommended for consideration for safety systems with improved sensor performance



To allow the simulation and testing of scenarios with realistic precipitation amounts that can be observed in real-world crashes, GIDAS data was linked to rainfall amounts around the crash site as measured in weather stations of the German Meteorological Service. The



results in Table 39 show that the subjective intensity label “light” in GIDAS can be mapped to the median value of 0.42mm/h, “moderate” to the median value of 0.84mm/h, and “heavy” to the median value of 1.2mm/h, with the 90th percentiles (indicating the rainfall amount that includes 90% of GIDAS crashes with the given rain intensity label) are 1.5 mm/h for “light,” 3.6mm/h for “moderate” and 5.8mm/h for “heavy”.

4.5.4 Most common crash scenarios for powered two-wheelers

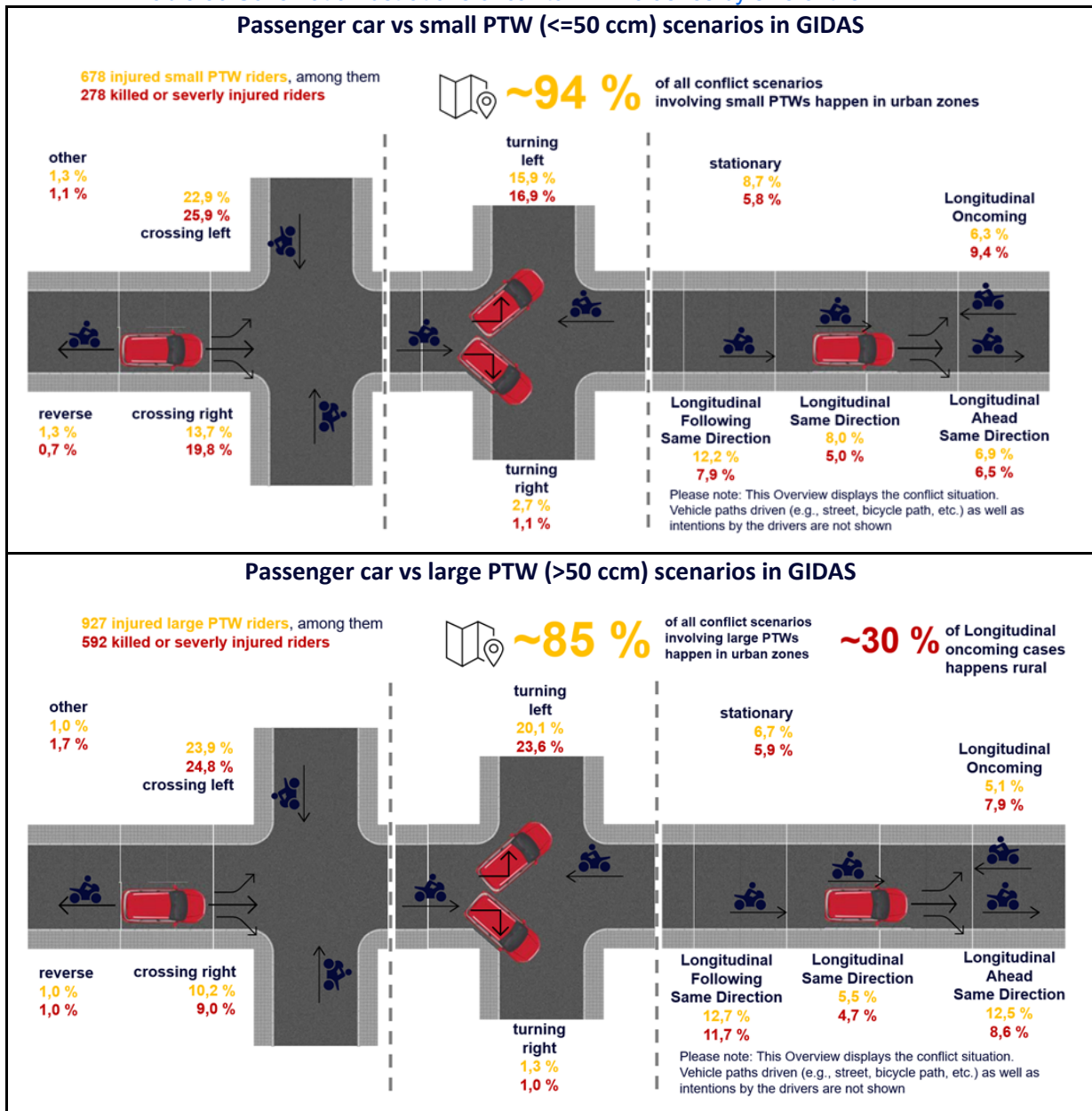
While no use cases for car-to-PTW crashes are defined in this report due to the project focus, the corresponding crashes were analyzed and clustered similarly to the car-to-bicyclist crashes to gain a full understanding of the frequency of scenarios in car-to-VRU crashes. Small PTWs (≤ 50 ccm) and large PTWs (> 50 ccm) were considered separately to identify potentially different characteristics of the corresponding crashes. The analysis is described in sections 4.3.3.3 and 4.3.3.4; the overview slides Figure 74 and Figure 75 are reproduced in Table 50 below for easier access.

Besides the crash data analysis in GIDAS, additional analysis was conducted in the data from the MAIDS and 2BeSafe projects for a better understanding of car-to-PTW crashes that may have implications on the modelling of PTW behavior in traffic simulation. The performed analysis showed clear information about conditions that are safety-critical for PTWs. According to analysis of MAIDS data excluding cases where the primary contributing factor was rider impairment or mechanical problems, crashes occur frequently with scenarios related to junctions, highlighting the importance of this kind of infrastructure in scenario definition. This conclusion can be extended with the cases reporting severe injuries. Around 58% of the severe injuries of the data analyzed were reported in a scenario related to junctions. Thus, defining a scenario that is safety-critical for PTWs riders should consider car-PTW interaction at junctions.

This conclusion is supported by the results of the preliminary analysis of the naturalistic data collected in the framework of the 2BeSafe project. The results identified the presence of a junction as a common factor in half of the conflicts between PTW and another vehicle in which the PTW rider required the most intense evasive braking maneuvers. The most frequent conflict requiring braking by the PTW rider was that avoiding a rear-end collision with a car at a junction.



Table 50 Schematic illustrations of car-to-PTW crashes by size of the PTW



5. Discussion and outlook

In this deliverable, the use cases for further analysis in the SAFE-UP project have been defined, based on the analysis of field data. This section discusses the method used for the selection of use cases and describes the limitations related to the underlying data that are important for the interpretation of the results. The open points and further directions related to the usage of use cases are described in Section 5.2.

5.1 Discussion of the method, results, and limitations

The results in this deliverable are based on the analysis of field data, i.e., road crash data and naturalistic driving data, both from real-world traffic. The first step of the analysis was to get an overview of EU level results based on data from the CARE database. Basing the direction of analysis on the corresponding results ensures the relevance of further steps for improved road safety at EU level. Additionally, the results of the CARE analysis may provide necessary input to safety benefit assessment in WP5 aiming to evaluate the safety systems in SAFE-UP in terms of saved lives and avoided injuries on EU level.

The EU level overview of crashes is based on the analysis of CARE which contains information about all crashes with personal injury reported in the national data from EU countries. Consequently, although there are indications that the completeness of reporting may vary between different countries and there are inconsistencies between the usage of specific variables (see e.g., Dobberstein et al., (2021)), the results give a reasonably complete picture of the crash situation on EU level regarding injury crashes. On the other hand, the CARE-based results do not include property damage only (PDO) crashes, i.e., they may not be representative for PDO crashes in the EU. This could be a challenge when comparing simulation-based results to real-world crash patterns, considering that it is difficult to tell the injury level of a simulated crash. The analysis of simulation-based crashes should be limited to injurious crashes to make a fair comparison.

Additionally, the initial safety-critical situations in this report are related to crashes rather than situations that had a high crash risk but typically did not end up in a crash. Such situations could also be of interest, considering that changes in future traffic related to the introduction of AVs or other factors could potentially change the characteristics of such situations and possibly increase the corresponding crash risk. For the identification of such high-risk situations, further analysis of naturalistic driving data could be relevant. The corresponding analysis of NDD is planned in T2.2, see Section 5.2 for further details.

Finally, this deliverable mostly addresses current safety-critical scenarios while the goal with SAFE-UP WP2 work is to find scenarios that will be relevant in the future. This is intentional; the expected future scenarios will be output from the Aimsun Next traffic simulations in tasks T2.2 – T2.5. The main purpose of T2.1 was to give a general overview of the current situation and provide thereby a foundation for the SAFE-UP project activities and specify starting



points that other tasks can work with until the final future scenarios are available. However, even the analysis in T2.1 included a future view when it was most relevant; for example, in the analysis of use cases for car occupant protection, only modern cars were included, and single vehicle crashes were disregarded as they were not considered relevant for AVs. Additionally, in Section 4.4, an outlook based on an initial analysis of crash data from the in-depth crash database IGLAD was given, to get a preliminary indication of how the distribution of crashes might change in the future because of a widespread fleet penetration of currently available active safety systems.

5.2 Suggested future directions and open points

The use cases suggested for further analysis in different parts of the project are all summarized in Section 4.5. That section is meant to provide an overview of initial safety-critical scenarios without having to read all details in other sections. However, it is a key point with this report that the selection of scenarios to be addressed can be extended or modified as needed in further project work. Specifically, appropriate ranges of crash configuration parameters for car occupant protection are provided in Table 10 and Table 11. Regarding VRU protection, the analyses in Sections 4.3.1 and 4.3.2 and four tables in the Appendix (from Table 51 to Table 54) can be used as a catalogue of relevant scenarios that includes various characteristics for each scenario (e.g., regarding weather, light conditions, infrastructural aspects, crash causation, kinematic parameters, and trajectories of the participants in the last seconds before the crash).

An additional point where further investigation is planned is the method of extrapolating results based on locally collected data (such as GIDAS, collected in two regions in Germany) to EU level. Such an extrapolation will be highly relevant when evaluating the safety benefit of safety systems in SAFE-UP in terms of saved lives and avoided injuries on EU level in WP5. Different extrapolation methods will be investigated in T5.3 for weighting data from IGLAD to EU level, also considering the representation of specific groups of VRUs (e.g., children/elderly, road workers, etc.), and the results will be applied to the method presented in Section 4.4. It is then planned to apply the most suitable extrapolation method for the safety benefit assessment.

Another relevant aspect that is only partly answered in this deliverable and is thus currently an open point is a more complete analysis of parameters related to driver behavior in critical and non-critical situations. Having such data is important for a correct calibration of the traffic simulations in T2.2 - T2.5; therefore, further NDD analysis based on data from the SePIA database (SePIA, 2021) as well as analysis of the TASC database is planned for a better characterization of the relevant aspects. As indicated in Section 4.5.1, such an analysis may also be relevant for the identification of safety-critical scenarios that typically do not lead to crashes today but could potentially have high crash risk in future traffic. The timeline for accessing data in these databases was not compatible with the timing of T2.1 and the need of other tasks to get access to the results described in this report, hence the corresponding analyses are planned to be performed in T2.2.



6. Conclusions

In this document, use cases for SAFE-UP systems for car occupant protection, advanced intervention systems and sensor systems working in adverse weather conditions have been defined by extensive analysis of crash data from several databases. The use cases were defined in the form of crash scenarios with pre-crash information for the active safety systems for VRU protection and with crash configurations (including, e.g., velocities and angles at the time of impact) for car occupant protection. Objective rainfall amounts have also been defined that may be relevant for simulating and testing sensor performance in adverse weather conditions. All use cases are briefly summarized in Section 4.5.

The initial safety-critical scenarios described in this report will be studied further in the project to derive the final scenarios representing our best estimate of future traffic. Until that time, the analysis described in this report may be the base for further project work. The use cases are recommendations to serve as starting points; detailed data about additional parameters and additional scenarios are provided in this deliverable, which allows the selection of additional scenarios or the replacement of certain recommended scenarios.



7. References

- 2BeSafe. (2021, 08 30). *Webpage of the EU project 2-wheeler Behavior and Safety*. Retrieved from <https://www.2besafe.eu/>
- Adjenughwure, K., Huertas-Leyva, P., Prinz, F., Tejada, A., & Wang, X. (2021). *SAFE-UP deliverable D2.5: Description metrics for traffic interactions*.
- Andrey, J., Mills, B., Leahy, M., & Suggett, J. (2003). Weather as a Chronic Hazard for Road Transportation in Canadian Cities. *Natural Hazards* 28.
- Attal, F., Boubezul, A., Oukhellou, L., & Espié, S. (2013). Riding patterns recognition for Powered two-wheelers users' behaviors analysis. *16th International IEEE Conference on Intelligent Transportation Systems (ITSC 2013)* (pp. 2033-2038). doi: 10.1109/ITSC.2013.6728528.
- Attal, F., Boubezul, A., Oukhellou, L., & Espié, S. (2015). Powered Two-Wheeler Riding Pattern Recognition Using a Machine-Learning Framework. *IEEE Transactions on Intelligent Transportation Systems* 16, 457-487.
- Baldanzini, N., Huertas-Leyva, P., Savino, G., & Pierini, M. (2016). Rider Behavioral Patterns in Braking Manoeuvres. *Transportation Research Procedia*, 4374-4383, <https://doi.org/10.1016/j.trpro.2016.05.359>.
- BMVBW. (2002). *German Federal Ministry of Transport, Mobilität in Deutschland Ergebnisbericht (in German)*.
- CADaS. (2021, 08 30). *Common Accident Data Set glossary, version 3.7*. Retrieved from https://ec.europa.eu/transport/road_safety/sites/default/files/cadas_glossary_v_3_7.pdf
- CARE. (2021, 08 30). *Information about the CARE database*. Retrieved from https://ec.europa.eu/transport/road_safety/specialist/statistics_en
- Davoodi, S. R., & Hamid, H. (2013). Motorcyclist braking performance in stopping distance situations. *Journal of Transportation Engineering* 139.
- DENSE. (2017a). *DENSE Deliverable 2.1: Characteristics of Adverse Weather Conditions*.
- DENSE. (2017b). *DENSE Deliverable 2.2: System needs and benchmarking*.
- DESTATIS. (2020a). *German Federal Statistical Office (Destatis), Verkehrsunfälle - Kraftrad- und Fahrradunfälle im Straßenverkehr 2019 (in German)*. Artikelnummer: 5462408-19700-4, Statistisches Bundesamt (Destatis).
- DESTATIS. (2020b). *German Federal Statistical Office (Destatis), Verkehrsunfälle - Unfälle unter dem Einfluss von Alkohol oder anderen berauschenden Mitteln im Straßenverkehr 2019*. Retrieved from Artikelnummer: 5462404-19700-4



- DESTATIS. (2021a, July 6). *German Federal Statistical Office (Destatis) - Verkehrsunfälle - Verletzte bei Verkehrsunfällen nach Art der Verkehrsbeteiligung (in German) 8 April 2021. [Online].* Retrieved from <https://www.destatis.de/DE/Themen/Gesellschaft-Umwelt/Verkehrsunfaelle/Tabellen/verletzte-fahrzeugart.html>
- DESTATIS. (2021b, July 6). *German Federal Statistical Office (Destatis) - Verkehrsunfälle - Getötete bei Verkehrsunfällen nach Art der Verkehrsbeteiligung (in German), April 8, 2021.* Retrieved from <https://www.destatis.de/DE/Themen/Gesellschaft-Umwelt/Verkehrsunfaelle/Tabellen/getoetete-fahrzeugart.html>
- DESTATIS. (2021c, July 6). *German Federal Statistical Office (Destatis), Destatis Verkehrsunfallkalender 2020.* Retrieved from <https://service.destatis.de/DE/verkehrsunfallkalender/>
- Dingus, T. A. (2006). *The 100-car naturalistic driving study, Phase II-results of the 100-car field experiment.* No. DOT-HS-810-593. United States. Department of Transportation. National Highway Traffic Safety Administration.
- Dobberstein, J., Lich, T., & Schmidt, D. (2019). *Accident data analysis - remaining accidents and crash configurations of automated vehicles in mixed traffic.* Available online at http://osccarproject.eu/wp-content/uploads/2020/04/OSCCAR_D_1.1.pdf: Deliverable 1.1 in the EU project OSCCAR.
- Dobberstein, J., Schmidt, D., Östling, M., Lindman, M., Bálint, A., & Höschele, P. (2021). *Deliverable D1.3 in the EU project OSCCAR.*
- DWD. (2020, December 10a). *German Meteorological Service, Climate Data Center.* Retrieved from https://opendata.dwd.de/climate_environment/CDC/
- DWD. (2020, December 10c). *German Meteorological Service, Datensatzbeschreibung: Historische 10-minütige Stationsmessungen der Niederschlagshöhe in Deutschland (in German).* Retrieved from https://opendata.dwd.de/climate_environment/CDC/observations_germany/climate/10_minutes/precipitation/historical/BESCHREIBUNG_obsgermany_climate_10min_precipitation_historical_de.pdf
- DWD. (2020b, December 10b). *German Meteorological Service, Wetterlexikon - Niederschlagsintensität.* Retrieved from <https://www.dwd.de/DE/service/lexikon/Functions/glossar.html?lv2=101812&lv3=101906>
- Eurostat. (2021, July 6). *Eurostat - Road accident fatalities - statistics by type of vehicle, Eurostat - Statistics Explained - Data by CARE Database, June 24, 2021. [Online].* Retrieved from https://ec.europa.eu/eurostat/statistics-explained/index.php?title=Road_accident_fatalities_-_statistics_by_type_of_vehicle&stable=0&redirect=no#Ratios_of_persons_killed_in_passenger_cars_crashes_differed_vastly_also_in_2018



- Eurostat. (2021). *Eurostat Data Browser - Persons killed in road crashes by type of vehicle (CARE data)*.
- Evgenikos, P., Yannis, G., Folla, K., Bauer, R., Machata, K., & Brandstaetter, C. (2016). How Safe are Cyclists on European Roads? *Transportation Research Procedia* 14, 2372-2381, <https://doi.org/10.1016/j.trpro.2016.05.269>.
- Fahrenkrog, F., Wang, L., Platzer, T., Fries, A., Raisch, F., & Kompaß, K. (2019). Prospective safety effectiveness assessment of automated driving functions - from the methods to the results. *26th International Technical Conference on the Enhanced Safety of Vehicles (ESV)*. Eindhoven, Netherlands.
- FARS. (2021, July 02). *Information about the Fatality Analysis Reporting system*. Retrieved from <https://www-fars.nhtsa.dot.gov/Main/index.aspx>
- GDV. (2016). *Crash type catalogue of the German Insurance Association (Unfalltypen-Katalog, Gesamtverband der Deutschen Versicherungswirtschaft)*, in German. Available at <https://udv.de/de/publikationen/broschueren/unfalltypen-katalog>.
- Huertas-Leyva, P., Baldanzini, N., Savino, G., & Pierini, M. (2021). Human error in motorcycle crashes: A methodology based on in-depth data to identify the skills needed and support training interventions for safe riding. *Traffic Injury Prevention*, 294-300.
- IGLAD. (2021, 08 30). *Information about the Initiative for the Global Harmonisation of Accident Data*. Retrieved from <http://iglad.net/web/page.aspx?refid=11>
- Infas. (2019). *German Federal Ministry of Transport and Digital Infrastructure, Mobilität in Deutschland – MiD (in German)*.
- JAAD. (2021, 08 30). *Description of the Joint Attention in Autonomous Driving dataset*. Retrieved from <https://paperswithcode.com/dataset/jaad>
- Kompf, M. (2020, December 10). *Algorithmen - Entfernungsberechnung (in German)*. Retrieved from <https://www.kompf.de/gps/distcalc.html>
- NSC. (2021, July 2). Retrieved from "injuryfacts.nsc.org": National Safety Council, "injuryfacts.nsc.<https://injuryfacts.nsc.org/home-and-community/safety-topics/bicycle-deaths/>
- Nugent, M., & Bálint, A. (2021, 08 30). *Task 2.1 Definition of Safety-Critical Scenarios [Graphical summary]*. Retrieved from <https://www.safe-up.eu/resources>
- Odriozola, M. d., Vilchez, S., Östling, M., D'Addetta, G. A., Merdivan, D., Bálint, A., . . . Zimmer, A. (2021). *SAFE-UP Deliverable D4.1: Use case definition*.
- Rasouli, A., Kotseruba, I., & Tsotsos, J. K. (2017). Are They Going to Cross? A Benchmark Dataset and Baseline for Pedestrian Crosswalk Behavior. *International Conference on Computer Vision (ICCV) workshop, Venice, Italy*. Computer Vision Foundation. Available online at:



https://openaccess.thecvf.com/content_ICCV_2017_workshops/papers/w3/Rasouli_Are_They_Going_ICCV_2017_paper.pdf.

Retting, R. (2018). *Pedestrian Traffic Fatalities by State*. Washington D.C.: Sam Schwartz Consulting, Governors Highway Safety Association.

SePIA. (2021, August 30). *Project information for Scenario-Based Platform for the Inspection of Automated Driving Functions (SePIA)*. Retrieved from <https://www.synchrone-mobilitaet.de/en/projects/sepia.html>

Sminkey, L. (2021, July 2). Retrieved from World Health Organisation: <https://www.who.int/news/item/11-12-2010-pedestrians-cyclists-among-main-road-traffic-crash-victims>

Stevens, S., Schreck, C., Saha, S., & Bell, J. K. (2019). Precipitation and Fatal Motor Vehicle Crashes: Continental Analysis with High-Resolution Radar Data. *Bulletin of the American Meteorological Society*.

Urban, M., Erbsmehl, C., Landgraf, T., Pohle, M., Mallada, J. L., Puente Guillen, P., & Tanigushi, S. (2020). Parameterization of Standard Test Scenarios of Automated Vehicles Using Accident Simulation Data. *Fédération Internationale des Sociétés d'Ingénieurs des Techniques de l'Automobile (FISITA Web Congress), 2020, online*.

Urban, M., Erbsmehl, C., Mallada, J. L., Puente Guillen, P., & Tanigushi, S. (2020). A Methodology for Building Simulation Files from Police Recorded Accident Data (for ADAS Assessment). *Fédération Internationale des Sociétés d'Ingénieurs des Techniques de l'Automobile (FISITA Web Congress), 2020, online*.

WHO. (2004). *World report on road traffic injury prevention*. Geneva.

WHO. (2018). *World Health Organization, Global status report on road safety 2018: summary*. WHO/NMH/NVI/18.20. Licence: CC BY-NC-SA 3.0 IGO.

Östling, M., Jeppsson, H., & Lübbe, N. (2019). Predicting crash configurations in passenger car to passenger car crashes to guide the development of future passenger car safety. *Proceedings of IRCOBI conference 2019, paper IRC-19-92* (pp. 626-643). Florence: <http://www.ircobi.org/wordpress/downloads/irc19/pdf-files/92.pdf>.

Östling, M., Lübbe, N., Jeppsson, H., & Puthan, P. P. (2019). Passenger car safety beyond ADAS: Defining remaining accident configurations as future priorities. *Passenger car safety beyond ADAS: Defining remaining accident configurations as future priorities. In The 26th International Technical Conference on the Enhanced Safety of Vehicles (paper 19-0091-O)*. Eindhoven, Netherlands.

...



Appendix

The following figures specify the time periods for car-involved crashes in rural areas (Figure 93 and Figure 95) and on motorways (Figure 94 and Figure 96), similarly to Figure 7 and Figure 8 in Section 4.1 for urban areas.

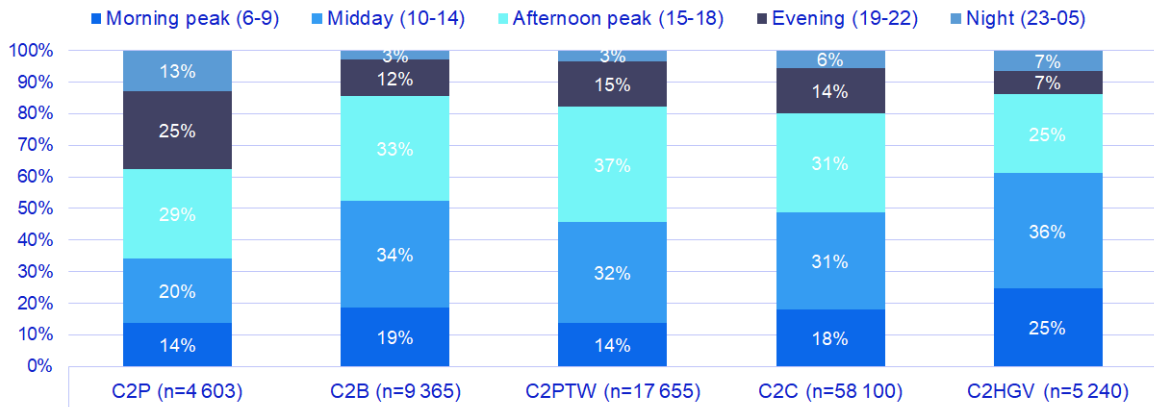


Figure 93 Time-of-the-day distribution of car-involved crashes of any injury level in rural areas in the EU in 2018

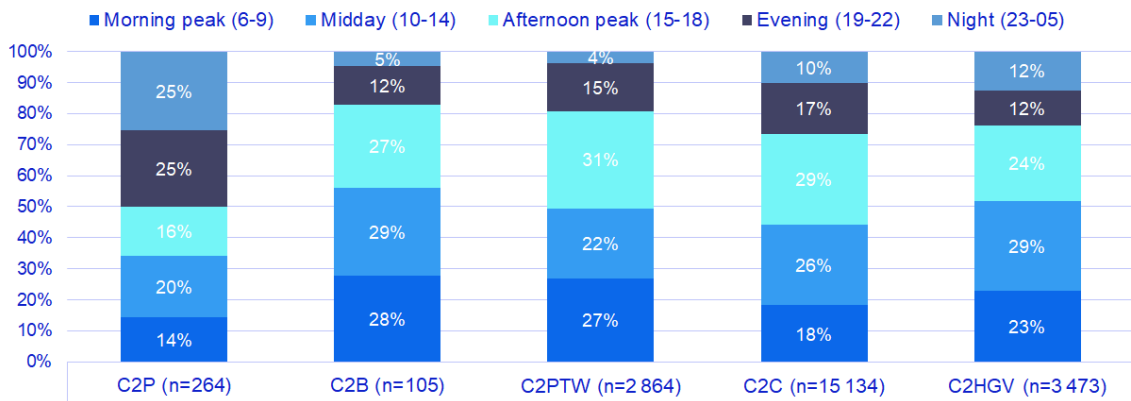


Figure 94 Time-of-the-day distribution of car-involved crashes of any injury level on motorways in the EU in 2018



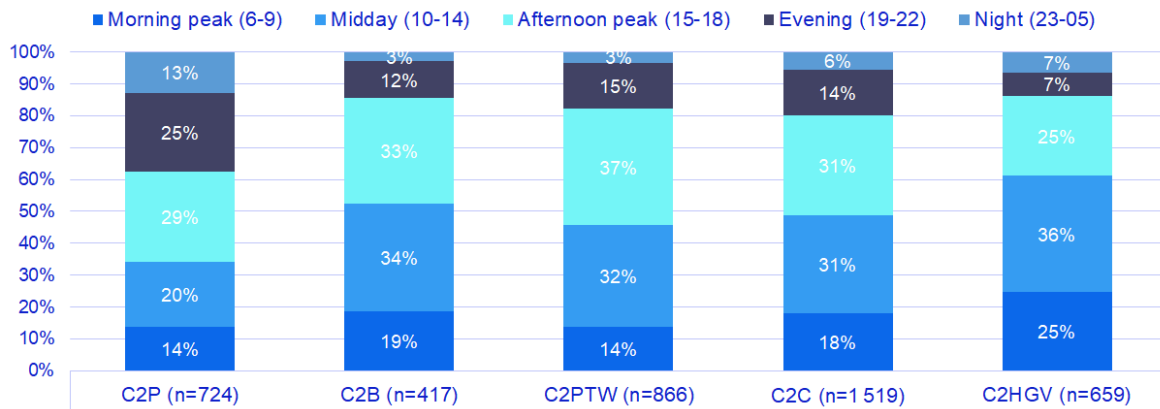


Figure 95 Time-of-the-day distribution of fatal car-involved crashes in rural areas in the EU in 2018

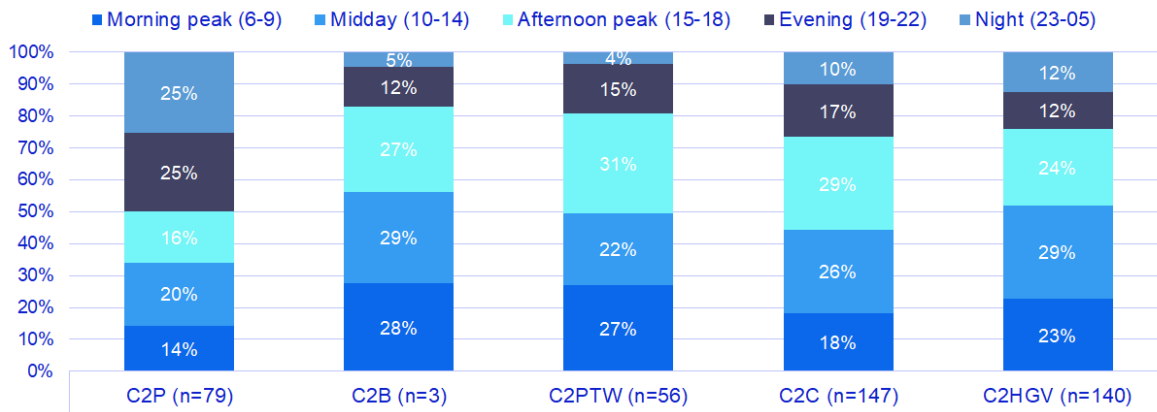


Figure 96 Time-of-the-day distribution of fatal car-involved crashes on motorways in the EU in 2018

Finally, the tables on the following pages summarize the environmental and kinematic parameters (Table 51 and Table 53) as well as results of a crash causation analysis (Table 52 and Table 54) for car-to-pedestrian and car-to-bicycle scenarios respectively, based on data from GIDAS.



Table 51 Summary statistics of environmental and kinematic parameters in car-to-pedestrian conflict scenarios

C2P scenario	# inj	# KSI	Away from junction [% of all inj]	Non-designated location [% of all inj]	Light conditions [% of all inj]			Night among KSI cases [%]	Precip (rain, snow, hail, sleet) [% of all inj]	Precip (rain, snow, hail, sleet) among KSI cases	Fog [% of all inj]	Init speed Q25, all inj [km/h]	Init speed Q75, all inj [km/h]	Coll speed Q25, all inj [km/h]	Coll speed Q75, all inj [km/h]	Passenger car (driver) classified as main causer [% of all inj]
					Daytime	Dawn	Night									
P-CLwoSO	522	300	55.4%	58.8%	52.3%	12.5%	35.2%	44.0%	21.5%	23%	0%	30	50	20	42	48%
P-CLwSO	423	216	70.9%	68.6%	71.4%	9.5%	19.1%	21.8%	12.3%	13.4%	1%	28	45	20	37	33%
P-CRwoSO	781	358	74.9%	54.9%	72.1%	8.6%	19.3%	23.2%	13.4%	14.5%	0%	26	48	17	40	45%
P-CRwSO	589	290	68.9%	76.9%	76.6%	7.7%	15.6%	19.7%	12.3%	12.8%	0%	26	45	19	38	27%
P-Long	117	43	90.7%	N/A	49.6%	7.7%	42.7%	58.1%	19.8%	23.3%	0%	20	58	20	50	89%
P-PCRev	257	82	79.0%	N/A	85.6%	7.0%	7.4%	4.0%	5.5%	4.9%	1%	0	6	5	10	99%
P-PCTurnL	376	142	2.4%	36.4%	54.0%	12.2%	33.8%	33.1%	25.3%	23.2%	0%	10	28	14	25	94%
P-PCTurnR	130	34	0%	23.8%	56.9%	10.8%	32.3%	35.3%	14.7%	11.8%	0%	11	25	10	20	92%



Table 52 Summary statistics of crash causation in car-to-pedestrian conflict scenarios

Scenario	Passenger Car (PC) and also its driver					Pedestrian (Ped)				
	Share of PC and its drivers w./o. a crash cause	# main causes for PC and its drivers	Main Cause of PC and its drivers with the highest share	# causes for PC and its drivers	Cause of PC and its drivers with the highest share	Share of Ped w./o. a crash cause	# main causes for Ped	Main Cause of Ped with the highest share	# causes for Ped	Cause of Ped with the highest share
P-CLwoSO	33%	350	Improper behavior towards ped at other places / 32%	469	Improper behavior towards ped at other places / 27%	26%	384	Improper behavior of pedestrians without paying attention to the traffic / 63%	526	Improper behavior of peds without paying attention to the traffic / 54%
P-CLwSO	49%	217	Improper behavior towards ped at stops / 36%	288	Improper behavior towards ped at stops / 31%	14%	363	Improper behavior of peds by suddenly emerging from behind obstacles obstructing the visibility / 45%	604	Improper behavior of peds without paying attention to the traffic / 46%
P-CRwoSO	41%	464	Improper behavior towards ped at other places / 25%	625	Improper behavior towards ped at other places / 21%	28%	562	Improper behavior of peds without paying attention to the traffic / 58%	766	Improper behavior of peds without paying attention to the traffic / 53%
P-CRwSO	52%	283	Improper behavior towards ped at other places / 25%	387	Improper behavior towards ped at other places / 24%	9.5%	533	Improper behavior of peds by suddenly emerging from behind obstacles obstructing the visibility / 48%	890	Improper behavior of peds without paying attention to the traffic / 46%
P-Long	7%	109	Improper behavior towards ped at other places / 64%	153	Improper behavior towards ped at other places / 52%	9.4%	49	Improper behavior of peds Failure to use footway / 27%	69	Improper behavior of peds Failure to use footway / 23%
P-PCRev	0.4%	256	Mistakes made when making U turn or reversing / 78%	408	Mistakes made when making U turn or reversing / 55%	82%	46	Improper behavior of peds without paying attention to the traffic / 27%	56	Improper behavior of peds without paying attention to the traffic / 45%
P-PCTurnL	4,3%	360	Improper behavior towards ped when turning / 77%	470	Improper behavior towards ped when turning / 63,4%	75%	93	Improper behavior of pedestrians without paying attention to the traffic / 44%	112	Improper behavior of peds without paying attention to the traffic / 42%
P-PCTurnR	3%	126	Improper behavior towards ped when turning / 66%	165	Improper behavior towards ped when turning / 56%	84%	21	Improper behavior of pedns without paying attention to the traffic / 38%	30	Improper behavior of peds without paying attention to the traffic / 43%



Table 53 Summary statistics of environmental and kinematic parameters in car-to-bicycle conflict scenarios

C2B scenario	# inj	# KSI	Away from junction [% of all inj]	Bicycle path not present [% of all inj]	Light conditions [% of all inj]			Night among KSI cases [%]	Precip (rain, snow, hail, sleet) [% of all inj]	Precip (rain, snow, hail, sleet) among KSI cases	Fog [% of all inj]	Init speed PC Q25, all inj [km/h]	Init speed PC Q75, all inj [km/h]	Coll speed PC Q25, all inj [km/h]	Coll speed PC Q75, all inj [km/h]	Init speed B Q25, all inj [km/h]	Init speed B Q75, all inj [km/h]	Coll speed B Q25, all inj [km/h]	Coll speed B Q75, all inj [km/h]	PC (driver) as main causer [% of all inj]
					Day	Dawn	Night													
B-CR	2705	597	9.7%	27.2%	86.3%	0%	13.7%	14.1%	7.2%	7.7%	0%	5	30	8	23	10	18	10	15	75%
B-CL	1707	397	7.6%	44.4%	78.2%	0%	21.8%	26.7%	11.4%	10.4%	0%	7	32	9	24	12	20	10	19	68%
B-LongSD	412	98	52.7%	68,9%	80.8%	0%	19.2%	30.6%	8.1%	9.2%	0%	20	50	15	45	12	20	12	20	67%
B-LongOD	197	39	23.9%	76.6%	78.7%	0%	21.3%	23.1%	6.6%	10.3%	0%	10	37	10	30	14	20	10	18	55%
B-PCRev	121	23	32.2%	57.0%	90.1%	0%	9.9%	8.7%	1.7%	0.0%	0%	0	5	4.5	10	10	18	10	15	98%
B-PCStat	480	72	90.6%	77.0%	82.5%	0%	17.5%	22.2%	4.6%	6.9%	0%	0	0	0	0	15	20	14	20	69%
B-PCTurnL	706	153	0.6%	39.9%	77.6%	0%	17.5%	24.8%	12.8%	11.8%	0%	11	29	14	23	12	21	10	19	95%
B-PCTurnR	944	118	0.7%	12.9%	83.7%	0%	16.3%	14.4%	8.4%	7.6%	0%	10	30	10	20	14	20	10	19	95%



Table 54 Summary statistics of crash causation in car-to-bicycle conflict scenarios

Scenario	Passenger Car (PC) and also its driver					Bicyclists (Cyc)				
	Share of PC and its drivers w./o. a crash cause	# main causes for PC and its drivers	Main Cause of PC and its drivers with the highest share	# causes for PC and its drivers	Cause of PC and its drivers with the highest share	Share of Cyc w./o. a crash cause	# main causes for Cyc	Main Cause of Cyc with the highest share	# causes for Cyc	Cause of Cyc with the highest share
B-CR	16,5%	2 259	Failure to observe the traffic signs regulating the priority / 62%	3 036	Failure to observe the traffic signs regulating the priority / 46%	34%	1 337	Unlawful use of the carriageway or of other parts of the road (e.g. footway) / 54,5%	2 285	Unlawful use of the carriageway or of other parts of the road (e.g. footway) / 44,5%
B-CL	25%	1 284	Failure to observe the traffic signs regulating the priority / 69%	1 637	Failure to observe the traffic signs regulating the priority / 55%	56%	760	Failure to observe the rule "right has priority over left" / 25%	1 005	Failure to observe the rule "right has priority over left" / 19%
B-LongSD	23,5%	315	Other mistakes made when overtaking / 22%	417	Other mistakes made when overtaking / 20,4%	53%	192	Mistakes made when turning (§ 9) left (except pos. 33, 40) / 32%	262	Mistakes made when turning (§ 9) left (except pos. 33, 40) / 25%
B-LongOD	39,5%	119	Failure to observe the traffic signs regulating the priority / 30%	159	Failure to observe the traffic signs regulating the priority / 23%	41%	116	Mistakes made when turning (§ 9) left (except pos. 33, 40) / 31%	174	Mistakes made when turning (§ 9) left (except pos. 33, 40) / 21%
B-PCRev	0%	121	Mistakes made when making U-turn or reversing / 86%	160	Mistakes made when making U-turn or reversing / 68%	72%	34	Unlawful use of the carriageway or of other parts of the road (e.g. footway) / 35%	39	Unlawful use of the carriageway or of other parts of the road (e.g. footway) / 33%
B-PCStat	29%	340	Behavior contrary to traffic regulations when getting on or off a vehicle / 86%	403	Behavior contrary to traffic regulations when getting on or off a vehicle / 74%	53%	225	Other mistakes made by driver / 50%	304	Other mistakes made by driver / 44,4%
B-PCTurnL	3%	685	Mistakes made when turning (§ 9) left (except pos. 33, 40) / 87%	916	Mistakes made when turning (§ 9) left (except pos. 33, 40) / 67%	73%	193	Unlawful use of the carriageway or of other parts of the road (e.g. footway) / 39%	236	Unlawful use of the carriageway or of other parts of the road (e.g. footway) / 35,6%
B-PCTurnR	2%	925	Mistakes made when turning (§ 9) (except pos. 33, 40) / 85,9%	1 204	Mistakes made when turning (§ 9) (except pos. 33, 40) / 67%	67%	308	Unlawful use of the carriageway or of other parts of the road (e.g. footway) / 56%	373	Unlawful use of the carriageway or of other parts of the road (e.g. footway) / 50%

